

# Valuation of natural gas storage contracts with the COS method

MASTER'S THESIS



Hendrik Jonker

Delft University of Technology

Supervised by

Prof.Dr.Ir C.W. Oosterlee

Dr. A.I. Borovykh



August 16, 2019



# Contents

<b>Acknowledgements</b>	<b>IV</b>
<b>Summary</b>	<b>VI</b>
<b>1 Introduction</b>	<b>1</b>
1.1 Natural Gas and the need for storage . . . . .	1
1.1.1 The natural gas market . . . . .	2
1.2 Determining the value of gas storage . . . . .	2
1.2.1 Intrinsic approach . . . . .	2
1.2.2 Extrinsic approach . . . . .	3
1.2.3 Existing valuation methods for gas storage facilities . . . . .	3
1.3 Hedging . . . . .	3
1.3.1 Hedging a gas storage facility . . . . .	5
1.4 Modelling the natural gas spot price process . . . . .	7
1.4.1 A mean-reverting model with constant mean . . . . .	7
1.4.2 A mean-reverting model with seasonality . . . . .	8
1.4.3 A mean-reverting model with seasonality and jumps . . . . .	9
1.5 Risk neutral measure . . . . .	9
1.5.1 Parameter estimation . . . . .	10
1.6 Structure of this thesis . . . . .	10
<b>2 COS method for European and Bermudan Options</b>	<b>11</b>
2.1 European option . . . . .	11
2.2 Bermudan option . . . . .	11
2.3 Fourier cosine series expansion . . . . .	12
2.4 Fourier Pairs . . . . .	13
2.5 The characteristic function . . . . .	14
2.6 COS method for European options . . . . .	14
2.6.1 The coefficients $V_k$ for vanilla options . . . . .	16
2.6.2 Multiple strike prices . . . . .	17
2.7 COS method for Bermudan options . . . . .	17
2.7.1 Recovering the coefficients $V_k(t_m)$ . . . . .	18
2.8 An approximation method for the characteristic function: Adjoint expansion . . . . .	21
2.8.1 Adjoint expansion for the Ornstein-Uhlenbeck process . . . . .	21
2.9 Interval of integration $[a, b]$ . . . . .	24
<b>3 Extended COS method and Least Squares Monte Carlo</b>	<b>25</b>
3.1 Options with multiple early exercise rights . . . . .	25
3.1.1 Recovering the coefficients $V_k^j(t_m)$ . . . . .	27
3.2 Least Squares Monte Carlo . . . . .	30
3.2.1 LSMC for Bermudan options . . . . .	30
3.2.2 LSMC for options with multiple early exercise rights . . . . .	32

<b>4</b>	<b>Natural gas storage contracts</b>	<b>35</b>
4.1	Relation to options with multiple early exercise rights . . . . .	35
4.2	Defining a natural gas storage contract . . . . .	35
4.3	The dynamic programming formulation . . . . .	37
4.4	LSMC method for a natural gas storage contract . . . . .	39
4.5	COS method for natural gas storage contracts . . . . .	40
4.5.1	Recovering the coefficients $V_k(t_m, \nu)$ . . . . .	40
4.5.2	Determining the contract value . . . . .	41
4.5.3	COS method for a process with a seasonality function . . . . .	42
4.5.4	Variation of the amount of gas in storage with the COS method . . . . .	43
<b>5</b>	<b>Numerical results</b>	<b>45</b>
5.1	Testing the COS and LSMC methods . . . . .	45
5.2	A put option with multiple exercise rights . . . . .	46
5.3	Test with the approximated characteristic function for the OU model . . . . .	47
5.4	Tests with natural gas storage contracts . . . . .	48
5.4.1	Contract values with the LSMC and COS method . . . . .	52
5.4.2	Average volume of gas in storage with LSMC . . . . .	52
5.4.3	An experiment with few nomination dates . . . . .	57
<b>6</b>	<b>Conclusions and Outlook</b>	<b>59</b>
6.1	Conclusions . . . . .	59
6.2	Outlook . . . . .	59
	<b>Appendices</b>	<b>62</b>
<b>A</b>	<b>Algorithms</b>	<b>63</b>
A.1	LSMC algorithm . . . . .	64
A.2	Extended LSMC algorithm . . . . .	65
<b>B</b>	<b>Comparison of two numerical integration techniques</b>	<b>67</b>
<b>C</b>	<b>Models for the dynamics of the underlying</b>	<b>71</b>
C.1	Geometric Brownian Motion . . . . .	71
C.2	Merton jump-diffusion . . . . .	72
C.3	Kou jump-diffusion . . . . .	72
C.4	Ornstein-Uhlenbeck mean-reverting process . . . . .	72
<b>D</b>	<b>Variations with the COS method</b>	<b>73</b>
	<b>References</b>	<b>75</b>

# Acknowledgements

This thesis marks the end of the period of studying for my master's degree Applied Mathematics at the TU Delft. The research which is being reported on in this work was carried out in direct collaboration with Anastasia Borovykh and Kees Oosterlee as part of my internship at CWI. First of all I thank them for their guidance and support during my research and their helpful comments when I was writing on this thesis. A special thanks goes to Kees for his trust in me to do my internship at CWI and for the guidance he gave in selecting my elective courses.

My gratitude also goes to my math teachers from secondary school, in particular Jan Mulder and Leen Reichard, of which the last one unfortunately already passed away, who woke up my interest in mathematics.

A big thanks goes to all the nice people from DSZ Wave and especially to the guys and girls in my waterpolo team. They made that I could clear my mind in busy times and they gave me a warm welcome in the city of Delft.

I would also like to thank some people that I met in Enschede, where I finished my bachelor's degree in Applied Mathematics. I would like to thank Lilian Spijker of the University of Twente, whose door was always open to discuss study related topics or just for a small talk. Her stimulation really helped to finish my bachelor's degree. I would also like to thank the people from W.S.G. Abacus in Enschede where I got to know the student life and where I have made many friends during my time in Enschede.

Last but not least I would like to thank all my friends, family and colleagues (a special thanks to Daphne for pushing me to the library in Middelburg) for their trust in successful finishing my work and the nice times they gave to me in my spare time.



# Summary

Since the liberalization of the energy markets, the storage of energy is decoupled from the production and sales. In Western-Europe the storage of natural gas becomes more and more important because production fields get depleted and governments force companies to slow down their production because of tremors in the ground. Natural gas needs to be imported from countries that are far away, like for example Russia. To provide in security of supply and to ensure there is enough natural gas when the demand is high, it is important to store natural gas nearby.

To determine the value of a gas storage facility in a reliable way we need an efficient market. For an efficient market is needed that the financial instruments, like futures contracts and options on natural gas, are liquidly traded on the exchange. If this condition is met, we are able to determine the value of storage according to market prices.

The COS method was already presented as an efficient method for pricing a broad spectrum of financial derivatives and can be used in combination with all processes for the underlying for which a characteristic function is known. For processes whose characteristic function is not available, the adjoint expansion method can be used to obtain an approximation of the characteristic function. In this work the COS method will be presented as an efficient method for determining the value of gas storage contracts which is competitive with existing valuation methods for natural gas storage contracts.



# Chapter 1

## Introduction

### 1.1 Natural Gas and the need for storage

The content of sections 1.1 and 1.2 is based on the content in [16] and [7]. Natural gas is, as the name already suggests, a naturally occurring mixture of hydrocarbons, primarily consisting of methane. It is formed during the decomposition of organic materials in deep layers of the earth in very many years. Natural gas is an important source of energy. Despite the fact that natural gas produces carbon dioxide when it is burnt and it is a greenhouse gas in itself, natural gas is seen as the least polluting among the fossil fuels. Natural gas becomes liquid at temperatures around  $-162\text{ }^{\circ}\text{C}$  (depending on pressure and its composition) and then it is known as Liquefied Natural Gas (LNG). When liquefying natural gas, its volume decreases with around 600 times, which makes storage and transport more efficient.

In The Netherlands and North-Western Europe, the production of natural gas decreases, because natural gas reservoirs become more and more depleted. In The Netherlands the main production fields had to slow down their production due to tremors in the earth and all the consequences for the local residents. To become not too dependent on the supply from other countries and to ensure security of supply, it is important to store natural gas nearby. So gas storage facilities provide flexibility in the delivery of gas when demand is bigger than production. Also the transition to renewable energies as solar and wind energy plays a role in the need for gas storage. The supply of renewable energies is heavily dependent on weather conditions. If the supply of these energies cannot meet the demand of energy, natural gas can still offer a solution to this problem. A third reason to store natural gas is because its price is known to be seasonal dependent. It is often profitable to buy and store natural gas when the price is low (summer) and to withdraw from the storage and possibly sell if the price is high (winter).

There are multiple ways to store large amounts of natural gas, among these are depleted gas and oil fields, empty salt caverns and empty aquifers. A gas storage facility always has three main operating characteristics: working gas volume, withdrawal rate and injection rate. The working gas volume is the part of the capacity that can be used to store gas, The withdrawal rate is the rate at which gas can be withdrawn from the storage and the injection rate is the rate at which gas can be injected into the storage.

Since the liberalization of the energy markets in the beginning of the 21st century, the production, storage and sales of energy are decoupled. So since then the storage of natural gas became a service on its own and there was a particular need to price this service.

An example of a commercial gas storage facility is Gas Storage Bergermeer (GSB), located near Alkmaar in the Netherlands, that started its service in 2014. At this storage facility the gas is stored in an empty gas field and it is the biggest gas storage facility of Europe. This facility makes use of the depleted Bergermeer gas reservoir and has a working capacity of 45.6 TWh. It is an open-access gas storage, which means that users do not need to purchase entry or exit capacity. Storage is sold in so called Standard Bundled Units (SBU). A standard bundled unit at GSB consists of 1,000 kWh storage capacity, 0.427 kW injection capacity and 0.579 kW withdrawal capacity. Capacity for future storage years is sold in periodic auctions.

### 1.1.1 The natural gas market

Gas storage facilities are usually connected to virtual markets where the gas can be traded (in this way gas in the transport network can be easily transferred between parties). One of the biggest virtual market places in Europe for example is the Dutch Title Transfer Facility (TTF). GSB is connected to the TTF where it delivers its service. The gas can be traded over the counter (OTC) or on an exchange. OTC transactions can be customized to the preferences of the two trading parties, where the products on the exchanges are standardized and the counter party is not necessarily known. Two exchanges that are designated for the Dutch gas market are ICE ENDEX and ECC. ICE ENDEX organizes the capacity auctions of SBU's for GSB. On these exchanges they offer different standardized products. One can think of futures contracts and options. ICE ENDEX is also the place where the secondary trading of storage contracts takes place. Here the customers can trade SBU's, unbundled capacity (injection/withdrawal capacity or storage space) and gas in storage.

Storage services are important for a properly working gas market in the sense that they provide in the need for individual traders to store the commodity they trade.

## 1.2 Determining the value of gas storage

Since the liberalization of the Energy markets in Europe the storage service is decoupled from the production, sales and transportation services. Therefore it became more important to have a good estimation of the value of gas storage. In determining the value of gas storage we distinguish two types of value: the value of the gas storage facility and the value of gas storage services.

The costs of a gas storage facility are made up of operating costs (costs to inject and withdraw), maintenance costs, initial investments (a big part of this is the cushion gas, which needs to be in the storage to have enough pressure for operating) and costs for the location. The profit that the owner of a gas storage facility makes usually consists of the revenues from selling storage service contracts.

The question is: what is a client willing to pay for these storage contracts? Of course if the client is an energy company that really needs to have gas in storage to provide in security of supply, he is willing to pay more than if the client is just a trader of gas and wants to make profit by buying low and selling high. But, if the gas market is liquid, the value of these storage contracts primarily depends on the market prices for gas, since all players can buy and sell gas at any moment on the market.

In determining the value of a gas storage facility, we do only consider storage that is used to trade in the market. For a company of course a storage facility can have additional value, for example it provides security of supply.

In the sequel if we write about the value of a gas storage facility, we actually mean the value of the service to make use of a certain amount of working capacity, with corresponding withdrawal and injection rates, that can be created by trading gas on the gas spot market. (Of course if this is done for the full capacity of the storage facility, this can be used in the valuation of the physical gas storage facility).

The value of a gas storage facility heavily depends on the trading strategy that is followed. We roughly distinguish two different approaches: The intrinsic and the extrinsic approach. Below we will explain their differences. We always assume that the trading is asset-backed, which means that the gas that is bought can be injected in the storage facility and the gas that is sold can be withdrawn from the gas storage facility.

### 1.2.1 Intrinsic approach

The intrinsic value of a gas storage facility is the value based on the forward curves. We can distinguish two types of intrinsic value.

The first one is the tradable intrinsic value. The tradable intrinsic value is the value that can be locked in today based on the current forward curves. Capturing the tradable intrinsic value is a static strategy, which comes down to buy gas in cheap periods and sell gas in expensive periods. This strategy is risk-less because all traded volumes and prices are known beforehand.

The second one is the rolling intrinsic value. The strategy resulting in the rolling intrinsic value is a dynamic strategy. The initial intrinsic trading strategy is changed (for example daily or weekly, also depending on transaction costs) if forward curves change. The advantage is that it cannot perform worse than the initial intrinsic trading strategy, because the strategy is changed only when more profit can be made. Changing the trading strategy is also called a roll. In determining the rolling intrinsic value, forward curves need to be simulated.

### 1.2.2 Extrinsic approach

The extrinsic approach is based on the real options approach and exploits the volatility of the gas spot price. When we follow a trading strategy based on this approach, usually gas is injected if the gas spot price drops and gas is withdrawn if the gas spot price rises. The extrinsic approach values the storage contract taking into account future optionality. The extrinsic value of a storage contract is the expected value that can be created by following the optimal trading strategy. In determining the extrinsic value the spot price needs to be simulated and it is essential that this process is realistic for the real spot price process of gas

By trading according to the strategy following from the extrinsic approach, it is not certain at all that the owner of the gas storage contract can collect the calculated extrinsic value. The money he actually makes can be more or less, depending on the actual development of the gas spot price. Because the gas spot price is quite volatile, there can be a high variance in realized value with the extrinsic approach. To reduce this variance, it is wise to combine this approach with an additional hedging strategy.

### 1.2.3 Existing valuation methods for gas storage facilities

We distinguish roughly two types of methods in the valuation of a gas storage facility. The first type are the simulation based methods. Among these methods is the forest of trees method, which is suitable to one factor models. Another simulation based method is based on the algorithm presented by Longstaff and Schwartz, which they introduced in their famous paper [18]. Boogert and de Jong are well known for applying this method in the context of natural gas storage valuation. Their simulation based method is for example very well suited to handle multi-factor models.

The second type are the partial integro differential equation (PIDE) methods. In [5], the authors derived the Hamilton-Jacobi-Bellman (HJB) equation for the stochastic control problem that characterizes the valuation of a gas storage facility. Subsequently they solve this HJB equation with a semi-Lagrangian method. Also in [28] the authors solve a PIDE to value a natural gas storage facility and determine optimal operating strategies.

## 1.3 Hedging

Holding a position in a certain stock exposes the holder to a certain amount of risk, because the spot price movement of the stock is uncertain. If the stock price drops, the holder of the stock will lose money. To limit or eliminate the risk of losing money, the holder can decide to additionally trade in a derivative on this stock, to keep the same level of wealth. A classical example is to use an option to offset the price movements of a stock. This method to reduce the risk is often called delta hedging, where delta represents the change of the value of the option in relation to the stock price movement. Here we will give a classical example (Based on the derivations of the Black-Scholes equation as done in [27] and [3])

on how to set up a hedging portfolio.

We assume stock price  $S$  follows a geometric Brownian motion

$$dS_t = \mu S_t dt + \sigma S_t dW_t^{\mathbb{P}}, \quad (1.1)$$

where  $W_t^{\mathbb{P}}$  is a Wiener process under the market measure  $\mathbb{P}$ . We also assume the existence of a riskless bank account  $B$ , paying the risk-free rate  $r$

$$dB_t = rB_t dt. \quad (1.2)$$

Now we construct a hedging portfolio, which we assume to be riskless, consisting of an option  $v(t, S_t)$  that is written on the underlying  $S$  and  $\Delta$  units of  $S$

$$\Pi_t = v(t, S_t) + \Delta S_t. \quad (1.3)$$

By Itô's lemma, the price of the option follows an Itô process with the same Wiener Process  $W_t^{\mathbb{P}}$

$$dv(t, S_t) = \left( \frac{\partial v(t, S_t)}{\partial t} + \mu S_t \frac{\partial v(t, S_t)}{\partial S_t} + \frac{1}{2} \sigma^2 S_t^2 \frac{\partial^2 v(t, S_t)}{\partial S_t^2} \right) dt + \sigma S_t \frac{\partial v(t, S_t)}{\partial S_t} dW_t^{\mathbb{P}}. \quad (1.4)$$

We assume that the portfolio is self-financing, so no money is injected or removed from the portfolio. The change in value of the portfolio is only due to changes in the value of  $S$  and the option written on it, which amounts to

$$d\Pi_t = dv(t, S_t) + \Delta dS_t, \quad (1.5)$$

$$d\Pi_t = \left( \frac{\partial v}{\partial t} + \mu S_t \frac{\partial v(t, S_t)}{\partial S_t} + \frac{1}{2} \sigma^2 S_t^2 \frac{\partial^2 v(t, S_t)}{\partial S_t^2} + \Delta \mu S_t \right) dt + \left( \sigma S_t \frac{\partial v(t, S_t)}{\partial S_t} + \Delta \sigma S_t \right) dW_t^{\mathbb{P}}. \quad (1.6)$$

Because we assumed the portfolio to be riskless and the only risk involved is in the Brownian motion part, we hedge this risk by setting

$$\Delta = -\frac{\partial v(t, S_t)}{S_t} \quad (1.7)$$

Because the no-arbitrage principle, the portfolio should pay the same risk-free rate  $r$  as the bank account

$$d\Pi_t = r\Pi_t dt = r(v(t, S_t) + \Delta S_t). \quad (1.8)$$

If we now equate (1.6) and (1.8), we end up with the famous Black-Scholes option pricing PDE

$$\frac{\partial v}{\partial t} + \frac{1}{2} \sigma^2 S_t^2 \frac{\partial^2 v(t, S_t)}{\partial S_t^2} + r S_t \frac{\partial v(t, S_t)}{\partial S_t} - r v(t, S_t) = 0. \quad (1.9)$$

Although we are not especially interested in this Black-Scholes option pricing PDE, it follows from the delta hedging argument and (in combination with the final condition  $v(T, S_T) = h(S_T)$ , where  $h$  is the payoff function of the option) it tells us what the option price should be at any time  $t$  before the options expiration date. Delta actually tells us how many units of stock we have to buy/sell to compensate the change in our option value due to the stock price movement.

A so-called perfect hedge does not exist. If you want to hedge a position continuously, you have to re-balance that position continuously, which is unfeasible. Re-balancing also brings costs with it, therefore sometimes it is better to keep a position instead of hedging it. In practice hedges are set in longer time intervals (daily, weekly or even monthly). Another necessary condition is that the contracts that can be used as a hedge must be liquidly traded on the exchange. A trader can possibly use derivatives on a similar stock that behaves almost the same as the stock in his/her portfolio.

### 1.3.1 Hedging a gas storage facility

Holding a certain amount of commodity, in our case gas, also exposes the trader to a certain amount of risk because the spot price movement of gas is also uncertain.

As stated earlier, when a storage manager follows the extrinsic approach and follows the resulting optimal strategy, on average the storage manager will realize the calculated value. But because in the extrinsic approach we make use of the gas spot price, for which the volatility is relatively high compared to forward prices, there is a high amount of risk involved. In order to reduce this risk, the spot trading strategy can be combined with a hedging strategy. In the commodity world they often use futures or forward contracts or options on these contracts to (partly) hedge away these price risks. The main reason to use these instruments is that they are (strongly) correlated to the gas spot price. The idea of futures and forward contracts is the same, for the difference please see the blog: *Futures and Forward contracts on commodities* on page 5. Because futures contracts are the most liquid instruments, in the sequel we will write about futures contracts.

On the commodities exchange one can trade not only natural gas futures contracts but also natural gas option contracts. These natural gas option contracts are options on the natural gas futures contracts. At the expiration date such a gas options contract automatically turns into the corresponding gas futures contract if the price of this contract is better than the spot price. Since a gas option gives the holder the right but not the obligation to buy or sell gas at a predetermined price, hedging with gas options is more flexible than hedging with gas futures. For now we only consider the case of hedging with gas futures contracts, so the gas storage trader ends up with a portfolio consisting of gas in storage + additional futures contracts. The main idea is that the hedging volume of the futures contracts neutralizes the movement in the portfolio value due to gas spot price movements.

A last thing to keep in mind is the type of settlement of these futures contracts. We distinguish physical settlement and cash settlement. When a futures contract is physically settled, the buyer has to take off the amount of gas and the seller has to deliver the amount of gas. In cash settled futures contracts, the difference between the spot price and the price in the contract is paid or received and there is no physical transfer of gas. So for hedging purposes, cash settled futures contracts are preferred, because physically settled futures contracts need additional constraints such that they are asset-backed.

#### **Futures and Forward contracts on commodities**

Futures contracts are agreements between two parties to buy or sell a certain amount of the underlying commodity at a fixed price at a pre-determined date in the future. A futures contract is settled on its expiration date. We distinguish cash settlement and physical settlement. If a futures contract is financially settled, the seller of the commodity does not deliver the commodity but receives or pays the difference between the spot price of the commodity and the cash position of the transaction agreed upon. If a futures contract is physically settled, the seller of the commodity has to deliver the commodity physically (and in return the buyer has to take off the commodity).

Futures contracts are highly standardized instruments traded on an exchange. The exchange takes the role as counterparty for both sides. Trading futures contracts also obliges both counterparties to deposit on a margin account and this margin is updated daily mark-to-market to the corresponding contract by interim transactions. Therefore there is almost no counterparty risk (the risk that the counterparty for what reason does not fulfill its obligations) in trading futures contracts.

Forward contracts are the same as futures contracts in the sense that they are agreements between two parties to buy or sell a certain amount of the underlying commodity at a fixed price at a pre-determined date in the future. The difference is that forward contracts are traded over-the-counter (OTC) and therefore customizable. The advantage of these contracts is that they can be constructed in such a way that they fulfill the special needs of both parties. The drawback of forward contracts is that holders are exposed to counterparty risk.

We also want to mention here that the (rolling) intrinsic strategy is a hedging strategy in itself, because it limits the risk the trader is exposed to.

In [6] four different hedging strategies that can be combined with the spot trading strategy are distinguished. These are the static intrinsic and static delta hedge, which are set in place only at the beginning of the storage year, and the dynamic intrinsic and dynamic delta hedge, which are rebalanced every month. The static intrinsic hedge is actually just applying the intrinsic strategy, where the dynamic intrinsic hedge is actually just applying the rolling intrinsic strategy. These (rolling) intrinsic strategies can be seen as a hedging strategy in itself, because these strategies also limit the risk the trader is exposed to.

What the authors in [6] very well in their backtest results in the Appendix is that the expected gas storage value of the intrinsic approach (which is a certain value, as explained in the section about the intrinsic approach) is lower than the expected gas storage value of the rolling intrinsic approach which in turn is lower than the expected gas storage value of the extrinsic approach. When concentrating on the realized value with the spot trading strategy without hedge, it can be seen that the realized gas storage value is much lower than the expected spot trading strategy. However, combined with the delta hedging strategy, it can be seen that the realized gas storage value is very close to the expected gas storage value. Their conclusion is therefore that the spot trading strategy, combined with dynamic delta hedging results in the highest realized gas storage value.

In [13] they describe this form of delta hedging a little bit more technically. Let  $F(t_m, T_i)$  denote the value of a futures contract at time  $t_m$  with expiration date  $T_i$ , for  $i = 1 \dots I$ , where  $F(t_m, T_1)$  is the prompt futures contract and  $F(t_m, T_I)$  is the futures contract that expires last in future. Note that if  $t_m \geq T_i$ ,  $F(t_m, T_i) = 0$ , because the futures contract stops trading after its expiration date.

The delta hedging strategy now comes down to add to the trading strategy that is based on the gas spot price at time  $t_m$ , a strategy of trading  $\Delta(t_m, T_i)$  of futures contracts. In total the hedging strategy consists of trading the following futures contracts:

$$\sum_{m=0}^M \sum_{i=1}^I \Delta(t_m, T_i) (F(t_{m+1}, T_i) - F(t_m, T_i)). \quad (1.10)$$

Note that  $\Delta(t_m, T_i) = 0$ , for  $t_m \geq T_i$ , also because the futures contract stops trading after its expiration date.

Because the price process of a futures contract is a martingale under the risk-neutral measure  $\mathbb{Q}$ , we have

$$\mathbb{E}_{\mathbb{Q}}[F(t_{m+1}, T_i) | \mathcal{F}_{t_m}] = F(t_m, T_i). \quad (1.11)$$

Now using the tower property for martingales, the expectation of this additional futures trading strategy at initial date  $t_0$  under the risk-neutral measure is given by

$$\mathbb{E}_{\mathbb{Q}} \left[ \sum_{m=0}^M \sum_{i=1}^I \Delta(t_m, T_i) (F(t_{m+1}, T_i) - F(t_m, T_i)) \middle| \mathcal{F}_{t_0} \right] = 0. \quad (1.12)$$

For the total expectation of our portfolio  $\Pi$  we need the expectation of the spot trading strategy in equation (4.5), which is introduced in Section 4.2. The total expectation of our portfolio  $\Pi$  at initial date  $t_0$  under the optimal decisions  $\Delta\nu^*$  is given by

$$\mathbb{E}_{\mathbb{Q}}[\Pi_{t_0} | \mathcal{F}_{t_0}] = \sup_{\Delta\nu^*} \mathbb{E}_{\mathbb{Q}} \left[ \sum_{m=1}^M e^{-rt_m} h(S(t_m), \Delta\nu(t_m)) + e^{-rt_{M+1}} q(t_{M+1}, S(t_{M+1}), \nu(t_{M+1})) \middle| \mathcal{F}_{t_0} \right] \quad (1.13)$$

$$+ \mathbb{E}_{\mathbb{Q}} \left[ \sum_{m=1}^M \sum_{i=1}^I \Delta(t_m, T_i) (F(t_{m+1}, T_i) - F(t_m, T_i)) \middle| \mathcal{F}_{t_0} \right] \quad (1.14)$$

$$= \sup_{\Delta\nu^*} \mathbb{E}_{\mathbb{Q}} \left[ \sum_{m=1}^M e^{-rt_m} h(S(t_m), \Delta\nu(t_m)) + e^{-rt_{M+1}} q(t_{M+1}, S(t_{M+1}), \nu(t_{M+1})) \middle| \mathcal{F}_{t_0} \right]. \quad (1.15)$$

So the expectation of our hedge portfolio is the same as the expectation of the gas spot trading strategy without hedge, but if we choose the  $\Delta(t_m, T_i)$  in a smart way, it is very likely that the variance of the realized value with our hedge portfolio will decrease.

The question remains: how to choose this delta? A heuristic strategy that is widely employed is mentioned in [6]. There they let the hedge volumes depend on the expected future injections and withdrawals. They buy the volume of expected cumulative injections and withdrawals between the expiry of two subsequent futures contracts beforehand by trading in the last of these two futures contracts.

This hedging strategy comes down to the  $\Delta_1$  strategy mentioned in [13].

$$\Delta_1(t_m, T_i) = \mathbb{E}_{\mathbb{Q}} \left[ \sum_{t_m \leq t_j < T_i} \Delta \nu^*(t_j) \middle| \mathcal{F}_{t_m} \right] \quad \text{if } i = 1, \quad (1.16)$$

$$= \mathbb{E}_{\mathbb{Q}} \left[ \sum_{T_{i-1} \leq t_j < T_i} \Delta \nu^*(t_j) \middle| \mathcal{F}_{t_m} \right] \quad \text{if } i > 1, \quad (1.17)$$

$$(1.18)$$

where  $\Delta \nu^*(t_j)$  denotes the optimal injection or withdrawal at time  $t_j$  that follows directly out of the extrinsic approach.

## 1.4 Modelling the natural gas spot price process

There are three main characteristics that are typical when looking at historical time series of the spot price process for natural gas, these are mean-reversion, seasonality and the occurrence of spikes or jumps. Because modeling the spot price process is not the scope of this work, we use spot price models that can capture these characteristics but we do not say anything about how well these models can mimic the real spot price process. We consider roughly speaking three different spot price models: A mean-reverting model with constant mean, a mean-reverting model with a time-dependent mean (to capture the seasonality) and a mean-reverting model with time-dependent mean and jumps.

### 1.4.1 A mean-reverting model with constant mean

In the first model by Schwartz [26], the spot price is driven by the following SDE:

$$dS(t) = \kappa(\mu - \log(S(t)))S(t) dt + \sigma S(t) dW(t), \quad (1.19)$$

where  $\kappa$  is the rate of mean-reversion,  $\mu$  is the long term mean of the process and  $\sigma$  is the volatility. Substituting  $X(t) = \log(S(t))$  and applying Itô's lemma yields

$$dX(t) = \left( \kappa(\mu - X(t)) - \frac{1}{2}\sigma^2 \right) dt + \sigma dW(t) \quad (1.20)$$

$$= \kappa(\theta - X(t)) dt + \sigma dW(t), \quad (1.21)$$

where  $\theta = \mu - \frac{\sigma^2}{2\kappa}$ . This last expression can be recognized as an Ornstein-Uhlenbeck process whose characteristics are given in Appendix C.4.

Because in Section 5.3 we will do an experiment with a European option where the process of the underlying asset is modelled according to this model, we also derive here the dynamics of the  $\log(S(t)/K)$  process. Instead of substituting  $X(t) = \log(S(t))$  in the step from (1.19) to (1.20) we substitute  $X(t) =$

$\log(S(t)/K)$ . Now applying Itô's lemma yields

$$dX(t) = \left( \kappa(\mu - X(t) - \log(K)) - \frac{1}{2}\sigma^2 \right) dt + \sigma dW(t) \quad (1.22)$$

$$= \kappa(\theta - X(t)) dt + \sigma dW(t), \quad (1.23)$$

where  $\theta = \mu - \log(K) - \frac{\sigma^2}{2\kappa}$ . So the strike price  $K$  appears in the parameter  $\theta$  that is inserted into the Ornstein-Uhlenbeck process.

### 1.4.2 A mean-reverting model with seasonality

The following model is based on the previous model stemming from the paper presented by Lucia and Schwartz [19]. This model is used for example by Boogert and de Jong [2] in their Monte Carlo valuation of gas storage contracts. Lucia and Schwartz use a model where the log-spot price follows a zero mean-reverting process plus a deterministic function  $f(t)$  which represents the seasonality component:

$$\log(S(t)) = f(t) + Y(t), \quad (1.24)$$

where the dynamics of  $Y(t)$  are given by

$$dY(t) = -\kappa Y(t) dt + \sigma dW(t), \quad (1.25)$$

where  $\kappa$  is the speed of mean reversion and  $\sigma$  is the volatility (Lucia and Schwartz use a time-dependent volatility  $\sigma(t)$ , but for simplicity we assume the volatility to be constant).

To get to the dynamics for  $S(t)$ , we can rewrite Equation (1.24) by taking exponents on both sides as

$$S(t) = F(t)e^{Y(t)}, \quad (1.26)$$

where  $F(t) := e^{f(t)}$ . Now applying Itô's lemma yields

$$dS(t) = \kappa(\mu(t) - \log(S(t)))S(t) dt + \sigma S(t) dW(t), \quad (1.27)$$

with the time-dependent mean reverting level  $\mu(t)$  given by

$$\mu(t) = \frac{1}{\kappa} \left( f'(t) + \frac{\sigma^2}{2} \right) + f(t). \quad (1.28)$$

Substituting  $X(t) = \log(S(t))$  and applying Itô's lemma once more yields

$$dX(t) = \left( \kappa(\mu(t) - X(t)) - \frac{1}{2}\sigma^2 \right) dt + \sigma dW(t) \quad (1.29)$$

$$= \kappa(\theta(t) - X(t)) dt + \sigma dW(t), \quad (1.30)$$

where  $\theta(t) = \mu(t) - \frac{\sigma^2}{2\kappa} = \frac{1}{\kappa}f'(t) + f(t)$ . This last expression can be recognized as the mean reverting Hull-White model.

In the paper [31], the authors provide the characteristic function for this process, which reads

$$\phi(\omega; x; \tau) = e^{i\omega x e^{-\kappa\tau} + A(\omega, \tau)}, \quad (1.31)$$

with

$$A(\omega, \tau) = i\omega \int_0^\tau (f'(T-s) + \kappa f(T-s)) e^{-\kappa s} ds + \frac{1}{4\kappa} \omega^2 \sigma^2 (e^{-2\kappa\tau} - 1). \quad (1.32)$$

### 1.4.3 A mean-reverting model with seasonality and jumps

Cartea and Figueroa extended in their paper [4] the model of Lucia and Schwartz to account for jumps. Their starting point is again Equation (1.24), but they extended the dynamics for  $Y(t)$  with a term that accounts for the jumps:

$$dY(t) = -\kappa Y(t) dt + \sigma dW(t) + \log(J(t)) dX_{\mathcal{P}}(t), \quad (1.33)$$

where  $X_{\mathcal{P}}(t)$  is a Poisson process with intensity  $\lambda$  and  $J(t)$  is an i.i.d. process which represents the jump size.  $W(t)$ ,  $J(t)$  and  $X_{\mathcal{P}}(t)$  are assumed to be mutually independent processes.

#### The Poisson process

For a Poisson process with intensity  $\lambda$ , it follows that

$$dX_{\mathcal{P}}(t) = \begin{cases} 1 & \text{with probability } \lambda dt \\ 0 & \text{with probability } 1 - \lambda dt, \end{cases} \quad (1.34)$$

for a sufficiently small time interval  $dt$ .

In their paper Cartea and Figueroa assume that the process  $J(t)$  is log-normal, i.e.  $\log(J(t)) \sim \mathcal{N}(\mu_J, \sigma_J^2)$ . This model can be easily adapted when considering other processes for the jump size, like the model by Kou in [17].

Now applying a variant of Itô's lemma for stochastic processes containing both a Brownian motion and a Poisson process results in the following dynamics for  $S(t)$ :

$$dS(t) = \kappa(\mu(t) - \log(S(t)))S(t) dt + \sigma S(t) dW(t) + S(t)(J(t) - 1) dX_{\mathcal{P}}(t), \quad (1.35)$$

with the time-dependent mean reverting level  $\mu(t)$  given by

$$\mu(t) = \frac{1}{\kappa} \left( f'(t) + \frac{\sigma^2}{2} \right) + f(t). \quad (1.36)$$

Substituting  $X(t) = \log(S(t))$  and applying the same variant of Itô's lemma once more yields

$$dX(t) = \left( \kappa(\mu(t) - X(t)) - \frac{1}{2}\sigma^2 \right) dt + \sigma dW(t) + \log(J(t)) dX_{\mathcal{P}}(t) \quad (1.37)$$

$$= \kappa(\theta(t) - X(t)) dt + \sigma dW(t) + \log(J(t)) dX_{\mathcal{P}}(t), \quad (1.38)$$

where  $\theta(t) = \mu(t) - \frac{\sigma^2}{2\kappa} = \frac{1}{\kappa} f'(t) + f(t)$ .

The characteristic function for this process is given by:

$$\phi(\omega; x; \tau) = e^{i\omega x e^{-\kappa\tau} + A(\omega, \tau) + B(\omega, \tau)}, \quad (1.39)$$

with  $A(\omega, \tau)$  as in (1.32) and

$$B(\omega, \tau) = \lambda\tau \left( e^{i\omega\mu_J - \frac{1}{2}\omega^2\sigma_J^2} - 1 \right), \quad (1.40)$$

as the part induced by the jump process.

## 1.5 Risk neutral measure

In financial models, where things are uncertain, we are always dealing with a probability space  $(\Omega, \mathcal{F}, \mathbb{P})$ . In this triplet,  $\Omega$  denotes the sample space and is the set of all possible states of the world.  $\mathcal{F}$  is a  $\sigma$ -algebra on  $\Omega$ , representing all possible events. Finally,  $\mathbb{P}$  is a probability measure that assigns a

probability to every event in  $\mathcal{F}$ . The measure  $\mathbb{P}$  is called the real world measure (also physical measure or market measure).

The risk-neutral measure (or equivalent martingale measure), usually denoted with  $\mathbb{Q}$ , is the measure under which the discounted price process of an asset is a martingale.

$$\mathbb{E}_{\mathbb{Q}} [e^{-rT} S(T) | \mathcal{F}_t] = S(t) \quad (1.41)$$

$\mathcal{F}_t \subset \mathcal{F}$  is the filtration on  $(\Omega, \mathcal{F})$  up to time  $t$ .

The fundamental theorem of asset pricing states that in a complete market there exists a unique risk-neutral probability measure that is equivalent to the real-world probability measure (denoted with  $\mathbb{P}$ ) if and only if there are no arbitrage opportunities.

In this work all valuation is done under the risk neutral measure. For the GBM and Merton model we correct the drift such that the asset price process is a martingale under the risk-neutral measure. For the models of the Ornstein-Uhlenbeck type, we assume that the parameters are already corrected for the market price of risk.

### 1.5.1 Parameter estimation

In estimating the model parameters, also called calibrating the model, it is essential to know under what measure this is done. If calibration is done on historical market data, we are working under the real-world measure  $\mathbb{P}$  and the process is fitted to historical market data. It is important to note that calibration under the risk neutral measure  $\mathbb{Q}$  will lead to different model parameters.

The estimation of model parameters is not in the scope of this thesis. But we want to use some realistic parameters in our experiments in Chapter 5. For the models that were introduced in previous section we use the empirical study in the paper [1] to choose some realistic parameters. Despite the fact that this study is done for electricity prices, we assume similar behaviour for natural gas spot prices. For a general explanation on how to estimate the model parameters we additionally refer to the paper [4].

## 1.6 Structure of this thesis

In Chapter 2 we start with the recap of the COS method for the valuation of European and Bermudan options. In Chapter 3 we extend the COS method to options with multiple exercise rights at discrete exercise dates. This will help us to ultimately employ the COS method for the valuation of gas storage contracts in Chapter 4. In Chapter 3 we will also introduce the method of Longstaff and Schwartz for the valuation of Bermudan options and options with multiple exercise rights. This simulation based method will be used to compare our results with the results that are obtained with the COS method. In Chapter 4 we introduce the natural gas storage contracts after which we describe the existing valuation method for these contracts that is used by Boogert and de Jong. In the same chapter we will derive the COS method for the valuation of natural gas storage contracts. Finally in Chapter 5 we report about some numerical experiments with the described methods that we have done during this research and in Chapter 7 we conclude.

## Chapter 2

# COS method for European and Bermudan Options

The COS method is a numerical integration method based on Fourier cosine expansions. It is an efficient method to recover a probability density function from its characteristic function. Before introducing the COS method, we start with recalling the definitions of European and Bermudan options, both of which are financial derivatives: their price depends on the price of its underlying asset  $S$ . Let  $S(t)$  denote the price of the asset  $S$  at time  $t$ . The holder of an option has the right, but not the obligation, to buy (call) or sell (put) the underlying asset at a predetermined strike price  $K$  at a predetermined time, which we call the exercise or expiration date.

### 2.1 European option

For European options it is only allowed to exercise at the expiration date  $T$ . Therefore, the value  $v$  of a European option can be computed with the risk-neutral valuation formula, which states that the value of an option at time  $t_0$  can be expressed as the discounted expected value of the option at time  $T$ :

$$v(t_0, S(t_0)) = e^{-r\Delta t} \mathbb{E}_{\mathbb{Q}}[v(T, S(T)) | \mathcal{F}_{t_0}]. \quad (2.1)$$

Here  $r$  is the risk-neutral interest rate,  $\Delta t = T - t_0$  and  $\mathbb{E}_{\mathbb{Q}}$  means that the expectation is taken with respect to the risk-neutral measure.

At time  $T$ , the value of the option is just the payoff of the option. The payoff function  $g$  for the vanilla options (which we will use in this throughout this report) is given by

$$g(t, S(t)) = \begin{cases} \max\{S(t) - K, 0\}, & \text{for a call,} \\ \max\{K - S(t), 0\}, & \text{for a put.} \end{cases} \quad (2.2)$$

### 2.2 Bermudan option

A Bermudan option is an option that can be exercised once at a set of predefined exercise dates before expiry. Let  $M$  denote the number of exercise dates before expiry and assume these dates are equally spaced, so that  $t_{m-1} - t_m = \Delta t$  for  $m = 1 \dots M$ . The resulting set of dates is given by:  $0 = t_0 < t_1 < \dots < t_M = T$  (see also Figure 2.1), where exercise is possible on all dates except the starting date  $t_0$ .



Figure 2.1: Time lattice for a natural gas storage contract

The price of a Bermudan option can be found via backward reasoning. At the expiry date  $t_M$ , if the option is not exercised on any exercise date before maturity, the value of the option is simply equal to the payoff:  $v(t_M, S(t_M)) = g(t_M, S(t_M))$ . On exercise date  $t_{M-1}$ , we have to decide on the following:

- If we exercise the option we receive the payoff  $g(t_{M-1}, S(t_{M-1}))$ .
- If we do not exercise the option we do not receive the payoff. the option however can still represent a value if we can exercise it profitably at  $t_M$ . This value is called the continuation value at  $t_{M-1}$  and is denoted by  $c(t_{M-1}, S(t_{M-1}))$ .

The decision we should take at time  $t_{M-1}$  is the decision which results in the highest value of the option at time  $t_{M-1}$ . The value of the option at time  $t_{M-1}$  is given by:

$$v(t_{M-1}, S(t_{M-1})) = \max\{g(t_{M-1}, S(t_{M-1})), c(t_{M-1}, S(t_{M-1}))\}.$$

The continuation value  $c(t_{M-1}, S(t_{M-1}))$  can be computed with the risk-neutral valuation formula:

$$c(t_{M-1}, S(t_{M-1})) = e^{-r\Delta t} \mathbb{E}_{\mathbb{Q}}[v(t_M, S(t_M)) | \mathcal{F}_{t_{M-1}}], \quad (2.3)$$

where  $\mathcal{F}_{t_{M-1}}$  denotes the filtration representing the information up to and including time  $t_{M-1}$ . It should be noticed that in this first step  $c(t_{M-1}, S(t_{M-1}))$  just equals the price of a European option at time  $t_{M-1}$  with expiration date  $t_M$ .

Now applying this reasoning backwards in time we get that for a general time point  $t_{m-1}$  the option value is given by:

$$v(t_{m-1}, S(t_{m-1})) = \max\{c(t_{m-1}, S(t_{m-1})), g(t_{m-1}, S(t_{m-1}))\}, \quad \text{for } m = M, \dots, 2.$$

For  $m = M, \dots, 1$ , the continuation values  $c(t_{m-1}, S(t_{m-1}))$  can be computed by successive application of the risk-neutral valuation formula

$$c(t_{m-1}, S(t_{m-1})) = e^{-r\Delta t} \mathbb{E}_{\mathbb{Q}}[v(t_m, S(t_m)) | \mathcal{F}_{t_{m-1}}]. \quad (2.4)$$

Now we have all the ingredients to calculate the continuation values backwards in time. Since the option can not be exercised at  $t_0$ , the option value at  $t_0$  equals the continuation value at  $t_0$ . Summarizing, we have the following dynamic programming problem which can also be found in [9]:

### The dynamic programming formulation

$$\begin{cases} v(t_M, S(t_M)) & = g(t_M, S(t_M)) \\ c(t_{m-1}, S(t_{m-1})) & = e^{-r\Delta t} \mathbb{E}_{\mathbb{Q}}[v(t_m, S(t_m)) | \mathcal{F}_{t_{m-1}}], \quad \text{for } m = M, \dots, 1 \\ v(t_{m-1}, S(t_{m-1})) & = \begin{cases} \max\{c(t_{m-1}, S(t_{m-1})), g(t_{m-1}, S(t_{m-1}))\} & \text{for } m = M, \dots, 2 \\ c(t_{m-1}, S(t_{m-1})) & \text{for } m = 1. \end{cases} \end{cases} \quad (2.5)$$

## 2.3 Fourier cosine series expansion

For a function supported on the interval  $[0, \pi]$ , its Fourier cosine series expansion is defined as

$$f(\theta) = \frac{1}{2}A_0 + \sum_{k=1}^{\infty} A_k \cdot \cos(k\theta), \quad (2.6)$$

with

$$A_k = \frac{2}{\pi} \int_0^{\pi} f(\theta) \cos(k\theta) d\theta. \quad (2.7)$$

For ease of notation we define

$$f(\theta) := \sum'_{k=0}^{\infty} A_k \cdot \cos(k\theta), \quad (2.8)$$

where  $\sum'$  indicates that the first term in the summation is multiplied by  $\frac{1}{2}$ .

For a function supported on the interval  $[a, b] \in \mathbb{R}$ , its Fourier cosine series expansion can be obtained by using the following change of variables:

$$\theta := \frac{x-a}{b-a}\pi. \quad (2.9)$$

It then reads

$$f(x) = \sum'_{k=0}^{\infty} A_k \cdot \cos\left(k\pi \frac{x-a}{b-a}\right), \quad (2.10)$$

with

$$A_k = \frac{2}{b-a} \int_a^b f(x) \cos\left(k\pi \frac{x-a}{b-a}\right) dx. \quad (2.11)$$

## 2.4 Fourier Pairs

For calculating the expectation given in (2.4), we need the transition probability distribution  $\Gamma(t_0, x; T, y)$ . This is nothing more than the probability distribution of the underlying process  $y$  at time  $T$ , given that the value of the process is  $x$  at time  $t_0$ . For certain processes the analytical expression for this transition probability function is unknown, but the characteristic function can be derived analytically.

The COS method exploits the availability of the characteristic function which is given by the Fourier transform of its probability density function in the second spatial variable:

$$\hat{\Gamma}(t_0, x; T, \omega) = \int_{-\infty}^{\infty} e^{iy\omega} \Gamma(t_0, x; T, y) dy. \quad (2.12)$$

If we consider an underlying processes with stationary increments, the transition probability density function depends only on the current state  $x$  and  $\tau := T - t_0$ . In the remaining of this section for ease of notation we omit the dependence on  $\tau$  and define:

$$\hat{\Gamma}(t_0, x; T, \omega) =: \phi(x; \omega) \quad \text{and} \quad \Gamma(t_0, x; T, y) =: f(y|x), \quad (2.13)$$

which is the same notation as used in [10] and [11].

In the subsequent derivation of the COS method for European options we will use the so-called Fourier pair

$$\phi(x; \omega) = \int_{-\infty}^{\infty} e^{iy\omega} f(y|x) dy. \quad (2.14)$$

Since the probability distribution of the density function  $f(y|x)$  has almost no mass in the tails, we can approximate the integral by integrating from  $a$  to  $b$  such that we get the approximation

$$\tilde{\phi}(x; \omega) := \int_a^b e^{iy\omega} f(y|x) dy. \quad (2.15)$$

## 2.5 The characteristic function

In general, characteristic functions can be written in the form

$$\phi(\omega; x; \tau) = e^{iux\beta} \varphi(\omega; \tau), \quad (2.16)$$

where  $\varphi(\omega; \tau)$  does not depend on  $x$ . For processes with independent increments  $\beta = 1$ . Since the exponential Lévy processes do have independent increments, their characteristic functions can be written in the form

$$\phi(\omega; x; \tau) = e^{iux} \varphi(\omega; \tau), \quad (2.17)$$

where  $\phi(\omega, \tau) := \phi(\omega; 0, \tau)$ .

For all processes for which  $\beta = 1$  the COS method offers some nice properties. One of these properties is that European option prices for many strike prices can be computed simultaneously, which we will show in Paragraph 2.6.2. For the valuation of Bermudan options, the FFT-based algorithm can be used to efficiently calculate the continuation value coefficients in  $O(N \log_2 N)$  operations as the authors showed in the paper [11].

If  $\beta \neq 1$  this FFT-based algorithm cannot be used. For example for the Ornstein-Uhlenbeck process  $\beta = e^{-\kappa\tau}$ . Under the Ornstein-Uhlenbeck process the computation of the continuation value coefficients can only be done in  $O(N^2)$  operations.

In the paper [29], the authors proposed an approximation of the characteristic function of the Ornstein-Uhlenbeck process such that it can be written in the form of Equation (2.17). They rewrite the characteristic function of the Ornstein-Uhlenbeck process (C.15) as

$$\phi_{ou}(\omega; x, \tau) = e^{i\omega x} e^{A(\omega, \tau) - i\omega x(1 - e^{-\kappa\tau})} =: e^{i\omega x} \psi(\omega; x, \tau). \quad (2.18)$$

Subsequently they approximate  $\psi(\omega; x, \tau)$  with  $\psi(\omega; \mathbb{E}[x | \mathcal{F}_0], \tau)$ , such that it is in the form of Equation (2.17). In combination with this approximated characteristic function the FFT-based algorithm can be used to efficiently calculate the continuation value coefficients in an efficient way.

In Paragraph 2.8.1 we introduce the so-called adjoint expansion method to approximate the characteristic function of the Ornstein-Uhlenbeck process in a different way. With this approximation the characteristic function can be written in the form

$$e^{i\omega x} \sum_{k=0}^n (x - \bar{x})^k g_{n,k}(t, T, \omega), \quad (2.19)$$

where the coefficients  $g_{n,k}$  do not depend on  $x$ . In [3] the authors showed that if the characteristic function can be written in this form, then also the FFT-based algorithm can be used to calculate the continuation value coefficients.

## 2.6 COS method for European options

Recalling formula (2.1) for the valuation of European options and defining  $x$  to be the state of the asset price process at time  $t_0$  and  $y$  the state of the asset price process at time  $T$  we have

$$v(t_0, x) = e^{-r\Delta t} \mathbb{E}_{\mathbb{Q}}[v(T, y) | \mathcal{F}_{t_0}] = e^{-r\Delta t} \int_{-\infty}^{\infty} v(T, y) f(y|x) dy. \quad (2.20)$$

Using the same truncation range as for the integral in (2.15), we can also approximate the integral in (2.20) by integrating from  $a$  to  $b$  so that we get the following approximation for the option value

$$v(t_0, x) \approx e^{-r\Delta t} \int_a^b v(T, y) f(y|x) dy. \quad (2.21)$$

Now we replace  $f(y|x)$  by its Fourier cosine series expansion (see (2.10) and (2.11)) such that we get

$$v(t_0, x) \approx e^{-r\Delta t} \int_a^b v(T, y) \sum_{k=0}^{\infty'} A_k(x) \cdot \cos\left(k\pi \frac{y-a}{b-a}\right) dy, \quad (2.22)$$

with

$$A_k(x) = \frac{2}{b-a} \int_a^b f(y|x) \cos\left(k\pi \frac{y-a}{b-a}\right) dy. \quad (2.23)$$

Interchanging integration and summation gives

$$v(t_0, x) \approx e^{-r\Delta t} \sum_{k=0}^{\infty'} A_k(x) \cdot \int_a^b v(T, y) \cos\left(k\pi \frac{y-a}{b-a}\right) dy. \quad (2.24)$$

Now letting  $V_k$  be the Fourier cosine series coefficients of the value of the option at maturity in  $y$

$$V_k := \frac{2}{b-a} \int_a^b v(y, T) \cos\left(k\pi \frac{y-a}{b-a}\right) dy, \quad (2.25)$$

and inserting in (2.24) gives

$$v(t_0, x) \approx \frac{b-a}{2} e^{-r\Delta t} \sum_{k=0}^{\infty'} A_k(x) \cdot V_k. \quad (2.26)$$

Since the Fourier cosine series coefficients decay rapidly when  $k$  goes to infinity, we can truncate the series summation to  $N$  terms to further approximate the value of the option:

$$v(t_0, x) \approx \frac{b-a}{2} e^{-r\Delta t} \sum_{k=0}^{N-1} A_k(x) \cdot V_k. \quad (2.27)$$

By Euler's formula we have that the cosine is the real part of the complex exponential function, thus we can rewrite the coefficients from (2.23) as

$$A_k(x) = \frac{2}{b-a} \Re \left\{ \int_a^b f(y|x) \exp\left(ik\pi \frac{y-a}{b-a}\right) dy \right\} \quad (2.28)$$

$$= \frac{2}{b-a} \Re \left\{ \int_a^b f(y|x) \exp\left(\frac{ik\pi y}{b-a}\right) dy \cdot \exp\left(\frac{-ik\pi a}{b-a}\right) \right\} \quad (2.29)$$

$$= \frac{2}{b-a} \Re \left\{ \tilde{\phi}\left(x; \frac{k\pi}{b-a}\right) \cdot \exp\left(\frac{-ik\pi a}{b-a}\right) \right\} \quad (2.30)$$

where  $\Re\{\cdot\}$  denotes taking the real part of the argument and in the last step we used (2.15)

Inserting this in (2.27) leads to

$$v(t_0, x) \approx e^{-r\Delta t} \sum_{k=0}^{N-1} \Re \left\{ \tilde{\phi}\left(\frac{k\pi}{b-a}; x\right) e^{-ik\pi \frac{a}{b-a}} \right\} V_k, \quad (2.31)$$

The last approximation uses the original characteristic function  $\phi$  instead of the approximated one  $\phi_1$ . Ultimately the COS formula for pricing European options for general underlying processes is given by

$$v(t_0, x) \approx e^{-r\Delta t} \sum_{k=0}^{N-1} \Re \left\{ \phi\left(\frac{k\pi}{b-a}; x\right) e^{-ik\pi \frac{a}{b-a}} \right\} V_k, \quad (2.32)$$

## 2.6.1 The coefficients $V_k$ for vanilla options

Recalling that the value of a vanilla option at maturity is given by the payoff at maturity, we have

$$V_k = \frac{2}{b-a} \int_a^b v(T, y) \cos\left(k\pi \frac{y-a}{b-a}\right) dy \quad (2.33)$$

$$= \frac{2}{b-a} \int_a^b g(T, y) \cos\left(k\pi \frac{y-a}{b-a}\right) dy \quad (2.34)$$

$$(2.35)$$

The payoff function for vanilla options is given in (2.2). We assume that the characteristic function of the  $\log(S(t)/K)$  price process is available and therefore we need to represent the payoff also as a function of  $\log(S(t)/K)$  instead of  $S(t)$ . The state variables  $x$  and  $y$  of the  $\log(S(t)/K)$  price process are defined as follows:

$$x := \log(S(0)/K), \quad \text{and} \quad y := \log(S(T)/K). \quad (2.36)$$

The payoff function represented as a function of  $\log(S(t)/K)$  is given by

$$g(T, y) \equiv \begin{cases} \max\{Ke^y - K, 0\}, & \text{for a call,} \\ \max\{K - Ke^y, 0\}, & \text{for a put.} \end{cases} \quad (2.37)$$

The coefficients  $V_k$  become

$$V_k = \begin{cases} \frac{2}{b-a} \int_0^b K (e^y - 1) \cos\left(k\pi \frac{y-a}{b-a}\right) dy, & \text{for a call} \\ \frac{2}{b-a} \int_a^0 K (1 - e^y) \cos\left(k\pi \frac{y-a}{b-a}\right) dy, & \text{for a put} \end{cases} \quad (2.38)$$

When we now use Result 3.1 from [10] which defines,

$$\chi_k(c, d) := \int_c^d e^y \cos\left(k\pi \frac{y-a}{b-a}\right) dy \quad (2.39)$$

$$= \frac{1}{1 + \left(\frac{k\pi}{b-a}\right)^2} \left[ \cos\left(k\pi \frac{d-a}{b-a}\right) e^d - \cos\left(k\pi \frac{c-a}{b-a}\right) e^c \right. \\ \left. + \frac{k\pi}{b-a} \sin\left(k\pi \frac{d-a}{b-a}\right) e^d - \frac{k\pi}{b-a} \sin\left(k\pi \frac{c-a}{b-a}\right) e^c \right], \quad (2.40)$$

and,

$$\psi_k(c, d) := \int_c^d \cos\left(k\pi \frac{y-a}{b-a}\right) dy \quad (2.41)$$

$$= \begin{cases} \left[ \sin\left(k\pi \frac{d-a}{b-a}\right) - \sin\left(k\pi \frac{c-a}{b-a}\right) \right] \frac{b-a}{k\pi}, & k \neq 0, \\ (d-c), & k = 0, \end{cases} \quad (2.42)$$

the coefficients  $V_k$  for the vanilla options are given by,

$$V_k^{call} = \frac{2}{b-a} K (\chi_k(0, b) - \psi_k(0, b)), \quad (2.43)$$

and,

$$V_k^{put} = \frac{2}{b-a} K (-\chi_k(a, 0) + \psi_k(a, 0)). \quad (2.44)$$

## 2.6.2 Multiple strike prices

For the special case of processes for which the characteristic function can be written in the form of (2.16), including the exponential Lévy processes, the valuation formula can handle multiple strike prices simultaneously. The valuation formula for multiple strikes is given by,

$$v(\mathbf{x}, t_0) \approx \mathbf{K} e^{-r\Delta t} \cdot \Re \left\{ \sum_{k=0}^{N-1} \varphi \left( \frac{k\pi}{b-a} \right) U_k \cdot e^{-ik\pi \frac{\beta\mathbf{x}-a}{b-a}} \right\}. \quad (2.45)$$

where  $\varphi \left( \frac{k\pi}{b-a} \right) := \phi \left( \frac{k\pi}{b-a}; 0 \right)$  and,

$$U_k = \begin{cases} \frac{2}{b-a} (\chi_k(0, b) - \psi_k(0, b)) & \text{for a call,} \\ \frac{2}{b-a} (-\chi_k(a, 0) + \psi_k(a, 0)) & \text{for a put.} \end{cases} \quad (2.46)$$

Here  $\mathbf{K}$  is a vector of strike prices  $K_i$  and therefore  $\mathbf{x}$  is also a vector, with elements  $\log(S_0/K_i)$ . For a full derivation we refer to the paper [10].

## 2.7 COS method for Bermudan options

This section contains the contents of the paper [11]. Here we briefly repeat the most important results. For an extensive derivation of the concepts and an error analysis we refer to the aforementioned paper.

The COS method for Bermudan options uses the same idea as the COS method for European options, but now the COS method is used to approximate the continuation values  $c(t_{m-1}, S(t_{m-1}))$  in the dynamic programming formulation of (2.5). Defining  $x$  to be the state of the asset price process at time  $t_{m-1}$  and  $y$  the state of the asset price process at time  $t_m$  we have

$$c(t_{m-1}, x) = e^{-r\Delta t} \mathbb{E}_{\mathbb{Q}}[v(t_m, y) | \mathcal{F}_{t_{m-1}}], \quad \text{for } m = M, \dots, 1 \quad (2.47)$$

Recalling that for the European options we had

$$v(t_0, x) = e^{-r\Delta t} \mathbb{E}_{\mathbb{Q}}[v(T, y) | \mathcal{F}_{t_0}], \quad (2.48)$$

we can immediately use the COS formula for pricing European options in (2.32), with the only remark that the coefficients  $V_k$ , defined by

$$V_k(t_m) := \frac{2}{b-a} \int_a^b v(t_m, y) \cos \left( k\pi \frac{y-a}{b-a} \right) dy, \quad (2.49)$$

depend on  $t_m$ .

Therefore the COS formula for the approximation of the continuation value  $\hat{c}(x, t_{m-1})$  for general underlying processes is given by

$$\hat{c}(t_{m-1}, x) := e^{-r\Delta t} \sum_{k=0}^{N-1} \Re \left\{ \phi \left( \frac{k\pi}{b-a}; x \right) e^{-ik\pi \frac{a}{b-a}} \right\} V_k(t_m). \quad (2.50)$$

Since from the dynamic programming formulation in (2.5) it follows that the option value at  $t_0$  is equal to the continuation value at  $t_0$ , an approximation of the option value at  $t_0$  is given by

$$v(t_0, x) \approx \hat{c}(t_0, x) = e^{-r\Delta t} \sum_{k=0}^{N-1} \Re \left\{ \phi \left( \frac{k\pi}{b-a}; x \right) e^{-ik\pi \frac{a}{b-a}} \right\} V_k(t_1). \quad (2.51)$$

So if we can recover the coefficients  $V_k(t_1)$ , we can approximate the option value at  $t_0$ . The authors of the paper [11] showed that the Fourier-cosine series coefficients  $V_k(t_m)$ ,  $k = 0, \dots, N-1$ , can be recovered from the coefficients  $V_j(t_{m+1})$ ,  $j = 0, \dots, N-1$ .

### 2.7.1 Recovering the coefficients $V_k(t_m)$

We first define

$$G_k(x_1, x_2) := \frac{2}{b-a} \int_{x_1}^{x_2} g(t_m, y) \cos\left(k\pi \frac{y-a}{b-a}\right) dy \quad (2.52)$$

to be the Fourier cosine series coefficients of the payoff function and

$$C_k(x_1, x_2, t_m) := \frac{2}{b-a} \int_{x_1}^{x_2} c(t_m, y) \cos\left(k\pi \frac{y-a}{b-a}\right) dy \quad (2.53)$$

to be the Fourier cosine series coefficients of the continuation value function.

The coefficients  $V_k(t_m)$  can be recovered in a backward manner. At time  $t_M$  the option value equals the payoff and the coefficients depend just on the payoff function. (actually they are the same as the coefficients derived in Paragraph 2.6.1)

$$V_k(t_M) = \begin{cases} G_k(0, b), & \text{for a call,} \\ G_k(a, 0), & \text{for a put,} \end{cases} \quad (2.54)$$

At all time points  $t_m$ , where  $m < M$ , the option value  $v(t_m, y)$  equals the maximum of the continuation value and the payoff:

$$v(t_m, y) = \max\{c(t_m, y), g(t_m, y)\}. \quad (2.55)$$

If there is a point  $x_m^*$  where the continuation value equals the payoff such that  $c(t_m, x_m^*) = g(t_m, x_m^*)$ , we call this point the early exercise point at time  $t_m$ . For now we assume that there exists an  $x_m^* \in [a, b]$ .

For a put option it holds that on the interval  $[a, x_m^*]$  the continuation value is less or equal than the payoff:  $c(t_m, y) \leq g(t_m, y)$ . On the interval  $[x_m^*, b]$  the continuation value is greater or equal than the payoff:  $c(t_m, y) \geq g(t_m, y)$ . Therefore we can split the integral in definition (2.49) of the option value coefficients at time  $t_m$  into two parts:

$$V_k(t_m) = \frac{2}{b-a} \int_a^b v(t_m, y) \cos\left(k\pi \frac{y-a}{b-a}\right) dy \quad (2.56)$$

$$= \frac{2}{b-a} \int_a^b \max\{g(t_m, y), c(t_m, y)\} \cos\left(k\pi \frac{y-a}{b-a}\right) dy \quad (2.57)$$

$$= \frac{2}{b-a} \int_a^{x_m^*} g(t_m, y) \cos\left(k\pi \frac{y-a}{b-a}\right) dy + \frac{2}{b-a} \int_{x_m^*}^b c(t_m, y) \cos\left(k\pi \frac{y-a}{b-a}\right) dy \quad (2.58)$$

$$= G_k(a, x_m^*) + C_k(x_m^*, b, t_m) \quad (2.59)$$

The same can be done for a call option if there is an early exercise point. Then on the interval  $[a, x_m^*]$  we have  $c(t_m, y) \geq g(t_m, y)$  and on the interval  $[x_m^*, b]$  we have  $c(t_m, y) \leq g(t_m, y)$ . Then the coefficients  $V_k(t_m)$  are given by:  $V_k(t_m) = C_k(a, x_m^*, t_m) + G_k(x_m^*, b)$ .

So for  $m = M-1, \dots, 1$  we have

$$V_k(t_m) = \begin{cases} C_k(a, x_m^*, t_m) + G_k(x_m^*, b), & \text{for a call,} \\ G_k(a, x_m^*) + C_k(x_m^*, b, t_m), & \text{for a put,} \end{cases} \quad (2.60)$$

In total,  $M-1$  early exercise points need to be determined, one for every exercise date  $t_1, \dots, t_{M-1}$ . Since the derivatives of  $\hat{c}(t_m, y)$  and  $g(t_m, y)$  can be derived easily, Newton's method can be used to determine these early exercise points at each time step.

To visually support the idea of splitting the integral in the definition of  $V_k(t_m)$ , in Figure 2.2 we show the contributions of  $G_k(a, x_m^*)$  and  $C_k(x_m^*, b, t_m)$  at time  $t_{M-1}$  for a certain put option. Figure 2.3 shows

in addition the 2 subsequent early exercise points.

Now it remains to determine the payoff coefficients  $G_k(x_1, x_2)$  and the continuation value coefficients  $C_k(x_1, x_2, t_m)$ .

Using the payoff function from (2.37) and the analytical expressions from (2.39) and (2.41) the coefficients  $G_k(x_1, x_2)$  can be determined analytically and for a put with  $x_2 \leq 0$  and a call with  $x_1 \geq 0$  we get

$$G_k(x_1, x_2) = \begin{cases} \frac{2}{b-a} K(\chi_k(x_1, x_2) - \psi_k(x_1, x_2)) & \text{for a call,} \\ \frac{2}{b-a} K(-\chi_k(x_1, x_2) + \psi_k(x_1, x_2)) & \text{for a put.} \end{cases} \quad (2.61)$$

Since in (2.60) we need to determine  $G_k(x_m^*, b)$  for a call and  $G_k(a, x_m^*)$  for a put and for a call  $x_m^* \leq 0$  and for a put  $x_m^* \geq 0$ , we can use the analytical expressions in (2.61).

For the coefficients  $C_k(x_1, x_2, t_m)$  we make use of the COS formula in (2.50). This approximation of the continuation value is inserted into (2.53) such that we get

$$\begin{aligned} \hat{C}_k(x_1, x_2, t_{M-1}) &= \frac{2}{b-a} \int_{x_1}^{x_2} \hat{c}(t_{M-1}, y) \cos\left(k\pi \frac{y-a}{b-a}\right) dy \\ &= \frac{2}{b-a} \int_{x_1}^{x_2} e^{-r\Delta t} \sum_{j=0}^{N-1} \Re \left\{ \phi\left(\frac{j\pi}{b-a}; y\right) e^{-ij\pi \frac{y-a}{b-a}} \right\} V_j(t_{M-1}) \cdot \cos\left(k\pi \frac{y-a}{b-a}\right) dy. \end{aligned} \quad (2.62)$$

$$(2.63)$$

Assuming that the characteristic function can be written in the form as introduced in (2.16), we can interchange summation and integration and take  $\varphi\left(\frac{j\pi}{b-a}\right)$  out of the integral.

$$\hat{C}_k(x_1, x_2, t_{M-1}) = e^{-r\Delta t} \sum_{j=0}^{N-1} \Re \left\{ \varphi\left(\frac{j\pi}{b-a}\right) V_j(t_{M-1}) \cdot \frac{2}{b-a} \int_{x_1}^{x_2} e^{-ij\pi \frac{y-a}{b-a}} \cos\left(k\pi \frac{y-a}{b-a}\right) dy \right\}. \quad (2.64)$$

Now we define

$$\mathcal{M}_{k,j}(x_1, x_2) := \frac{2}{b-a} \int_{x_1}^{x_2} e^{-ij\pi \frac{y-a}{b-a}} \cos\left(k\pi \frac{y-a}{b-a}\right) dy, \quad (2.65)$$

such that we can write

$$\hat{C}_k(x_1, x_2, t_{M-1}) = e^{-r\Delta t} \sum_{j=0}^{N-1} \Re \left\{ \varphi\left(\frac{j\pi}{b-a}\right) V_j(t_{M-1}) \cdot \mathcal{M}_{k,j}(x_1, x_2) \right\}. \quad (2.66)$$

now in turn can be recovered efficiently with an algorithm that makes use of the fast Fourier transform. This algorithm is not explained in detail here, but we refer to [11] and [3], where this efficient algorithm is explained in detail. For the remaining of this work, if we refer to the FFT-based algorithm, it is this algorithm we refer to.

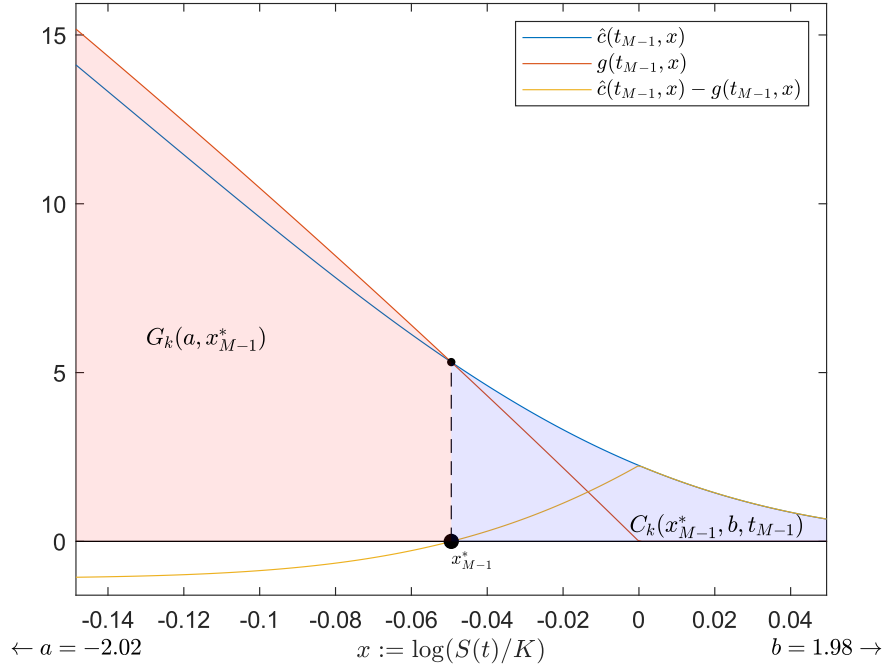


Figure 2.2: The contribution of  $G_k(a, x_{M-1}^*)$  (in red) and  $C_k(x_{M-1}^*, b, t_{M-1})$  (in blue) to the integral of the option value coefficients  $V_k(t_{M-1})$ . The point  $x_{M-1}^*$  is also shown, this is the point where the payoff function  $g(x, t_{M-1})$  equals the approximated continuation value function  $\hat{c}(t_{M-1}, x)$ . The figure is zoomed in on  $x_{M-1}^*$ , for the specific problem the integration range is  $[a, b] = [-2.02, 1.98]$ .

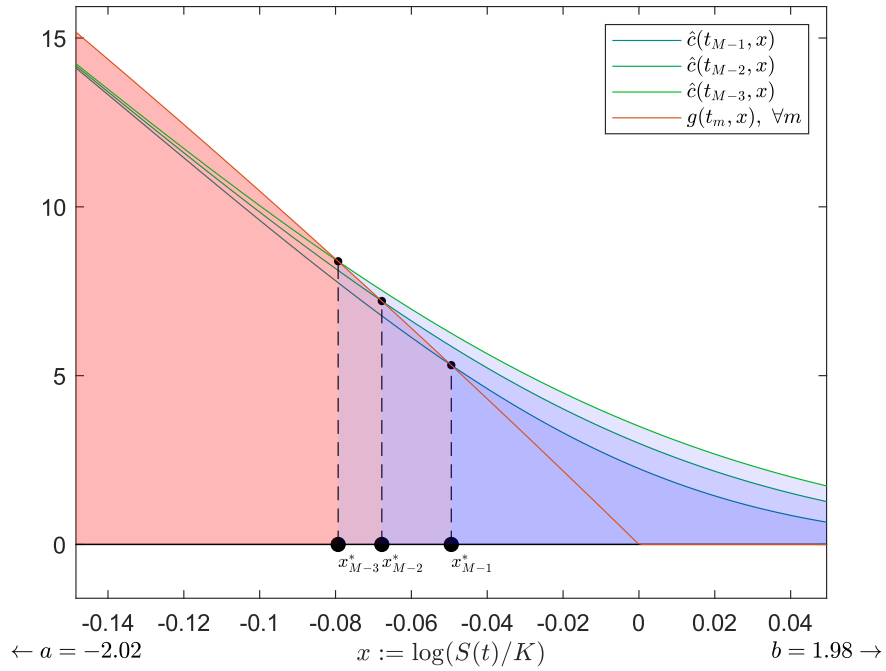


Figure 2.3: For  $t_{M-1}, t_{M-2}$  and  $t_{M-3}$  the early exercise points are shown. This figure shows the evolution of the approximated continuation value function back in time. The figure is zoomed in on  $x_{M-1}^*$ , for the specific problem the integration range is  $[a, b] = [-2.02, 1.98]$ .

## 2.8 An approximation method for the characteristic function: Adjoint expansion

In this section we follow the so-called adjoint expansion method, introduced in the paper [22]. This method can be used to approximate the characteristic function of local Lévy models for which a characteristic function is unknown. Here we propose this method to approximate the characteristic function of the Ornstein-Uhlenbeck process, such that it can be written in the form

$$e^{i\omega x} \sum_{k=0}^n (x - \bar{x})^k g_{n,k}(t, T, \omega), \quad (2.67)$$

where the coefficients  $g_{n,k}$  do not depend on  $x$ . In [3] the authors showed that if the characteristic function can be written in this form, then the FFT algorithm can be used to calculate the continuation values. We will follow approximately the same notation and we apply the method to our specific problem.

Suppose the dynamics for the log-price process  $X_t = \log(S_t)$  are given by

$$dX_t = \mu(t, X_t) dt + \sigma(t, X_t) dW_t. \quad (2.68)$$

The price of a European option with payoff  $h(S_T)$  is given by

$$v(t, X_t) = \mathbb{E}[\phi(X_T) | \mathcal{F}_t], \quad (2.69)$$

where  $\phi(x) = h(e^x)$ . Now by the Feynman-Kac formula,  $v$  can be expressed as the solution to the following Cauchy problem

$$\begin{cases} Lu(t, x) = 0, & t \in [0, T), x \in \mathbb{R} \\ u(T, x) = \phi(x), & x \in \mathbb{R}, \end{cases} \quad (2.70)$$

where  $L$  is the integro-differential operator

$$Lu(t, x) = \partial_t u(t, x) + \mu(t, x) \partial_x u(t, x) + \frac{\sigma^2(t, x)}{2} \partial_{xx} u(t, x). \quad (2.71)$$

The expectation in (2.69) can be written as an integral with respect to the transition distribution of  $y$  at time  $T$  given  $x$  at time  $t < T$ , which we shall denote here as  $\Gamma(t, x; T, y)$

$$v(t, x) = \int_{-\infty}^{\infty} \phi(y) \Gamma(t, x; T, y) dy. \quad (2.72)$$

Now the corresponding characteristic function of the log-price process is given by the Fourier transform of this transition distribution (in the sequel we denote taking the Fourier transform on a function with a hat)

$$\hat{\Gamma}(t, x; T, y) = \int_{-\infty}^{\infty} e^{i\omega y} \Gamma(t, x; T, y) dy. \quad (2.73)$$

### 2.8.1 Adjoint expansion for the Ornstein-Uhlenbeck process

Because for the Ornstein-Uhlenbeck process we have  $\mu(t, x) = \kappa(\theta - x)$  and  $\sigma(t, x) = \sigma$  is a constant, we Taylor expand the coefficients  $\mu(t, x)$  around some point  $\bar{x}$  up to first order with

$$\mu_0 = \kappa(\theta - \bar{x}), \quad (2.74)$$

$$\mu_1 = -\kappa. \quad (2.75)$$

We use this to approximate the integro-differential operator  $L$  and the first order approximation of  $L$  in (2.71) is given by

$$L_1 = L_0 + (x - \bar{x}) \mu_1 \partial_x, \quad (2.76)$$

where

$$L_0 = \partial_t + \mu_0 \partial_x + \frac{1}{2} \sigma^2 \partial_{xx}. \quad (2.77)$$

For the process under consideration higher order approximations are not possible because the higher order derivatives of  $\mu(t, x)$  with respect to  $x$  are equal to 0.

Now it comes down to solve two Cauchy problems

$$\begin{cases} L_0 G^0(t, x; T, y) = 0, & t \in [0, T], x \in \mathbb{R} \\ G^0(T, x; T, y) = \delta_y(x). \end{cases} \quad (2.78)$$

and

$$\begin{cases} L_0 G^1(t, x; T, y) = -(L_1 - L_0)G^0(t, x; T, y), & t \in [0, T], x \in \mathbb{R} \\ G^1(t, x; T, y) = 0, & x \in \mathbb{R}. \end{cases} \quad (2.79)$$

Since  $L_1 - L_0 = (x - \bar{x})\mu_1 \partial_x$ , this results in

$$\begin{cases} L_0 u^1(t, x) = -(x - \bar{x})\mu_1 \partial_x u^0(t, x), & t \in [0, T], x \in \mathbb{R} \\ u^1(T, x) = 0, & x \in \mathbb{R}. \end{cases} \quad (2.80)$$

Now the first order approximation of  $\Gamma(t, x; T, y)$  is defined as

$$\Gamma^{(1)}(t, x; T, y) = G^0(t, x; T, y) + G^1(t, x; T, y) \quad (2.81)$$

and correspondingly

$$\hat{\Gamma}^{(1)}(t, x; T, y) = \hat{G}^0(t, x; T, y) + \hat{G}^1(t, x; T, y) \quad (2.82)$$

Now, because the operator  $L$  acts on  $x$  and the characteristic function is a Fourier transform with respect to  $y$ , we need to use the adjoint operator  $\tilde{L}$  of  $L$ , which acts on  $y$ . For our problem, the adjoint operators  $\tilde{L}_0$  and  $\tilde{L}_1$  are given by:

$$\tilde{L}_0 = -\partial_T - \mu_0 \partial_y + \frac{1}{2} \sigma^2 \partial_{yy}, \quad (2.83)$$

and

$$\tilde{L}_1 - \tilde{L}_0 = -(y - \bar{y})\mu_1 \partial_y. \quad (2.84)$$

$L$  can be seen as the Kolmogorov forward operator, while  $\tilde{L}$  can be seen as the Kolmogorov backward operator. The adjoint (dual) Cauchy problems are formulated as follows:

$$\begin{cases} \tilde{L}_0 G^0(t, x; T, y) = 0, & T > t, y \in \mathbb{R} \\ G^0(t, x; t, y) = \delta_x(y). \end{cases} \quad (2.85)$$

and

$$\begin{cases} \tilde{L}_0 G^1(t, x; T, y) = -(\tilde{L}_1 - \tilde{L}_0)G^0(t, x; T, y), & T > t, y \in \mathbb{R} \\ G^1(t, x; t, y) = 0, & y \in \mathbb{R}. \end{cases} \quad (2.86)$$

To obtain the characteristic function these dual Cauchy problems can be solved directly in Fourier space, by taking the Fourier transform with respect to  $y$ . For (2.85) this results in the ordinary differential equation

$$\begin{cases} \partial_T \hat{G}^0(t, x; T, \omega) = \psi(\omega) G^0(t, x; T, \omega) & T > t \\ \hat{G}^0(t, x; t, \omega) = e^{i\omega x}, \end{cases} \quad (2.87)$$

where

$$\psi(\omega) = \mu_0 i\omega - \frac{1}{2}\sigma^2\omega^2 = i\kappa(\theta - \bar{x})\omega - \frac{1}{2}\sigma^2\omega^2. \quad (2.88)$$

which can be easily solved and has solution

$$\hat{G}^0(t, x, T, \omega) = e^{i\omega x + (T-t)\psi(\omega)}. \quad (2.89)$$

For (2.86) this results in the ordinary differential equation

$$\begin{cases} \partial_T \hat{G}^1(t, x; T, \omega) = \psi(\omega) \hat{G}^0(t, x; T, \omega) + \mu_1 i\omega (i\partial_\omega + \bar{x}) \hat{G}^0(t, x; T, \omega), & T > t \\ \hat{G}^1(t, x; t, \omega) = 0, \end{cases} \quad (2.90)$$

for which the solution is given by

$$\hat{G}^1(t, x; T, \omega) = - \int_t^T e^{\psi(\omega)(T-s)} \mu_1 i\omega (i\partial_\omega + \bar{x}) \hat{G}^0(t, x; s, \omega) ds, \quad (2.91)$$

$$= - \int_t^T e^{\psi(\omega)(T-s)} \mu_1 i\omega (i\partial_\omega + \bar{x}) e^{i\omega x + (s-t)\psi(\omega)} ds. \quad (2.92)$$

Now using

$$\partial_\omega (e^{i\omega x + (s-t)\psi(\omega)}) = e^{i\omega x + (s-t)\psi(\omega)} (ix + (s-t)\psi'(\omega)), \quad (2.93)$$

and inserting this into the integral for  $\hat{G}^1(t, x; T, \omega)$  results in

$$\hat{G}^1(t, x; T, \omega) = e^{i\omega x + (T-t)\psi(\omega)} \mu_1 \int_t^T (\omega(ix + (s-t)\psi'(\omega)) - i\omega\bar{x}) ds, \quad (2.94)$$

$$= e^{i\omega x + (T-t)\psi(\omega)} \mu_1 \left( \frac{\omega}{2} (T-t)^2 \psi'(\omega) + i\omega(T-t)(x - \bar{x}) \right). \quad (2.95)$$

Now, recalling (2.82), the first-order approximation of the characteristic function is ultimately given by

$$\hat{\Gamma}(t, x; T, \omega) \approx \hat{\Gamma}^{(1)}(t, x; T, \omega) = G^0(t, x; T, \omega) + G^1(t, x; T, \omega), \quad (2.96)$$

$$= e^{i\omega x + (T-t)\psi(\omega)} + e^{i\omega x + (T-t)\psi(\omega)} \mu_1 \left( \frac{\omega}{2} (T-t)^2 \psi'(\omega) + i\omega(T-t)(x - \bar{x}) \right) \quad (2.97)$$

$$= e^{i\omega x + (T-t)\psi(\omega)} \left( 1 + \mu_1 \left( \frac{\omega}{2} (T-t)^2 \psi'(\omega) + i\omega(T-t)(x - \bar{x}) \right) \right) \quad (2.98)$$

For this specific case if we write the first order approximation in the form suggested in [3], we end up with the following:

$$\hat{\Gamma}^{(1)}(t, x; T, \omega) := e^{i\omega x + (T-t)\psi(\omega)} (\hat{F}^0(t, x; T, \omega) + \hat{F}^1(t, x; T, \omega)), \quad (2.99)$$

with

$$\hat{F}^0(\omega; x, \tau) = g_0^{(0)}(T-t, \omega), \quad (2.100)$$

$$\hat{F}^1(\omega; x, \tau) = g_0^{(1)}(T-t, \omega) + g_1^{(1)}(T-t, \omega)(x - \bar{x}), \quad (2.101)$$

and

$$g_0^{(0)}(s, \omega) = 1, \quad (2.102)$$

$$g_0^{(1)}(s, \omega) = \mu_1 s^2 \frac{\omega}{2} \psi'(\omega), \quad (2.103)$$

$$g_1^{(1)}(s, \omega) = \mu_1 s i\omega. \quad (2.104)$$

$$(2.105)$$

Because we chose to expand the coefficients around  $\bar{x} = x$ , the formula for our specific case simplifies to

$$\hat{\Gamma}^{(1)}(t, x; T, \omega) = e^{i\omega x + (T-t)\psi(\omega)} \left( 1 + \mu_1 (T-t)^2 \frac{\omega}{2} \psi'(\omega) \right), \quad (2.106)$$

$$= e^{i\omega x + (T-t)(\mu_0 i\omega - \frac{1}{2}\sigma^2\omega^2)} \left( 1 - \kappa(T-t)^2 \frac{\omega}{2} (\mu_0 i - \sigma^2\omega) \right), \quad (2.107)$$

$$= e^{i\omega x + (T-t)(\kappa(\theta - \bar{x})i\omega - \frac{1}{2}\sigma^2\omega^2)} \left( 1 - \kappa(T-t)^2 \frac{\omega}{2} (\kappa(\theta - \bar{x})i - \sigma^2\omega) \right). \quad (2.108)$$

## 2.9 Interval of integration $[a, b]$

We define the domain of integration as follows

$$[a, b] := \left[ \xi_1 - L\sqrt{\xi_2 + \sqrt{\xi_4}}, \quad \xi_1 + L\sqrt{\xi_2 + \sqrt{\xi_4}} \right], \quad \text{with } L = 10, \quad (2.109)$$

as proposed in [9]. Here  $\xi_n$  denotes the  $n$ -th cumulant of the process that is defined by the characteristic function  $\phi(\omega; x; T)$ . The cumulants can be computed with

$$\xi_n := \frac{1}{i^n} \frac{\partial^n (\log(\phi(\omega; x; T)))}{\partial \omega^n} \Big|_{\omega=0}. \quad (2.110)$$

Taking parameter  $L = 10$  seems an appropriate choice for all the experiments in this work. For a more extensive analysis of the choice of this parameter  $L$  and the influence on the error propagation in the case of a Bermudan option we refer to the paper [11].

In theory a larger domain of integration should result in more accurate approximations of the option values. But when the domain of integration becomes larger, in general more terms need to be taken into the cosine series summation to reach the same level of accuracy.

## Chapter 3

# Extended COS method and Least Squares Monte Carlo

### 3.1 Options with multiple early exercise rights

In this section we will extend the framework for valuing a Bermudan option, which can be exercised once before its expiration date, to options that can be exercised multiple times before their expiration date. Since an option gives the holder the right to buy or sell the underlying asset at the strike price  $K$ , we call the number of times that an option can be exercised the number of rights, which we denote by  $R$ . So for a Bermudan option we have  $R = 1$ . It is only possible to exercise the option once at a single exercise date. We cannot have more rights than exercise dates, so we have  $R \leq M$ . We define  $\mathcal{R} := \{1, \dots, R\}$  to be the set of all possible numbers of rights left, which we will also call levels of rights left. The time lattice is the same as for the Bermudan option, see Figure 2.1, so the exercise dates are at discrete time points.

In the paper [29], the authors already considered the valuation of swing options with the COS method. They modelled the valuation of swing options with a continuous time model. In their model swing actions could be exercised at any time before expiry and a recovery time between subsequent swing actions is included. This method however is more complex than our setting, since we only consider discrete exercise points.

In the framework of options with multiple early exercise rights, the notation has to be extended. To denote the value of an option with  $j$  rights left, we introduce the superscript  $j$ . So  $v^j(t_m, S(t_m))$  denotes the value of the option with  $j$  rights left at time  $t_m$  when the spot price is  $S(t_m)$ . The most important thing that we need to describe is the connection between the number of rights left. To illustrate this: if we have 3 rights left and decide to exercise 1 right, we end up at the level of 2 rights left.

We introduce a simple example to get an idea how to handle multiple early exercise rights with the COS method. Suppose we have an option with only three exercise dates,  $0 = t_0 < t_1 < t_2 < t_3 = T$  and the number of rights  $R = 2$ . A schematic representation of this example is given in Figure 3.1. For this schematic representation the following notation is defined:  $PO_m := g(t_m, S(t_m))$ ,  $CV_m^j := c^j(t_m, S(t_m))$  and  $V_m^j := v^j(t_m, S(t_m))$ , where  $g$  is the payoff,  $c^j$  the continuation value for the level of  $j$  rights left and  $v^j$  the option value for the level of  $j$  rights left, all as functions of  $t_m$  and  $S(t_m)$ .

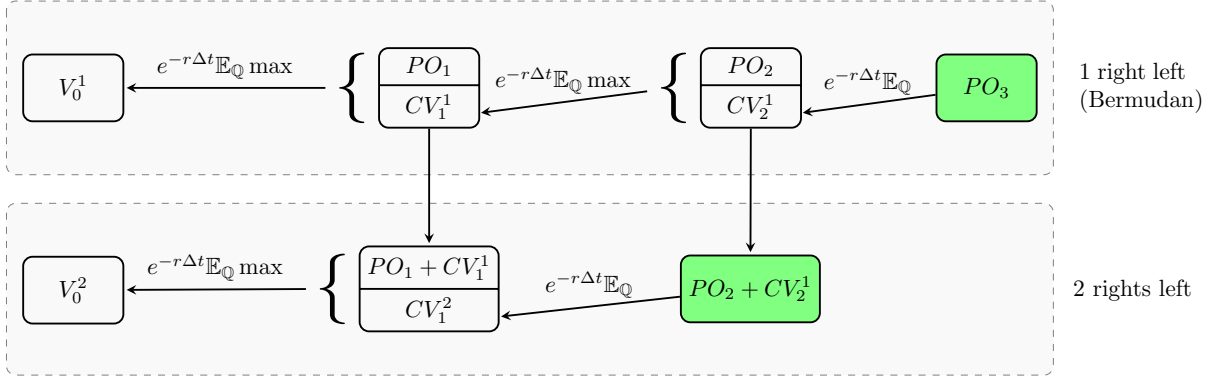


Figure 3.1: Schematic overview of the recursive scheme that is used in the example problem. The green nodes denote the initialization for each level of rights left.

In Section 2.7 the COS method for the level of one right left (Bermudan option) was already introduced and the continuation value  $c^1(t_2, S(t_2))$  can be computed with the risk-neutral valuation formula

$$c^1(t_2, S(t_2)) = e^{-r\Delta t} \mathbb{E}_Q[v^1(t_3, S(t_3)) | \mathcal{F}_{t_2}] \quad (3.1)$$

$$= e^{-r\Delta t} \mathbb{E}_Q[g(t_3, S(t_3)) | \mathcal{F}_{t_2}]. \quad (3.2)$$

For the level of two rights left we can do almost the same, but the difference is that the first continuation value is only calculated at time  $t_{M-1}$ . The continuation value  $c^2(t_1, S(t_1))$  can be computed with the risk-neutral valuation formula

$$c^2(t_1, S(t_1)) = e^{-r\Delta t} \mathbb{E}_Q[v^2(t_2, S(t_2)) | \mathcal{F}_{t_1}]. \quad (3.3)$$

The value of the option with two rights left one time step before maturity,  $v^2(t_2, S(t_2))$ , is equal to the payoff at time  $t_2$  plus the expected payoff at time  $t_3$  discounted to time  $t_2$ . This is because there are still two rights left and there are only two remaining exercise dates. Now we use (3.2) to see that the expected payoff at time  $t_3$  discounted to time  $t_2$  is equal to the continuation value of the option at time  $t_2$  with one right less. Putting that into equation (3.3) we get

$$c^2(t_1, S(t_1)) = e^{-r\Delta t} \mathbb{E}_Q[g(t_2, S(t_2)) + c^1(t_2, S(t_2)) | \mathcal{F}_{t_1}] \quad (3.4)$$

$$= e^{-r\Delta t} \mathbb{E}_Q[g(t_2, S(t_2)) | \mathcal{F}_{t_1}] + e^{-r\Delta t} \mathbb{E}_Q[c^1(t_2, S(t_2)) | \mathcal{F}_{t_1}] \quad (3.5)$$

$$= e^{-r\Delta t} \mathbb{E}_Q[g(t_2, S(t_2)) | \mathcal{F}_{t_1}] + e^{-r\Delta t} \mathbb{E}_Q[e^{-r\Delta t} \mathbb{E}_Q[g(t_3, S(t_3)) | \mathcal{F}_{t_2}] | \mathcal{F}_{t_1}] \quad (3.6)$$

$$= e^{-r\Delta t} \mathbb{E}_Q[g(t_2, S(t_2)) | \mathcal{F}_{t_1}] + e^{-r2\Delta t} \mathbb{E}_Q[g(t_3, S(t_3)) | \mathcal{F}_{t_1}], \quad (3.7)$$

where the first equality follows from the linearity of the expectation function, the second equality follows from (3.2) and the last equality follows from the tower rule. It can be seen that the first continuation value for the level of two rights left that is approximated at  $t_1$  is built up out of the two expected future payoffs discounted to  $t_1$ .

By applying this tower rule repetitively, the value of the option with  $j$  rights left at time  $t_{M-j+1}$  can be expressed as the payoff at time  $t_{M-j+1}$  plus the continuation value of the option with one right less at time  $t_{M-j+1}$

$$v^j(t_{M-j+1}, S(t_{M-j+1})) = g(t_{M-j+1}, S(t_{M-j+1})) + c^{j-1}(t_{M-j+1}, S(t_{M-j+1})) \quad \forall j \in \mathcal{R} \quad (3.8)$$

where we define the continuation value for the option with zero rights left as  $c^0(t_m, S(t_m)) = 0$  for all  $m$ . We call this the initialization for every level of rights left.

On the exercise dates before the initialization  $t_{m-1}$ ,  $m = M - j + 1, \dots, 2$  for every level of  $j$  rights left we have to decide on the following

- If we exercise the option we receive the payoff  $g(t_{m-1}, S(t_{m-1}))$  and continue with the option with one right less  $c^{j-1}(t_{m-1}, S(t_{m-1}))$ .

- If we do not exercise the option we do not receive the payoff and continue with the option with the same number of rights left  $c^j(t_{m-1}, S(t_{m-1}))$ .

The decision we should take at time  $t_{m-1}$  is the decision which results in the highest value of the option at time  $t_{m-1}$ . The value of the option with  $j$  rights left at time  $t_{m-1}$  is given by:

$$v^j(t_{m-1}, S(t_{m-1})) = \max\{c^j(t_{m-1}, S(t_{m-1})), c^{j-1}(t_{m-1}, S(t_{m-1})) + g(t_{m-1}, S(t_{m-1}))\}.$$

The continuation values  $c^j(t_{m-1}, S(t_{m-1}))$  can be computed with the risk-neutral valuation formula

$$c^j(t_{m-1}, S(t_{m-1})) = e^{-r\Delta t} \mathbb{E}_{\mathbb{Q}}[v^j(t_m, S(t_m)) | \mathcal{F}_{t_{m-1}}], \quad \forall j \in \mathcal{R}. \quad (3.9)$$

Now we have all the ingredients to calculate the continuation values backwards in time. Since the option can not be exercised at  $t_0$ , the option value at  $t_0$  equals the continuation value at  $t_0$ . Summarizing, we have the following dynamic programming problem:

### The dynamic programming formulation

$$\begin{cases} c^0(t_m, S(t_m)) & = 0 \quad \forall m \\ v^j(t_{M-j+1}, S(t_{M-j+1})) & = g(t_{M-j+1}, S(t_{M-j+1})) + c^{j-1}(t_{M-j+1}, S(t_{M-j+1})) \quad \forall j \in \mathcal{R} \\ c^j(t_{m-1}, S(t_{m-1})) & = e^{-r\Delta t} \mathbb{E}_{\mathbb{Q}}[v^j(t_m, S(t_m)) | \mathcal{F}_{t_{m-1}}] \quad \forall j \in \mathcal{R}, \text{ for } m = M, \dots, 1 \\ v^j(t_{m-1}, S(t_{m-1})) & = \max\{c^j(t_{m-1}, S(t_{m-1})), c^{j-1}(t_{m-1}, S(t_{m-1})) + g(t_{m-1}, S(t_{m-1}))\}, \\ & \quad \forall j \in \mathcal{R}, \text{ for } m = M - j + 1, \dots, 2 \\ v^j(t_0, S(t_0)) & = c^j(t_0, S(t_0)) \quad \forall j \in \mathcal{R}. \end{cases} \quad (3.10)$$

#### 3.1.1 Recovering the coefficients $V_k^j(t_m)$

To approximate the continuation values for the option with  $j$  rights left, we can use COS formula (2.50) directly with as only difference the dependence on the level of rights left:

$$\tilde{c}^j(t_{m-1}, x) = e^{-r\Delta t} \sum_{k=0}^{N-1} \Re \left\{ \phi \left( \frac{k\pi}{b-a}; x \right) e^{-ik\pi \frac{a}{b-a}} \right\} V_k^j(t_m), \quad \forall j \in \mathcal{R}. \quad (3.11)$$

From the dynamic programming formulation in (3.10) it follows that for an option with  $R$  exercise rights

$$v^R(t_0, x) \approx \hat{c}^R(t_0, x) = e^{-r\Delta t} \sum_{k=0}^{N-1} \Re \left\{ \phi \left( \frac{k\pi}{b-a}; x \right) e^{-ik\pi \frac{a}{b-a}} \right\} V_k^R(t_1). \quad (3.12)$$

So if we can recover the coefficients  $V_k^R(t_1)$ , we can approximate the option value for an option with  $R$  exercise rights at  $t_0$ .

Below we describe how to recover the option value coefficients at time  $t_m$  for  $j$  rights left which are defined as

$$V_k^j(t_m) := \frac{2}{b-a} \int_a^b v^j(t_m, y) \cos \left( k\pi \frac{y-a}{b-a} \right) dy. \quad (3.13)$$

The initialization for the level of one right left is exactly the same as the initialization for the Bermudan option in Paragraph 2.7.1 and thus

$$V_k^1(t_M) = \begin{cases} G_k(0, b), & \text{for a call,} \\ G_k(a, 0), & \text{for a put.} \end{cases} \quad (3.14)$$

The novelty occurs in the initialization for the level of two rights left. The initialization for the level of two rights left is at time  $t_{M-1}$ . The option value coefficients are given by

$$V_k^2(t_{M-1}) = \frac{2}{b-a} \int_a^b v^2(t_{M-1}, y) \cos\left(k\pi \frac{y-a}{b-a}\right) dy \quad (3.15)$$

$$= \frac{2}{b-a} \int_a^b (g(t_{M-1}, y) + c^1(t_{M-1}, y)) \cos\left(k\pi \frac{y-a}{b-a}\right) dy \quad (3.16)$$

$$= \frac{2}{b-a} \int_a^b g(t_{M-1}, y) \cos\left(k\pi \frac{y-a}{b-a}\right) dy + \frac{2}{b-a} \int_a^b c^1(t_{M-1}, y) \cos\left(k\pi \frac{y-a}{b-a}\right) dy \quad (3.17)$$

$$= G_k(a, b) + C_k^1(a, b, t_{M-1}). \quad (3.18)$$

Here we note that for the vanilla options

$$G_k(a, b) = \begin{cases} G_k(0, b), & \text{for a call,} \\ G_k(a, 0), & \text{for a put.} \end{cases} \quad (3.19)$$

Generalizing this derivation to the level of  $j$  rights left, the initialization for the level of  $j$  rights left is at time  $t_{M-j+1}$  and is given by

$$V_k^j(t_{M-j+1}) = G_k(a, b) + C_k^{j-1}(a, b, t_{M-j+1}). \quad (3.20)$$

From the dynamic programming formulation (3.10) it follows that for all  $j \in \mathcal{R}$  and  $m = M - j, \dots, 1$

$$v^j(t_m, y) = \max\{c^j(t_m, y), c^{j-1}(t_m, y) + g(t_m, y)\}. \quad (3.21)$$

As we did for the Bermudan option, we assume that there exists a point  $x_m^{*j}$  for which  $c^j(t_m, x_m^{*j}) = c^{j-1}(t_m, x_m^{*j}) + g(t_m, x_m^{*j})$ . This point is called the early exercise point at time  $t_m$  for the level of  $j$  rights left.

For a put option it holds that  $c^j(t_m, y) \leq c^{j-1}(t_m, y) + g(t_m, y)$  on the interval  $[a, x_m^{*j}]$ . On the interval  $[x_m^{*j}, b]$  it holds that  $c^j(t_m, y) \geq c^{j-1}(t_m, y) + g(t_m, y)$ . Therefore we can split the integral in definition (3.13) of the option value coefficients at time  $t_m$  into two parts:

$$V_k^j(t_m) = \frac{2}{b-a} \int_a^b v^j(t_m, y) \cos\left(k\pi \frac{y-a}{b-a}\right) dy \quad (3.22)$$

$$= \frac{2}{b-a} \int_a^b \max\{c^j(t_m, y), g(t_m, y) + c^{j-1}(t_m, y)\} \cos\left(k\pi \frac{y-a}{b-a}\right) dy \quad (3.23)$$

$$= \frac{2}{b-a} \int_a^{x_m^{*j}} c^j(t_m, y) \cos\left(k\pi \frac{y-a}{b-a}\right) dy + \frac{2}{b-a} \int_{x_m^{*j}}^b (g(t_m, y) + c^{j-1}(t_m, y)) \cos\left(k\pi \frac{y-a}{b-a}\right) dy \quad (3.24)$$

$$= C_k^j(x_m^{*j}, b, t_m) + G_k(a, x_m^{*j}) + C_k^{j-1}(a, x_m^{*j}, t_m), \quad (3.25)$$

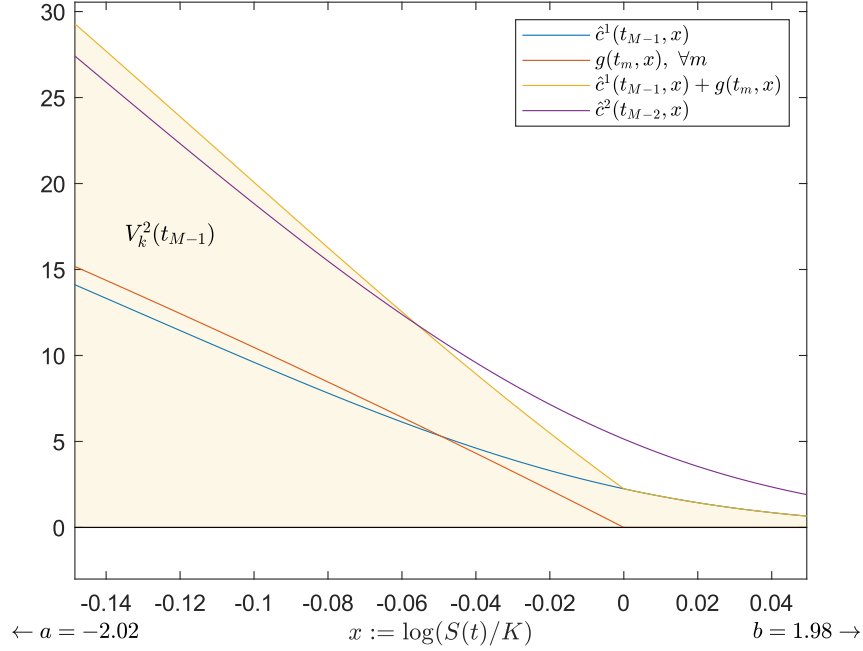


Figure 3.2: Integral of the option value coefficients  $V_k^2(t_{M-1})$ . The coefficients are the coefficients of the payoff function  $g(x, t_{M-1})$  plus the coefficients of the (estimated) continuation value function  $\hat{c}^1(x, t_{M-1})$ . Also the estimated continuation value function  $\hat{c}^2(x, t_{M-2})$  is shown, which is approximated with the coefficients  $V_k^2(t_{M-1})$ . The figure is zoomed in on  $x_{M-1}^*$ , for the specific problem the integration range is  $[a, b] = [-2.02, 1.98]$ .

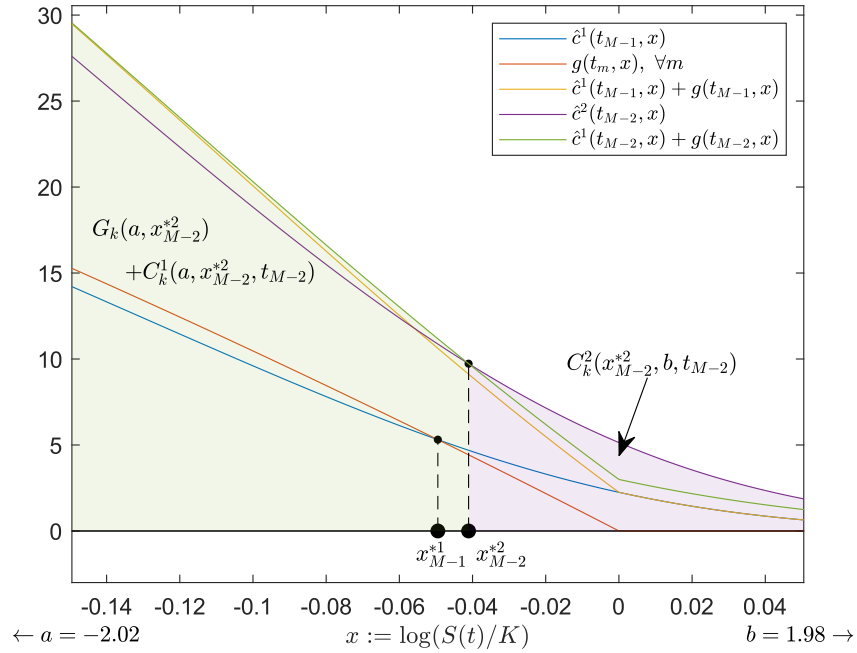


Figure 3.3: The contribution of  $G_k(a, x_{M-2}^{*2}) + C_k^1(a, x_{M-2}^{*2}, t_{M-2})$  (in green) and  $C_k^2(x_{M-2}^{*2}, b, t_{M-2})$  (in purple) to the integral of the option value coefficients  $V_k^2(t_{M-2})$ . The points  $x_{M-1}^*$  and  $x_{M-2}^{*2}$  are also shown.  $x_{M-2}^{*2}$  is the point where  $g(x, t_{M-2}) + \hat{c}^1(x, t_{M-2}) = \hat{c}^2(x, t_{M-2})$ . The figure is zoomed in on  $x_{M-1}^*$ , for the specific problem the integration range is  $[a, b] = [-2.02, 1.98]$ .

## 3.2 Least Squares Monte Carlo

As described in Section 2.2, the price of a Bermudan option can be found by solving the dynamic programming problem of (2.5). A good estimation of the continuation values is key in the valuation of Bermudan options and options with multiple early exercise rights. In Section 2.7 the COS method was introduced for estimating these continuation values. Another approach to estimate the continuation values is for example the Stochastic Grid Bundling Method (SGBM), which was introduced by the authors of [15]. Another popular method to estimate the continuation values of early exercise options is the method introduced by Longstaff and Schwartz [18]. This method makes use of a least squares regression to approximate the continuation values directly as a function of the spot price. Because this method is very intuitive we compare the results obtained with the COS method to the results obtained with this method. In the remainder of this work we write Least Squares Monte Carlo method, or LSMC, when referring to the method from Longstaff and Schwartz. In the subsequent sections we will first introduce the method for Bermudan options. After that, the method will be extended to price options with multiple early exercise rights. This extension was presented first by Dörr in [8]. Finally the method will be used to value gas storage contracts. Guideline here will be the paper by Boogert and De Jong [2] in which they used the LSMC method for the valuation of gas storage contracts.

As Longstaff and Schwartz mention in their paper, the key insight is that the continuation values can be estimated by using the, what they refer to as the, cross-sectional information in the simulated trajectories. To approximate the continuation values at time  $t_m$ , they regress the sum of realized future cash flows discounted to time  $t_m$  on basis functions of the spot price at time  $t_m$ .

The great advantage of the LSMC method is that it can be used in combination with a wide variety of models for the underlying spot price process. Once the trajectories of the spot price process are simulated, the algorithm can easily be applied. Before explaining the idea of the algorithm, we assume that the trajectories for the spot price are already simulated and the number of simulated trajectories is denoted by  $N$ .

### 3.2.1 LSMC for Bermudan options

In this section the attempt is to describe the LSMC method for Bermudan options in a clear way. We strongly recommend the illustrative example in the original paper by Longstaff and Schwartz [18] to support the readers understanding.

Before introducing the algorithm, for notational convenience we define  $PO_m^i := g(t_m, S^i(t_m))$  and  $CV_m^i := c(t_m, S^i(t_m))$ , where  $g$  is the payoff function and  $c$  the continuation value as function of  $t_m$  and  $S^i(t_m)$ . We also define  $CF_m^i$  to be the cash flow of trajectory  $i$  at time  $t_m$ .

As with the COS method, the algorithm is constructed in a backward manner. For every simulated trajectory of the spot price process the exercise strategy is determined individually. The option value at time  $t_0$  for an individual trajectory must be seen as the total value of all future cash flows discounted to  $t_0$  when the optimal exercise strategy is applied on a single realization of the spot price process. The ultimate option value is obtained by taking the average of these option values for all trajectories. The algorithm consists at every iteration of two stages:

- determining the function for estimating the continuation values as a function of the spot price,
- updating the exercise strategy and corresponding cash flows for the single trajectories.

In the subsequent part we will show how the information across the trajectories is used to approximate the continuation values and how the exercise strategies are updated for the single trajectories. The single trajectories of the spot price process are denoted by  $S^i, i = 1, \dots, N$ .

The algorithm starts with determining the cash flows at the final exercise date  $t_M$ . Since the option expires at this final exercise date, it is clear that the continuation value of the option is zero. So at  $t_M$  the value of the option depends only on the direct payoff. The cash flows for all trajectories are given by

$CF_m^i = \max\{0, PO_M^i\}$ . In the case of a negative payoff, the option is not exercised at all and the cash flow is zero. The exercise rule at  $t_M$  is straightforward: for every trajectory  $S^i$ , exercise the option if it is in the money.

In the next iteration the exercise date prior to the final exercise date is considered. At  $t_{M-1}$  there are two choices: to exercise the option or to not exercise the option. Of course a necessary condition for exercising the option is that it is in the money. But if it is in the money, should the holder exercise the option and collect a profit or should the holder wait until  $t_M$  and maybe even collect a bigger profit? This is where the continuation value comes into play. Recall the formula for the continuation value in the dynamic programming formulation (2.5):

$$c(t_{m-1}, S(t_{m-1})) = e^{-r\Delta t} \mathbb{E}_{\mathbb{Q}}[v(t_m, S(t_m)) | \mathcal{F}_{t_{m-1}}]. \quad (3.26)$$

Assuming that the above expectation function is unknown, the main idea is to approximate the continuation value at time  $t_{M-1}$  directly as a function of the spot price at time  $t_{M-1}$ .

In order to find a function that approximates the continuation value as a function of the spot price, a regression of the cash flows  $CF_M^i$ ,  $i = 1, \dots, N$ , discounted to time  $t_{M-1}$  is done on a finite set of  $P$  basis functions of the spot price values  $S^i(t_{M-1})$ ,  $i = 1, \dots, N$  at time  $t_{M-1}$ .

In this setting, the approximation of the continuation value for trajectory  $S^i$  is given by

$$CV_{M-1}^i \approx \sum_{p=1}^P a_p B_p(S^i(t_{M-1})), \quad \text{for all } i, \quad (3.27)$$

where  $B_p$ ,  $p = 1, \dots, P$  denote the basis functions as a function of  $S^i(t_{M-1})$ .

The goal is to find the coefficients  $a_p$ ,  $p = 1, \dots, P$  that fit the cross-sectional data best in a least squares sense. Finding these coefficients comes down to regress  $Y$  on  $X$ , where  $Y$  is a vector of length  $N$  such that  $Y^i = e^{-r\Delta t} CF_M^i$  and  $X$  is a vector of length  $N$  such that  $X^i = S^i(t_{M-1})$ .

For example, if the regression is done on a standard polynomial of degree 3 and if the coefficients  $a_p$ ,  $p = 1, \dots, 4$  are determined, the approximation of the continuation value for trajectory  $S^i$  at time  $t_{M-1}$  is given by:

$$CV_{M-1}^i \approx a_1 + a_2 S^i(t_{M-1}) + a_3 S^i(t_{M-1})^2 + a_4 S^i(t_{M-1})^3. \quad (3.28)$$

Once the continuation values at time  $t_{M-1}$  can be approximated for all trajectories  $S^i$ , the exercise strategy for the single trajectories can be updated. For time  $t_{M-1}$  the exercise rule is to exercise the option if and only if  $PO_{M-1}^i > CV_{M-1}^i$ . If the option is exercised, the cash flow at time  $t_{M-1}$  becomes  $CF_{M-1}^i = PO_{M-1}^i$ . Now it is important to notice that if for trajectory  $S^i$  the option is exercised at time  $t_{M-1}$ , the cash flow for trajectory  $S^i$  at time  $t_M$  is set to zero, because the option may be exercised only once.

This strategy is the generalized to all time steps prior to time  $t_{M-1}$ . For approximating the continuation values at times  $t_m$ ,  $m = M-2, \dots, 1$ , the regression is carried out on the sum of all future cash flows discounted to time  $t_m$  and the vector  $Y$  is given by

$$Y^i = DCF_m^i := \sum_{k>m} e^{-r(k-m)\Delta t} CF_k^i, \quad (3.29)$$

where  $DCF_m^i$  denote the sum of all future cash flows for trajectory  $S^i$  discounted to time  $t_m$ .

The exercise rule for trajectory  $S^i$  at time  $t_m$  becomes to exercise the option if and only if  $PO_m^i > CV_m^i$ . If the option is exercised, the cash flow at time  $t_m$  becomes  $CF_m^i = PO_m^i$ . Also here it is important to notice that if for trajectory  $S^i$  the option is exercised at time  $t_m$ , the cash flows for trajectory  $S^i$  at all times  $t_k$ , where  $k > m$ , are set to zero, because the option may be exercised only once.

Ultimately, when the exercise strategy is determined and the cash flows for every trajectory are known for all time steps  $t_m$ ,  $m = 1 \dots M$ , in order to determine the option value one has to discount the cash flows for every trajectory to time  $t_0$  and average over all trajectories. The LSMC approximation of the option value is given by

$$v(t_0, S(t_0)) \approx \frac{1}{N} \sum_{i=1}^N DCF_0^i. \quad (3.30)$$

For a pseudocode we refer to Algorithm 1 in Appendix A.1.

As explained, the LSMC method sums up the discounted future cash flows at every time step. Instead of discounting all future cash flows at every time step, it is also possible to keep track of all these future cash flows, which saves memory and computational time. This can be achieved by defining  $DCF_m^i$  as the maximum of the direct payoff and the continuation value at time  $t_{m+1}$ , discounted to time  $t_m$

$$DCF_m^i := e^{-r\Delta t} \max\{PO_{m+1}^i, CV_{m+1}^i\}, \quad (3.31)$$

where we used that the discounted future cash flows are already ‘contained’ in this continuation value. For a pseudocode that exploits this fact please see algorithm 2 in appendix A.1. We will call this algorithm the vectorized algorithm. In figure 3.4 an illustrative scheme of this variant of the LSMC method for a Bermudan option is given.

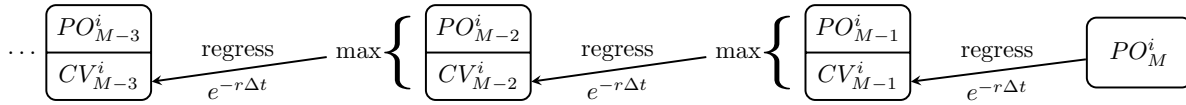


Figure 3.4: Schematic overview of the recursive scheme that is used in the LSMC algorithm for a single trajectory. From right to left we go back in time. The continuation value and payoff at time  $t_m$  are denoted by  $CV_m^i$  and  $PO_m^i$  respectively.

A pseudocode for the vectorized algorithm that is used to generate the results for the numerical experiments in Chapter 5 can be found in appendix A.1.

**Remark:** To increase the efficiency of the algorithm, Longstaff and Schwartz mention that in determining the continuation values at time  $t_m$  only trajectories that are in the money at time  $t_m$  ( $PO_m^i > 0$ ) should be used in the regression. This is because the continuation values are estimated better in the region where exercise is relevant and it also decreases the computational time needed for the regression.

### 3.2.2 LSMC for options with multiple early exercise rights

The idea of the LSMC method for options with multiple exercise rights is the same as the LSMC method for Bermudan options. Nevertheless, the method is a bit more involved, because it has to take care of the number of exercise rights left. For the extension of the LSMC algorithm for a Bermudan option to the algorithm for multiple exercise rights, we follow the extension of Dörr in [8] and the thesis of Olofsson [21]. In this section we do not contain specific examples of the method, but the authors strongly recommend the examples presented in these two theses for a better understanding.

The difference with the LSMC method for Bermudan options is that in the LSMC algorithm for options with multiple early exercise rights a regression is done to estimate the continuation values for every number of rights left. Therefore an extra dimension is added, which we call the dimension or level of exercise rights left. The algorithm has to update the cash flows for every level of exercise rights left up to  $R$ . In the remainder of this section we do only consider options where the number of rights  $R > 1$ , since the case  $R = 1$  is just a Bermudan option, which we already covered in Paragraph 3.2.1. We use the same notation as in that section, but now the superscript  $i, j$  is used instead of  $i$ , where  $j$  denotes the level of rights left.

Key is in the interconnection between the levels of exercise rights left. When exercising the option at a certain level of exercise rights left, the value of the option consists of the direct payoff plus the continuation value of the option with one exercise right less. Where in the algorithm for a Bermudan option in case of an exercise all future cash flows were set to zero, here the future cash flows are replaced by the future cash flows of the option with one exercise right less.

For every level of exercise rights left it is needed to approximate the continuation values. Not every iteration the continuation values need to be approximated for every level of exercise rights left. In the first iteration the continuation values for the level of one exercise right left at time  $t_{M-1}$  are approximated. At all levels with more exercise rights left we do not need to approximate the continuation values at time  $t_{M-1}$  since the exercise rule is to exercise if the option is in the money. This is due to the fact that when we are at time  $t_{M-1}$  and still have more than one exercise right left, it is always optimal to exercise if the option is in the money. In the second iteration the continuation values for the levels of one and two exercise rights left at time  $t_{M-2}$  are approximated. This causes that the first continuation value for the level of one right left (Bermudan option) that is approximated is the continuation value at time  $t_{M-1}$ . For the level of two rights left, the first continuation value that is approximated is at time  $t_{M-2}$ . In general, for the level of  $j$  rights left the first continuation value that is approximated is at time  $t_{M-j}$ .

Here we show how the algorithm works for the case  $R = 2$ . For every level of exercise rights left an initialization is done. For the level of one exercise right left the initialization is the same as for a Bermudan option and the first approximation of the continuation value is done at time  $t_{M-1}$ . For the level of two exercise rights left the initialization is to always exercise at  $t = t_M$  and  $t = t_{M-1}$  if the option is in the money. Not exercising a right makes no sense since the option expires at  $t_M$ . The cash flows for all trajectories are given by  $CF_{M-1}^{i,2} = \max\{0, PO_{M-1}^i\}$  and  $CF_M^{i,2} = \max\{0, PO_M^i\}$ . For the level of two exercise rights left the first approximation of the continuation value is done at time  $t_{M-2}$ . In order to find this approximation of the continuation value  $CV_{M-2}^{i,2}$  as a function of the spot price  $S_{M-2}^i$  at time  $t_{M-2}$ , the two future cash flows  $CF_{M-1}^{i,2}$  and  $CF_M^{i,2}$  are discounted to  $t_{M-2}$  and summed. Then the vector  $Y$  where is regressed on is given by

$$Y^i = DCF_{M-2}^{i,2} = e^{-r\Delta t}CF_{M-1}^{i,2} + e^{-r2\Delta t}CF_M^{i,2}. \quad (3.32)$$

Once the continuation values at time  $t_{M-2}$  can be approximated for all trajectories  $S^i$ , the exercise strategy for the single trajectories can be updated. The exercise rule at  $t_{M-2}$  with two rights left is not as straightforward as for the Bermudan option because if we decide to exercise, the number of rights left will decrease by 1. Therefore the exercise rule at  $t_{M-2}$  will be: exercise the option if and only if  $PO_{M-2}^i + CV_{M-2}^{i,1} > CV_{M-2}^{i,2}$ . If the option is exercised, the cash flow for trajectory  $S^i$  at time  $t_{M-2}$  becomes  $CF_{M-2}^{i,2} = PO_{M-2}^i$ . Now it is important to notice that if for trajectory  $S^i$  the option is exercised at time  $t_{M-2}$ , the exercise strategy and thus the cash flows for trajectory  $S^i$  at times  $t_{M-1}$  and  $t_M$  are replaced by the cash flows for trajectory  $S^i$  for the level of one exercise right left. This step is very important and prevents that the option is exercised more than there are exercise rights. Recall that in the case for a Bermudan option these future cash flows were set to zero.

Generalizing to the level of  $j = 1 \dots R$  rights left, the initialization is to always exercise the option at  $t = t_M \dots t_{M-j+1}$  if the option is in the money. For the level of  $j$  rights left, the first approximation of the continuation value is done at time  $t_{M-j}$ . For  $j$  rights left the vector  $Y$  where is regressed on is given by

$$Y^i = DCF_m^{i,j} := \sum_{k>m} e^{-r(k-m)\Delta t}CF_k^{i,j}. \quad (3.33)$$

Comparing this expression with (3.29), it can be seen that in the method for multiple exercise rights the approximation of the continuation values is actually the same as for a Bermudan option. The only difference is that continuation values are approximated for every level of rights left.

Once the continuation values at time  $t_m$  can be approximated for all trajectories  $S^i$  and all levels of rights left, the exercise strategy for the single trajectories can be updated. The exercise rule at  $t_m$  will

be: exercise the option if and only if  $PO_{M-2}^i + CV_{M-2}^{i,j-1} > CV_{M-2}^{i,j}$ . If the option is exercised, the cash flow at time  $t_m$  becomes  $CF_m^{i,j} = PO_m^i$ .

Now it is important to notice that if for trajectory  $S^i$  and the level of  $j$  exercise rights left the option is exercised at time  $t_m$ , the exercise strategy and thus the cash flows for trajectory  $S^i$  and the level of  $j$  exercise rights left at all times  $t_k, k > m$  are replaced by the cash flows at these times for trajectory  $S^i$  for the level of  $j - 1$  exercise right left.

For a schematic overview of the recursive scheme for multiple early exercise opportunities see Figure 3.5.

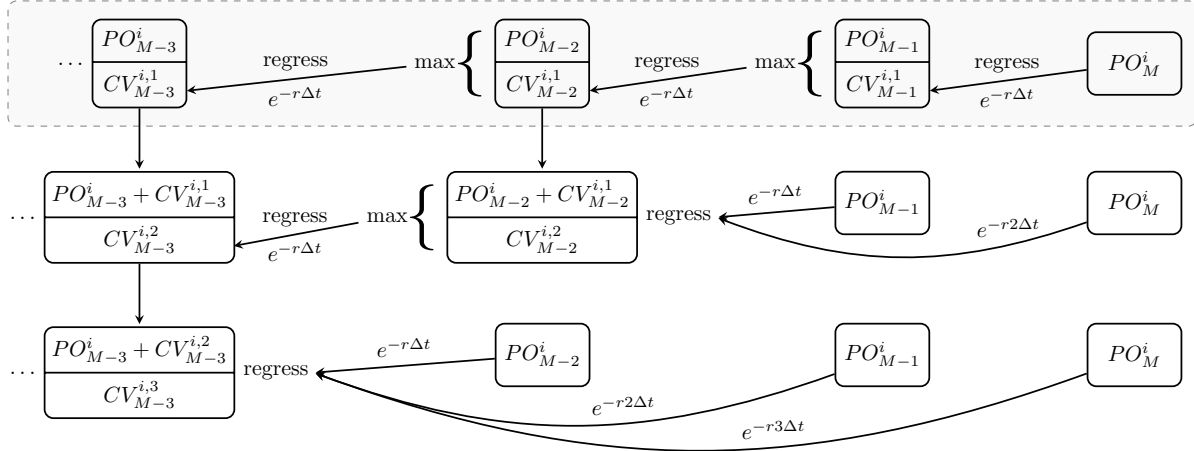


Figure 3.5: Schematic overview of the recursive scheme that is used in the LSMC algorithm for an option with multiple early exercise rights for a single trajectory. From right to left we go back in time and from bottom to top the number of rights left decreases.  $CV_m^{i,j}$  denotes the continuation value at time  $t_m$  with  $j$  rights left and  $PO_m^i$  denotes the payoff at time  $t_m$ . In the shaded area we recognize the scheme for a Bermudan option.

Because in the valuation we need the continuation values for every number of rights left up to  $R$ , we get the option values for  $r$  rights left, where  $1 < r < R$ , for free.

In all the tests in Chapter 5 we use as basis functions for the LSMC method the standard polynomials up to degree three. The experiments showed that this is good enough to approximate the continuation values. Also in [18] and [2] the authors mention that this is sufficient in the valuation.

## Chapter 4

# Natural gas storage contracts

Throughout this section we will primarily follow the paper of Boogert and de Jong [2] in defining a natural gas storage contract and the way to value it with a trading strategy based on the natural gas spot price.

### 4.1 Relation to options with multiple early exercise rights

The holder of an option with multiple early exercise rights has to decide when to exercise his rights. So at every exercise date he has to decide if he exercises a right or not. The holder of a gas storage contract has to decide which action he takes at every date before the settlement of the contract. For a natural gas storage contract the actions that can be taken are withdrawing, injecting or doing nothing. A natural gas storage contract therefore can be seen as an option with as many exercise rights as exercise dates ( $R = M$ ), with the difference that the payoff function depends on the action taken. Passing the request to inject or withdraw to the natural gas storage facility is also called a nomination.

The gas that the owner of the contract decides to inject or withdraw is traded on the market. Gas that is injected must be bought on the market, while gas that is withdrawn has to be sold on the market. Therefore a natural gas storage contract can have both positive (withdrawing) and negative (injecting) payoffs. Accepting a negative cash flow could be profitable if the resulting expected future cash flows are higher. This is an essential difference with options, since in general for options it holds that the cash flows are positive.

The last difference of natural gas storage contracts with options are the operational constraints and physical limitations of the natural gas storage facility. The volume in storage is limited by the capacity of the gas storage facility, and often there has to be a minimum amount of gas in storage (at least it can not be negative). Also the rates of injection and withdrawal are limited.

### 4.2 Defining a natural gas storage contract

The time lattice for a natural gas storage contract does not differ much from the time lattice for a Bermudan option. The only difference is that an extra date is included, the settlement date of the contract. So, when dealing with natural gas storage contracts we have the following set of equally spaced dates:  $0 = t_0 < t_1 < \dots < t_{M-1} < t_M = T < t_{M+1}$ , where  $t_{m-1} - t_m = \Delta t$  for  $m = 1 \dots M+1$ , where  $t_0$  is the start date and  $t_{M+1}$  is the settlement date of the contract. At all the intermediate dates the contract holder can submit a nomination. So every date where a nomination can be submitted (nomination date) corresponds to an exercise date of a Bermudan option.

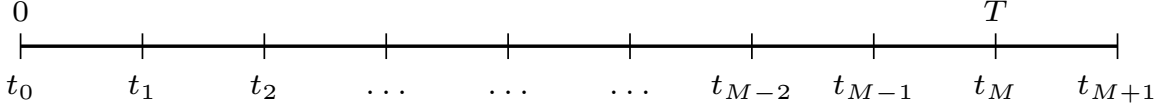


Figure 4.1: Time lattice for a natural gas storage contract.

The action that is nominated at time  $t_m$  is denoted by  $\Delta\nu(t_m)$ . This nomination corresponds to a volume change which is in place at the beginning of the next nomination date. So the volume change  $\Delta\nu(t_m) = \nu(t_{m+1}) - \nu(t_m)$ , where a positive volume change corresponds to an injection and a negative volume change corresponds to a withdrawal. Since the contract holder cannot take an action at times  $t_0$  and  $t_{M+1}$ , we have  $\Delta\nu(t_0) = 0$  and  $\Delta\nu(t_{M+1}) = 0$  by the definition of the contract.

At the settlement date  $t_{M+1}$  a penalty function  $q(t_{M+1}, S(t_{M+1}), \nu(t_{M+1}))$  is introduced which may depend on the volume of natural gas in storage and the natural gas spot price. This penalty function ensures that the volume of gas in storage at the settlement date equals the required volume of gas in storage at this date.

In contrast to the payoff function of an option, the payoff function of a natural gas storage contract depends not only on the gas spot price at time  $t_m$ , but also on the action that is taken. The payoff function is defined by

$$g(t_m, S(t_m), \Delta\nu(t_m)) := \begin{cases} -c(S(t_m))\Delta\nu(t_m) & \Delta\nu(t_m) > 0 \\ 0 & \Delta\nu(t_m) = 0 \\ -p(S(t_m))\Delta\nu(t_m) & \Delta\nu(t_m) < 0, \end{cases} \quad (4.1)$$

where  $c$  represent the cost of injection as a function of the natural gas spot price and  $p$  represent the profit of withdrawal as a function of the natural gas spot price. In the remainder of this work we will use  $c(S(t_m)) = p(S(t_m)) = S(t_m)$ . Boogert and de Jong showed in their work [2] how to include transaction costs and bid-ask spreads in these cost and profit functions.

The physical limitation of the natural gas storage facility impose that for all times  $t_m$ , the volume of natural gas in storage  $\nu(t_m)$  should satisfy

$$\nu^{min} \leq \nu(t_m) \leq \nu^{max}, \quad (4.2)$$

where  $\nu^{min}$  is the minimum volume of natural gas in storage and  $\nu^{max}$  is the maximum volume of natural gas in storage. The operational constraints of the natural gas storage facility are represented by a limitation on the volume change per nomination date. For  $m = 1 \dots M$  the volume change  $\Delta\nu(t_m)$  is assumed to satisfy

$$i^{min} \leq \Delta\nu(t_m) \leq i^{max}, \quad (4.3)$$

where  $i^{min} < 0$  is the maximum withdrawal rate and  $i^{max} > 0$  is the maximal injection rate. Often in practice  $i^{min}$  and  $i^{max}$  are functions of time  $t_m$  and volume  $\nu(t_m)$ . This is because when there is more natural gas in storage it is easier to withdraw because the pressure is higher. In this work for simplicity we assume that  $i^{min}$  and  $i^{max}$  are constants.

The set of allowed actions at time  $t_m$  is limited. For example it is not possible to inject into a full storage and it is not possible to withdraw from an empty storage. We define  $\mathcal{D}(t_m, \nu(t_m))$  to be the set of all allowed actions that can be taken at time  $t_m$  given the volume  $\nu(t_m)$

$$\mathcal{D}(t_m, \nu(t_m)) := \{\Delta\nu | \nu^{min} \leq \nu(t_m) + \Delta\nu \leq \nu^{max} \text{ and } i^{min} \leq \Delta\nu \leq i^{max}\}. \quad (4.4)$$

We finally obtain the following pricing problem

$$v(t_0, S(t_0)) := \sup_{\Delta\nu^*} \mathbb{E}_{\mathbb{Q}} \left[ \sum_{m=1}^M e^{-rt_m} g(t_m, S(t_m), \Delta\nu(t_m)) + e^{-rt_{M+1}} q(t_{M+1}, S(t_{M+1}), \nu(t_{M+1})) \right], \quad (4.5)$$

where  $\Delta\nu^* := \{\Delta\nu^*(t_1), \dots, \Delta\nu^*(t_M)\}$  denotes the optimal strategy that is taken.

For the remaining of this work we assume that we are given the contract details in Table 4.1 when we deal with gas storage contracts.

Start date	$t_0$
Settlement date	$t_{M+1}$
Nomination	$\Delta t$
Minimum volume	$\nu^{min}$
Maximum volume	$\nu^{max}$
Start volume	$\nu(t_0)$
End volume	$\nu(t_{M+1})$
Maximum withdrawal rate	$i^{min} < 0$
Maximum injection rate	$i^{max} > 0$

Table 4.1: Characteristics of a natural gas storage contract

### 4.3 The dynamic programming formulation

As we did for the Bermudan option and the option with multiple early exercise rights, we can also set up a dynamic programming formulation for the natural gas storage contract. To this end the storage volume is discretized into  $N_\nu - 1$  units of length  $\delta := (\nu^{max} - \nu^{min}) / (N_\nu - 1)$ . The resulting set of all  $N_\nu$  possible volume levels is denoted by  $\mathcal{V}$ . We assume that at every time step the set of possible volume levels is the same. Furthermore we assume that the nomination  $\Delta\nu(t_m)$  is a multiple of  $\delta$ .

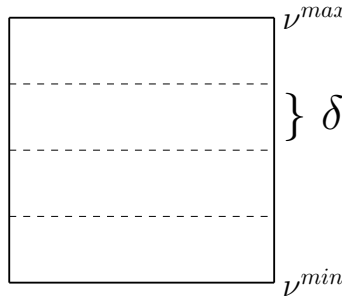


Figure 4.2: Discretization of the volume of the natural gas storage when  $N_\nu = 5$

On the one hand when valuing a natural gas storage contract it is not needed to keep track of the number of rights left because every nomination date the holder of the contract has the right to do an action. On the other hand, the dynamic program will be solved backwards in time and it is not known which volume levels will be visited in advance. Therefore, at every nomination date before the settlement date of the contract, the contract values for all possible volume levels  $\nu \in \mathcal{V}$  need to be calculated. Since these volume levels are not necessarily integer valued we take the dependence of the volume level on the contract value into the brackets of  $v$  (instead of using a superscript which we did for options with multiple early exercise rights). Let  $v(t_m, S(t_m), \nu(t_m))$  denote the value of the storage contract at time  $t_m$  when

the natural gas spot price is  $S(t_m)$  and the storage is at volume level  $\nu(t_m)$ .

At the settlement date  $t_{M+1}$ , for every volume level  $v \in \mathcal{V}$  the value of the natural gas storage contract equals the value of the penalty function:  $v(t_{M+1}, S(t_{M+1}), \nu) = q(t_{M+1}, S(t_{M+1}), \nu)$ .

For all time steps before the settlement date we need continuation values. The continuation value of a natural gas storage contract at time  $t_m$  does not only depend on the current volume level  $\nu(t_m)$ , but also on the nomination  $\Delta\nu(t_m) \in \mathcal{D}(t_m, \nu(t_m))$ . Let  $c(t_m, S(t_m), \nu(t_m), \Delta\nu(t_m))$  denote the continuation value at time  $t_m$  when the natural gas spot price is  $S(t_m)$ , the storage is at volume level  $\nu(t_m)$  and the nomination is  $\Delta\nu(t_m)$ . Note that if at time  $t_m$  the volume in storage is  $\nu(t_m)$  and  $\Delta\nu(t_m)$  is nominated to be injected or withdrawn, the volume in storage at time  $t_{m+1}$  is  $\nu(t_{m+1}) = \nu(t_m) + \Delta\nu(t_m)$ . This idea allows to reduce the dimension of the continuation value from four to three. The continuation values at time  $t_m$  can be written as a function of the sum of the volume level at time  $t_m$  and the nomination at time  $t_m$ :

$$c(t_m, S(t_m), \nu(t_m) + \Delta\nu(t_m)) = c(t_m, S(t_m), \nu(t_{m+1})). \quad (4.6)$$

So at time  $t_m$  it suffices to compute continuation values just for all the volume levels  $\nu \in \mathcal{V}$ .

To clarify this idea, we introduce the following example. Starting from certain volume levels and taking different actions can result in the same continuation value of the contract. For example:

$$c(t_m, S(t_m), 2, -1) = c(t_m, S(t_m), 1, 0) = c(t_m, S(t_m), 0, 1). \quad (4.7)$$

For these three continuation values it holds that

$$c(t_m, S(t_m), \nu(t_{m+1})) = c(t_m, S(t_m), 1). \quad (4.8)$$

See also Figure 4.4 which shows the connection between the volume levels, actions and continuation values for this specific example.

On all nomination dates  $t_{m-1}$ ,  $m = M+1, \dots, 2$  we have to decide what action to take. The action we should take at time  $t_{m-1}$  is the action which results in the highest value of the natural gas storage contract at time  $t_{m-1}$ . The contract value at time  $t_{m-1}$  is given by:

$$v(t_{m-1}, S(t_{m-1}), \nu(t_{m-1})) = \max_{\Delta\nu \in \mathcal{D}(t_{m-1}, \nu(t_{m-1}))} \{g(t_{m-1}, S(t_{m-1}), \Delta\nu) + c(t_{m-1}, S(t_{m-1}), \nu(t_{m-1}) + \Delta\nu)\}. \quad (4.9)$$

The continuation values  $c(t_{m-1}, S(t_{m-1}), \nu(t_m))$  can be computed by successive application of the risk-neutral valuation formula

$$c(t_{m-1}, S(t_{m-1}), \nu) = e^{-r\Delta t} \mathbb{E}_{\mathbb{Q}}[v(t_m, S(t_m), \nu) | \mathcal{F}_{t_{m-1}}] \quad \forall \nu \in \mathcal{V}. \quad (4.10)$$

Now we have all the ingredients to calculate the continuation and contract values backwards in time. Ultimately, since the contract holder cannot take an action at  $t_0$ , the contract value at  $t_0$  equals the continuation value at  $t_0$ . Summarizing we are left with the following dynamic programming problem:

### The dynamic programming formulation

$$\left\{ \begin{array}{l} v(t_{M+1}, S(t_{M+1}), \nu) = q(t_{M+1}, S(t_{M+1}), \nu) \quad \forall \nu \in \mathcal{V} \\ c(t_{m-1}, S(t_{m-1}), \nu) = e^{-r\Delta t} \mathbb{E}_{\mathbb{Q}}[v(t_m, S(t_m), \nu) | \mathcal{F}_{t_{m-1}}] \quad \forall \nu \in \mathcal{V}, \text{ for } m = M+1, \dots, 1 \\ v(t_{m-1}, S(t_{m-1}), \nu) = \max_{\Delta\nu \in \mathcal{D}(t_{m-1}, \nu)} \{g(t_{m-1}, S(t_{m-1}), \Delta\nu) + c(t_{m-1}, S(t_{m-1}), \nu + \Delta\nu)\} \\ \hspace{15em} \forall \nu \in \mathcal{V}, \text{ for } m = M+1, \dots, 2 \\ v(t_0, S(t_0), \nu) = c(t_0, S(t_0), \nu) \quad \forall \nu \in \mathcal{V} \end{array} \right. \quad (4.11)$$

## 4.4 LSMC method for a natural gas storage contract

In the LSMC algorithm for natural gas storage contracts, a regression is done for every allowed volume level for every time step. To give some intuition for the LSMC algorithm, we first introduce the recursive scheme for the following example where the allowed volume levels and actions are given by,

$$\mathbf{Example\ 1} := \begin{cases} \mathcal{V} = \{0, 1, 2\}, \\ \mathcal{D}(t_m, 0) = \{0, 1\}, & \forall m, \\ \mathcal{D}(t_m, 1) = \{-1, 0, 1\}, & \forall m, \\ \mathcal{D}(t_m, 2) = \{-1, 0\}, & \forall m. \end{cases} \quad (4.12)$$

Before introducing the algorithm, for notational convenience we define  $PO_m^i := g(t_m, S^i(t_m), \Delta\nu(t_m))$  and  $CV_m^{i,\nu} := c(t_m, S^i(t_m), \nu(t_{m+1}))$ , where  $g$  is the payoff function and  $c$  the continuation value as function of  $t_m$ ,  $S^i(t_m)$  and  $\nu(t_{m+1})$ . We also define  $CF_m^{i,\nu}$  to be the cash flow of trajectory  $i$  at time  $t_m$  for volume level  $\nu(t_m)$ . For **Example 1** the payoff is defined as,

$$PO_m^i := \begin{cases} S^i(t_m), & \text{if } \Delta\nu(t_m) = -1, \\ 0, & \text{if } \Delta\nu(t_m) = 0, \\ -S^i(t_m), & \text{if } \Delta\nu(t_m) = 1. \end{cases} \quad (4.13)$$

A difference with the Bermudan option is that at the settlement date of the gas storage contract a penalty function is included. The initialization of the LSMC algorithm at time  $t_{M+1}$  is done by assigning a (possible negative) cash flow to every trajectory for every volume level which is defined by the penalty function. To ensure an empty storage tank at the settlement date of the contract, we use the following penalty function:

$$q(t_{M+1}, S(t_{M+1}), \nu(t_{M+1})) = -1000 \cdot \nu(t_{M+1}). \quad (4.14)$$

The initialization for this penalty function is schematically shown in Figure 4.3.

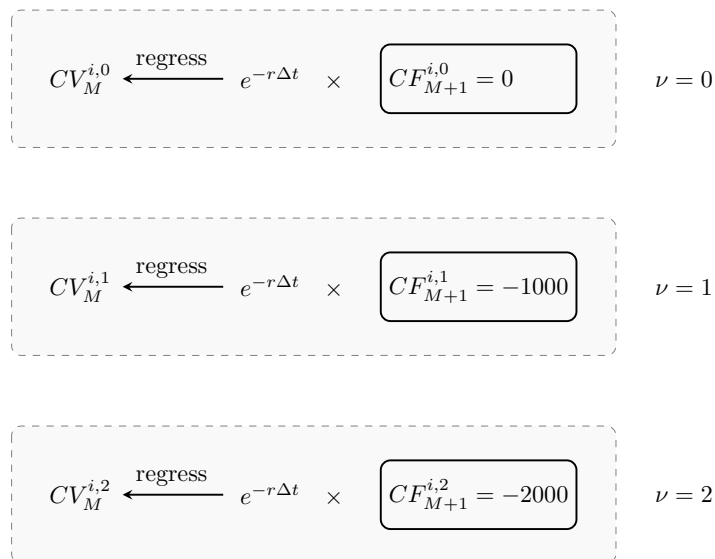


Figure 4.3: First iteration of the LSMC algorithm for the example problem in (4.12) with penalty function (4.14). The continuation values at time  $t_M$  are approximated based on a regression.

For the time steps  $t_m$ , where  $m = 1 \dots M - 1$ , the scheme is also somewhat different from the Bermudan option. We have now to deal with different volume levels, and each action leads to a specific continuation value and payoff, as can be seen in Figure 4.4.

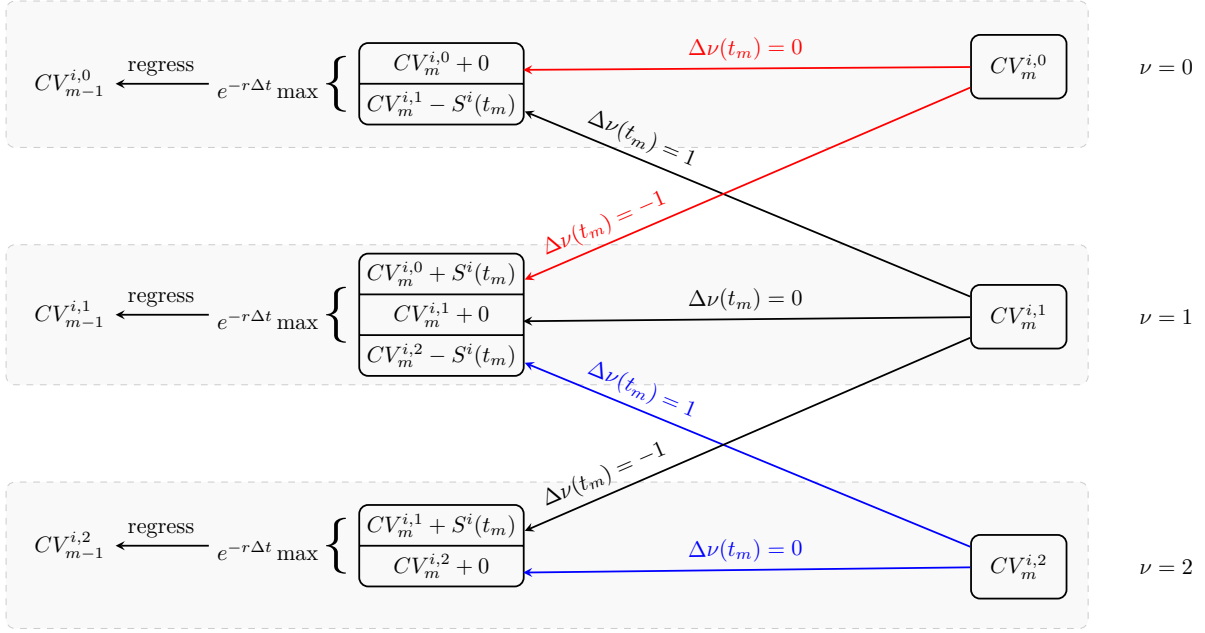


Figure 4.4: Schematic overview of the continuation value propagation for the problem with 3 allowed volume levels for an arbitrary time step  $t_{m-1}$ , where  $m = 2 \dots M$ . The main difference with the scheme for the Bermudan option is that the direct payoff depends on the action that is taken.

For the explanation how to obtain these continuation values with the LSMC method we refer to Chapter A.1. The procedure for the regression is exactly the same.

## 4.5 COS method for natural gas storage contracts

As far as the authors know, the valuation of gas storage contracts with the COS method is not done before. In this section the goal is to use the COS method for the valuation of natural gas storage contracts. Similar as for the Bermudan option and the option with multiple early exercise rights, the backbone is the dynamic programming formulation of the problem. The dynamic programming formulation (4.11) for the valuation of natural gas storage contracts can be found on page 38.

We copy the idea to discretize the volume of the storage. For every volume level  $\nu \in \mathcal{V}$  the continuation values need to be approximated with the COS method. The penalty function is treated as a payoff at time  $t_{M+1}$ .

In the valuation of options with the COS method we used the characteristic function of the  $\log(S(t)/K)$  price process. This was beneficial in determining the integration range for the payoff function. For the valuation of natural gas storage contracts however the payoff function is a direct function of the natural gas spot price and there is no strike price involved. Therefore in the natural gas storage contracts setting we will work with the  $\log(S(t))$  price process.

### 4.5.1 Recovering the coefficients $V_k(t_m, \nu)$

In this section we describe how to recover the option value coefficients at time  $t_m$  for volume level  $\nu$  which are defined as

$$V_k(t_m, \nu) := \frac{2}{b-a} \int_a^b v(t_m, y, \nu) \cos\left(k\pi \frac{y-a}{b-a}\right) dy. \quad (4.15)$$

For all volume levels  $\nu \in \mathcal{V}$  the Fourier cosine series coefficients of the contract value at the settlement date  $t_{M+1}$  are given by

$$V_k(t_{M+1}, \nu) = \frac{2}{b-a} \int_a^b q(t_{M+1}, y, \nu) \cos\left(k\pi \frac{y-a}{b-a}\right) dy, \quad \forall \nu \in \mathcal{V}, \quad (4.16)$$

where  $q(t_{M+1}, y, \nu)$  is the penalty function.

From the dynamic programming formulation (4.11) it follows that for all  $\nu \in \mathcal{V}$  and  $m = M, \dots, 1$

$$v(t_m, y, \nu) = \max_{\Delta\nu \in \mathcal{D}(t_m, \nu)} \{g(t_m, y, \Delta\nu) + c(t_m, y, \nu + \Delta\nu)\}. \quad (4.17)$$

In the valuation of Bermudan options and options with multiple early exercise rights, the maximum in the dynamic programming formulation is taken over two functions. Here it was easy to determine an early exercise point and the integral of the Fourier cosine series coefficients for the option value could be splitted up into two parts. In the valuation of natural gas storage contracts, at time  $t_m$  the maximum in the dynamic programming formulation has to be taken over all possible  $\Delta\nu \in \mathcal{D}(t_m, \nu)$ . Therefore in general it is difficult to say how many early decision points there are and how to determine them.

Instead of this we use a discrete Fourier cosine transform to approximate the integral of (4.15). The idea for this is taken from Appendix C in [25]. To this end the domain of integration is discretized into  $N_I$  grid-points and we define an equidistant  $y$ -grid

$$y_n := a + \left(n + \frac{1}{2}\right) \frac{b-a}{N_I} \quad \text{and} \quad \Delta y := \frac{b-a}{N_I}. \quad (4.18)$$

$$V_k(t_m, \nu) = \frac{2}{b-a} \int_a^b v(t_m, y, \nu) \cos\left(k\pi \frac{y-a}{b-a}\right) dy \quad (4.19)$$

$$\approx \sum_{n=0}^{N_I-1} \frac{2}{b-a} v(t_m, y_n, \nu) \cos\left(k\pi \frac{y_n-a}{b-a}\right) \Delta y \quad (4.20)$$

$$= \sum_{n=0}^{N_I-1} v(t_m, y_n, \nu) \cos\left(k\pi \frac{2n+1}{2N_I}\right) \frac{2}{N_I}. \quad (4.21)$$

The appearing DCT (DCT-II in the book [23]) can be easily calculated by the function `dct` of MATLAB. The numerical integration error is second order in  $N_I$  as shown in Appendix B.

## 4.5.2 Determining the contract value

Now for  $m = M+1, \dots, 2$  and for all volume levels we can approximate the continuation values with the COS method:

$$\hat{c}(t_{m-1}, x, \nu) = e^{-r\Delta t} \sum_{k=0}^{N-1} \Re \left\{ \phi\left(\frac{k\pi}{b-a}; x\right) e^{-ik\pi \frac{a}{b-a}} \right\} V_k(t_m, \nu), \quad \forall \nu \in \mathcal{V}. \quad (4.22)$$

For  $m = M, \dots, 1$  and we can recover the cosine series coefficients of the contract value as follows:

$$\begin{aligned} V_k(\nu, t_m) &= \frac{2}{b-a} \int_a^b v(y, \nu, t_m) \cos\left(k\pi \frac{y-a}{b-a}\right) dy, \quad \forall \nu \in \mathcal{V}, \\ &= \frac{2}{b-a} \int_a^b \max_{\Delta\nu \in \mathcal{D}(t_m, \nu)} \{c(t_m, y, \nu + \Delta\nu, t_m) + g(t_m, y, \Delta\nu)\} \cos\left(k\pi \frac{y-a}{b-a}\right) dy, \quad \forall \nu \in \mathcal{V}. \end{aligned} \quad (4.23)$$

With both (4.22) and (4.23) we can recover the coefficients  $V_k(\nu, t_1)$  for all volume levels  $\nu \in \mathcal{V}$ . Finally we can calculate the contract values at  $t_0$  with

$$\hat{v}(t_0, x, \nu) = \hat{c}(t_0, x, \nu) \approx e^{-r\Delta t} \sum_{k=0}^{N-1} \Re \left\{ \phi \left( \frac{k\pi}{b-a}; x \right) e^{-ik\pi \frac{a}{b-a}} \right\} V_k(t_1, \nu), \quad \forall \nu \in \mathcal{V}, \quad (4.24)$$

where we are especially interested in the contract value  $\hat{v}(t_0, x, \nu(0))$ , since the start volume  $\nu(0)$  is imposed.

### 4.5.3 COS method for a process with a seasonality function

When valuing natural gas storage contracts with the COS method where the natural gas spot price is modeled by the stochastic process introduced in Paragraph 1.4.2, we are dealing with a characteristic function that differs at every time step. Formula (1.32) actually holds only for a European option, where  $\tau := T - t_0$ .

When valuing Bermudan options or natural gas storage contracts, the characteristic function of the underlying process, given by  $\hat{\Gamma} \left( t_{m-1}, x; t_m, \frac{k\pi}{b-a} \right)$  (Returning to the notation of the characteristic function in (2.12)), depends on  $t_m$  and not on  $T$ . Therefore at every time step the characteristic function of the underlying process needs to be recalculated. The formula for the approximation of the continuation values can be written as

$$\hat{c}(x, \nu, t_{m-1}) = e^{-r\Delta t} \sum_{k=0}^{N-1} \Re \left\{ \hat{\Gamma} \left( t_{m-1}, x; t_m, \frac{k\pi}{b-a} \right) e^{-ik\pi \frac{a}{b-a}} \right\} V_k(t_m, \nu), \quad \forall \nu \in \mathcal{V}, \quad (4.25)$$

where the characteristic function of the underlying process is defined by

$$\hat{\Gamma} \left( t_{m-1}, x; t_m, \omega \right) := e^{i\omega x e^{-\kappa\tau} + A(\omega, \tau)}, \quad (4.26)$$

with

$$A(\omega, \tau) = i\omega \int_0^\tau (f'(t_m - s) + \kappa f(t_m - s)) e^{-\kappa s} ds + \frac{1}{4\kappa} \omega^2 \sigma^2 (e^{-2\kappa\tau} - 1) \quad (4.27)$$

and  $\tau := t_m - t_{m-1}$ .

We work this out for the following seasonality function,

$$f(t) = \log(15) - \frac{1}{10} \cos(2\pi t), \quad (4.28)$$

which we will also use in our numerical tests in Section 5.4. The derivative of (4.28) is given by,

$$f'(t) = \frac{1}{5} \sin(2\pi t). \quad (4.29)$$

Recalling the formula for  $A(\omega, \tau)$  in (4.27), the integral

$$\int_0^\tau (f'(t_m - s) + \kappa f(t_m - s)) e^{-\kappa s} ds, \quad (4.30)$$

for this specific seasonality function is given by,

$$\int_0^\tau \left( \frac{1}{5} \sin(2\pi(t_m - s)) + \kappa \left( \log(15) - \frac{1}{10} \cos(2\pi(t_m - s)) \right) \right) e^{-\kappa s} ds. \quad (4.31)$$

We define

$$I_1 := \int_0^\tau \frac{1}{5} \sin(2\pi(t_m - s))e^{-\kappa s} ds \quad (4.32)$$

$$= \frac{\pi e^{-\kappa\tau} (\kappa (e^{\kappa\tau} \sin(2\pi t_m) + \sin(2\pi(\tau - t_m))) - 2\pi e^{\kappa\tau} \cos(2\pi t_m) + 2\pi \cos(2\pi(\tau - t_m)))}{5(\kappa^2 + 4\pi^2)}, \quad (4.33)$$

$$I_2 := \int_0^\tau \kappa \log(15)e^{-\kappa s} ds = \log(15) (1 - e^{-\kappa\tau}), \quad (4.34)$$

$$I_3 := \int_0^\tau -\kappa \frac{1}{10} \cos(2\pi(t_m - s))e^{-\kappa s} ds \quad (4.35)$$

$$= -\kappa \frac{e^{-\kappa\tau} (2\pi (e^{\kappa\tau} \sin(2\pi t_m) + \sin(2\pi(\tau - t_m))) + \kappa e^{\kappa\tau} \cos(2\pi T) - \kappa \cos(2\pi(\tau - t_m)))}{10(\kappa^2 + 4\pi^2)}. \quad (4.36)$$

We define the characteristic function for this specific seasonality function as,

$$\hat{\Gamma}(t_{m-1}, x; t_m, \omega) := e^{i\omega x e^{-\kappa\tau} + A(\omega, \tau)}, \quad (4.37)$$

with

$$A(\omega, \tau) = i\omega(I_1 + I_2 + I_3) + \frac{1}{4\kappa}\omega^2\sigma^2 (e^{-2\kappa\tau} - 1). \quad (4.38)$$

and  $\tau := t_m - t_{m-1}$ .

The integrals  $I_1$ ,  $I_2$  and  $I_3$  have been verified with the help of Wolfram *Mathematica*<sup>®</sup> 10.

#### 4.5.4 Variation of the amount of gas in storage with the COS method

With the LSMC method for natural gas storage contracts we could calculate the optimal amount of natural gas in storage for every single trajectory by just following the optimal strategy for that trajectory. The optimal strategy follows directly out of the recursive algorithm. The average amount of natural gas in storage is obtained by taking the average of the optimal volumes for every trajectory.

If we want to determine an optimal strategy with the COS method, we still have to simulate some trajectories of the natural gas spot price process. If we subsequently insert the natural gas spot price into the estimated continuation value function  $\hat{c}(t_m, x, \nu)$ , where  $x$  denotes the log-spot price, we can calculate the continuation values for all volume levels  $\nu \in \mathcal{V}$  and determine the optimal decision. Taking this decision, we end up at volume level  $\nu(t_{m+1})$  and we repeat this procedure.



# Chapter 5

## Numerical results

All the experiments in this section are carried out on a computer with an Intel(R) Core(TM) i7-4700MQ CPU with clock rate 2.40GHz. Implementation of the code is done in MATLAB R2018a.

For all plain Monte Carlo and LSMC simulations we make use of antithetic variates to reduce the variance. For an explanation of this variance reduction technique we refer to Chapter three of the book [27].

All the 95% confidence intervals (c.i.) are constructed by repeating the experiment 10 times. How to construct these intervals for given sample mean and sample variance, see for example the book [12]. The reported CPU times are obtained by taking the average time over 10 runs.

### 5.1 Testing the COS and LSMC methods

To test and compare the COS method and the (Least Squares) Monte Carlo simulations for European and Bermudan options, we used two test scenarios. In the first test scenario, the underlying is driven by a GBM with parameters the same as in Table 1 in the paper [11]. For the second test scenario we chose a Merton jump-diffusion process with the same parameters as for the GBM model, supplemented with the parameters for the jump process. The parameters that are used for both test scenarios can be found in Table 5.1. The results for the test under the GBM model are presented in Table 5.2 and for the test under the Merton model the results are presented in Table 5.3. For the COS method we used  $N = 128$  and for the (LS)MC method we used  $N = 1 \cdot 10^6$ .

Test No.	Model	$S_0$	$K$	$T$	$r$	$\sigma$	Other Parameters
1	GBM	100	110	1	0.1	0.2	-
2	Merton	100	110	1	0.1	0.2	$\lambda = 0.1, \bar{\mu} = 0, \bar{\sigma} = 0.5$

Table 5.1: Parameters for test scenarios 1 and 2.

Option Style	Analytic	Time	COS	Time	(LS)MC 95% c.i.	Time
European Put	7.7152	0.1ms	7.715168113	0.05ms	7.7131-7.7189	0.07s
European Call	8.1831	0.1ms	8.183052129	0.05ms	8.1808-8.1890	0.07s
Bermudan Put	-	-	10.480	1.3ms	10.476-10.482	1.8s
Bermudan Call	-	-	8.1831	0.7ms	8.1756-8.1883	1.2s

Table 5.2: Calculated option prices and CPU times for Test No. 1.

Option Style	COS	Time	(LS)MC 95% c.i.	Time
European Put	9.1526	0.06ms	9.1504-9.1625	0.7s
European Call	9.6204	0.06ms	9.6017-9.6319	0.7s
Bermudan Put	11.288	1.4ms	11.2680-11.2761	2.8s
Bermudan Call	9.6204	0.8ms	9.6022-9.62898	2.1s

Table 5.3: Calculated option prices and CPU times for Test No. 2.

As expected, we observe from Tables 5.2 and 5.3 that the option prices under the Merton model are higher than the option prices under GBM. By setting  $\lambda$  or  $\sigma_J$  to zero, experiments showed that the option prices were the same as their value under GBM, which is what we expect.

It can be seen that the option prices that were calculated by means of the COS method fall within the confidence intervals that were constructed by means of the (LS)MC simulations, with one exception. The confidence interval obtained with the LSMC method for a Bermudan put under the Merton process seems a little bit shifted downwards. We blame this to the small jump parameter  $\lambda = 0.1$ , which make that many simulated trajectories are needed to get close to the real option value. An experiment with  $\lambda = 1$  showed indeed that the value obtained with COS is again in the confidence interval obtained with the LSMC method.

Also the expectation that the option prices under the Merton model are higher than the option prices under GBM are reflected in Tables 5.2 and 5.3. By setting the jump intensity  $\lambda$  or the jump standard deviation to zero, experiments showed that the option prices are the same as their counterpart under GBM, which is what we expect.

## 5.2 A put option with multiple exercise rights

In the following experiment we compare the value of a put option with multiple exercise rights obtained with the COS method to the value obtained with the extended LSMC method. We base the experiment on the one introduced in paper [14] in order to compare the obtained values to their results.

We assume that the underlying stock price is driven by a GBM process with  $S(0) = 35$  and parameters  $r = 0.0488$  and  $\sigma = 0.25$ . At every exercise date the strike price is  $K = 40$  and the payoff is the payoff of a put. Time to maturity is  $T = 0.5$  and we assume  $M = 12$  exercise dates.

Now for the number of exercise rights  $R = 1, \dots, 6$ , the option value is calculated. The results are presented in Table 5.4.

$R$	LSMC 95% c.i.			COS
	$N = 1000$	$N = 10000$	$N = 100000$	$N = 128$
1	5.3674-5.4034	5.3763-5.4093	5.3759-5.3843	5.3816
2	10.664-10.723	10.692-10.734	10.689-10.699	10.696
3	15.898-15.987	15.927-15.993	15.930-15.944	15.941
4	21.063-21.174	21.103-21.173	21.100-21.118	21.116
5	26.148-26.279	26.200-26.287	26.205-26.225	26.219
6	31.153-31.303	31.227-31.311	31.231-31.254	31.247
CPU time (sec.)	0.03	0.08	0.60	0.02

Table 5.4: Option values calculated by means of the extended LSMC method and the COS method. The values obtained by the COS method are in all the confidence intervals that were constructed with the LSMC method.

The corresponding option values that were obtained for the same experiment which are presented in Table 3.1 in the paper [14] are contained in all our confidence intervals. Moreover, these values are very close to the values we found with the COS method. This suggests that both the extended LSMC method as the COS method for options with multiple exercise rights work well.

### 5.3 Test with the approximated characteristic function for the OU model

For this experiment we will use the approximation of the characteristic function for the Ornstein-Uhlenbeck process that we derived in Paragraph 2.8.1. We will use the COS method to calculate the value of a European put option with strike  $K = 22$  where the underlying price process is modelled by the mean-reverting model with constant mean from Paragraph 1.4.1. As before we choose  $S(0) = 15$  and  $\mu = \log(20)$ . The errors  $v_{OU} - v_{app}$  are shown in Figure 5.1 for different values of  $\kappa$  and  $\sigma$ , where  $v_{OU}$  denotes the option value obtained with the original characteristic function for the OU model and  $v_{app}$  denotes the option value obtained with the approximated characteristic function for the OU process. For  $\kappa = 1$  and  $\sigma = 0.1$  the absolute errors for different values of  $T$  are shown in Table 5.5.

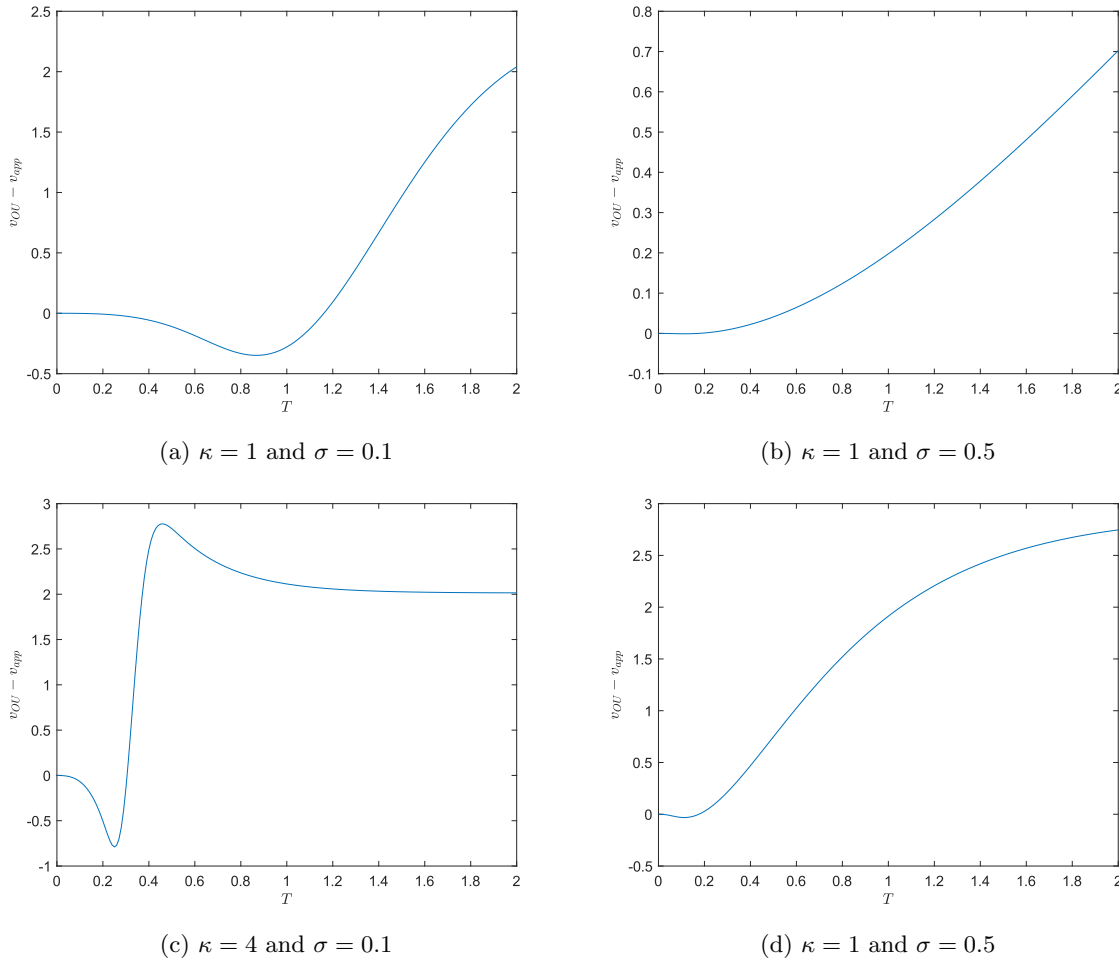


Figure 5.1: Error  $v_{OU} - v_{app}$  for different maturities  $T$ . Each subplot shows the approximation error for different parameter choices.

$T$	Absolute error
0.04	$9.56 \cdot 10^{-5}$
0.08	$5.63 \cdot 10^{-4}$
0.12	$1.71 \cdot 10^{-3}$
0.16	$3.86 \cdot 10^{-3}$
0.20	$7.33 \cdot 10^{-3}$

Table 5.5: Absolute error  $|v_{OU} - v_{app}|$  with parameters  $\kappa = 1$  and  $\sigma = 0.1$  for different small values of  $T$ .

In general for short maturities the value of the option obtained with the approximated characteristic function is close to the value obtained with the original characteristic function. For small parameter values of  $\kappa$  the approximation is better than for bigger parameter values of  $\kappa$ . Also for smaller parameter values of  $\kappa$  the approximation holds for longer times to maturity  $T$ .

## 5.4 Tests with natural gas storage contracts

In this section we perform several tests on the valuation of gas storage contracts with the COS and LSMC method. We consider tests under the three different models for the gas spot price which were introduced in Section 1.4. The three different tests are defined below.

### Gas Test 1

In the first test we model the natural gas spot price process according to the mean-reverting model with constant mean from Paragraph 1.4.1. The parameters are set as follows:  $S(0) = 15$ ,  $\kappa = 1$  and  $\mu = \log(20)$ . We compare the results for  $\sigma = 0.1$  (low volatility) and  $\sigma = 0.5$  (high volatility). For each choice of  $\sigma$ , six simulated spot price trajectories are shown in Figures 5.2 and 5.3.

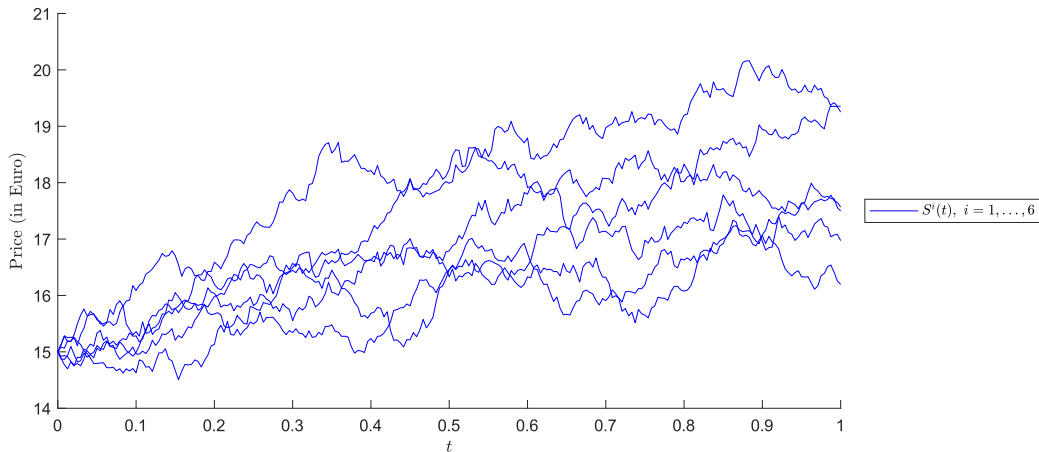


Figure 5.2: Six simulations of the spot price process that is used in Gas Test 1 with parameters  $\kappa = 1$ ,  $\sigma = 0.1$  and  $\mu = \log(20)$ . It can be observed that the price slowly reverts to the mean.

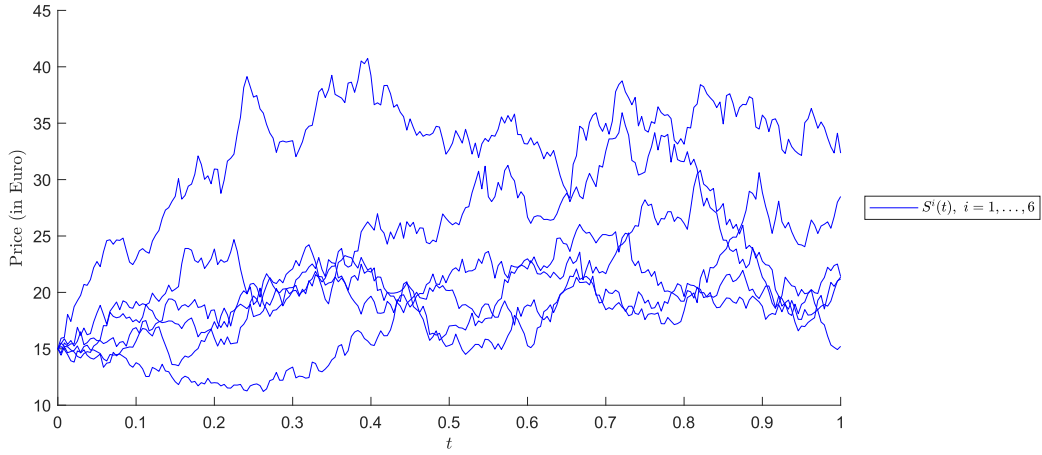


Figure 5.3: Six simulations of the spot price process that is used in Gas Test 1 with parameters  $\kappa = 1, \sigma = 0.5$  and  $\mu = \log(20)$ . It can be observed that the price is more volatile than the process in Figure 5.2 and therefore reverts faster to the mean.

### Gas Test 2

In the second test we use the mean-reverting model with seasonality from Paragraph 1.4.2 to model the natural gas spot price process. Also in this test we use  $\kappa = 1$  and for the function  $f$  we choose the function in (4.28). Again, we compare the results for  $\sigma = 0.1$  (low volatility) and  $\sigma = 0.5$  (high volatility). For each choice of  $\sigma$ , six simulated spot price trajectories are shown in Figures 5.4 and 5.5.

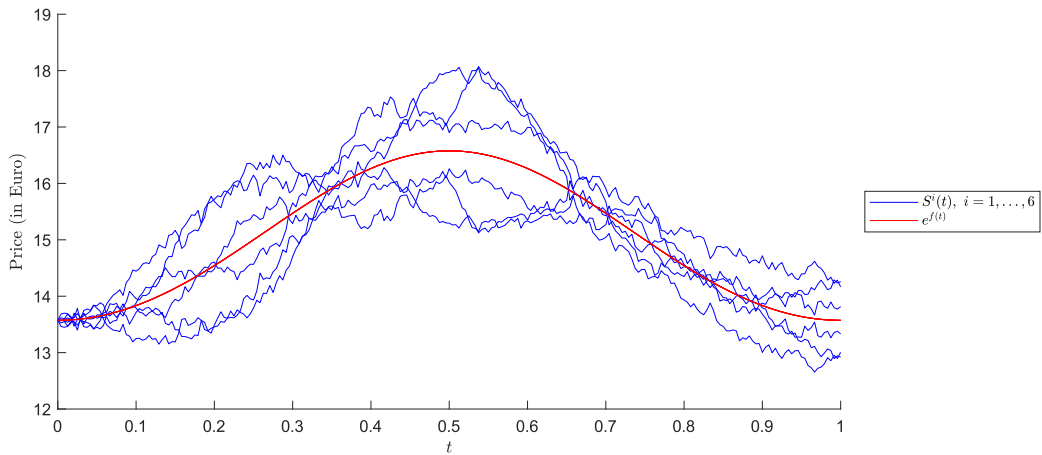


Figure 5.4: Six simulations of the spot price process that is used in Gas Test 2 with parameters  $\kappa = 1$  and  $\sigma = 0.1$ . It can be observed that the price mimics the seasonality function very well.

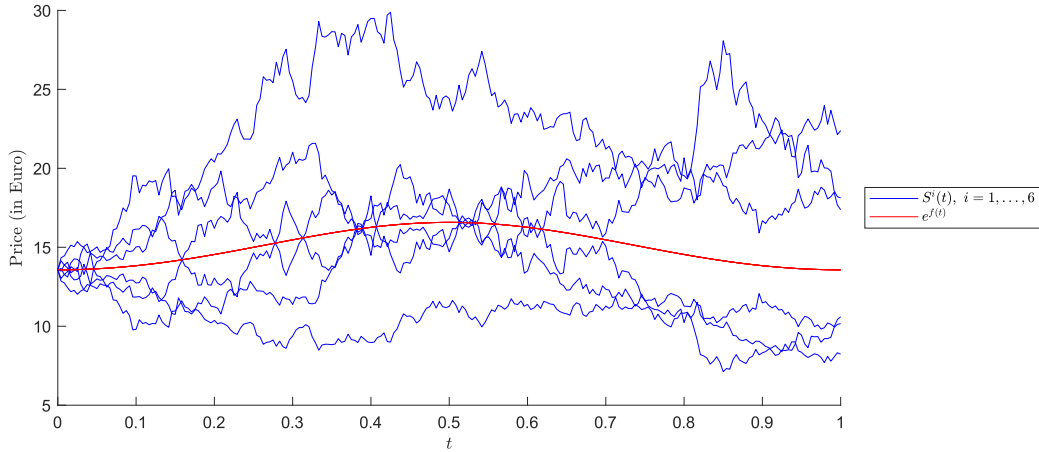


Figure 5.5: Six simulations of the spot price process that is used in Gas Test 2 with parameters  $\kappa = 1$  and  $\sigma = 0.5$ . It can be observed that the price is more volatile than the process in Figure 5.4.

### Gas Test 3

In the third test we model the natural gas spot price process according to the mean-reverting model with seasonality and jumps from Paragraph 1.4.3. As in Gas Test 2, we use the seasonality function (4.28). We set the jump parameters  $\lambda = 5$ ,  $\mu_J = 0$  and  $\sigma_J = 1$ , which is close to the parameters estimated for this model in the paper [1]. To ensure a fast mean-reversion of the jumps we set  $\kappa = 80$  and compensate for this in the so-called base process by setting  $\sigma$  high. We compare between  $\sigma = 0.5$  (low volatility) and  $\sigma = 3$  (high volatility). The idea for these high values for  $\kappa$  and  $\sigma$  also stems from the paper [1]. For each choice of  $\sigma$ , six simulated spot price trajectories are shown in Figures 5.6 and 5.7. In Figure 5.8 it can be seen that when we chose parameter  $\kappa$  too low, the jumps did not revert to the mean fast enough which did not result in the typical spikes.

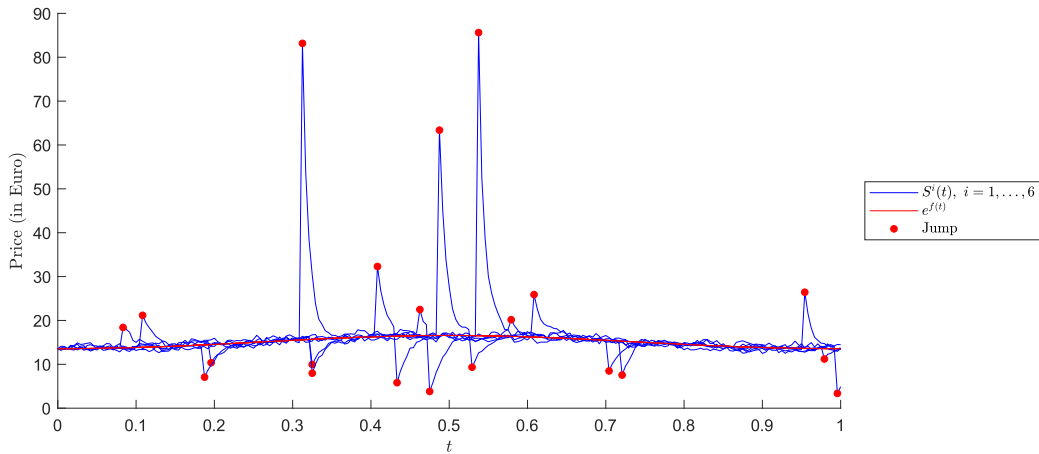


Figure 5.6: Six simulations of the spot price process that is used in Gas Test 3 with parameters  $\kappa = 80$ ,  $\sigma = 0.5$ ,  $\lambda = 5$ ,  $\mu_J = 0$  and  $\sigma_J = 1$ . It can be observed that this parameter choice results in a spiky behaviour of the spot price.

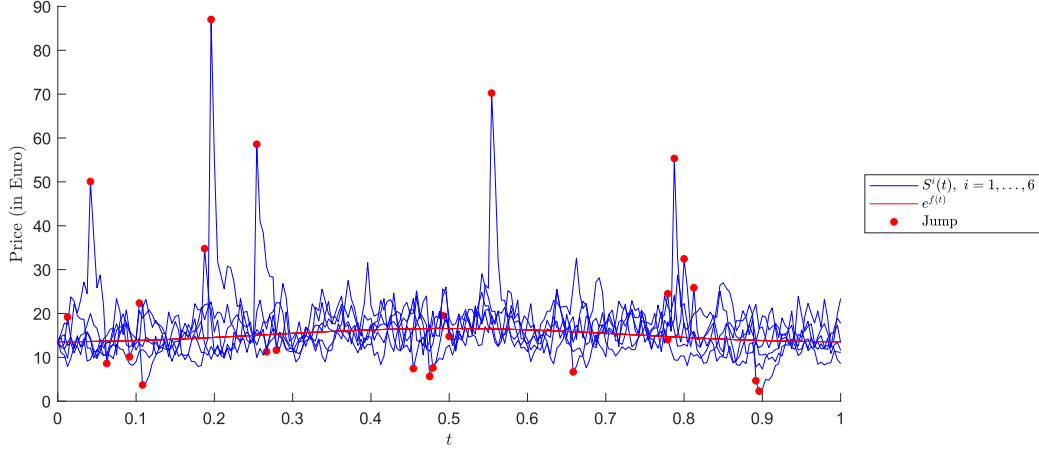


Figure 5.7: Six simulations of the spot price process that is used in Gas Test 3 with parameters  $\kappa = 80, \sigma = 0.5, \lambda = 5, \mu_J = 0$  and  $\sigma_J = 1$ . Besides the spiky behaviour of the spot price we now also observe that the spot price is more volatile.

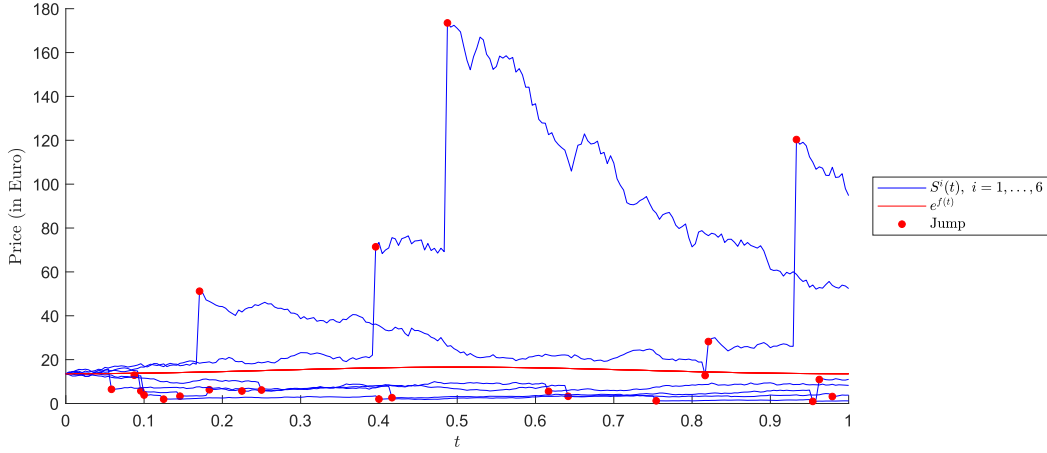


Figure 5.8: Six simulations of the spot price process that is used in Gas Test 3 with parameters  $\kappa = 1, \sigma = 0.5, \lambda = 5, \mu_J = 0$  and  $\sigma_J = 1$ . It can be observed that with this parameter choice the jumps do revert to the mean slowly.

In all the three tests we distinguish between slow storage ( $i^{max} = 1$  and  $i^{min} = -1$ ) and fast storage ( $i^{max} = 4$  and  $i^{min} = -6$ ). For all the three tests the contract details are given in Table 5.6

Start date	$t_0$	0
Last trading date	$T$	1
Nomination	$\Delta t$	1/240
Minimum volume	$\nu^{min}$	0
Maximum volume	$\nu^{max}$	100
Start volume	$\nu(0)$	0
End volume	$\nu(t_{M+1})$	0
Maximum withdrawal	$i^{min}$	-1 (slow), -6 (fast)
Maximum injection	$i^{max}$	1 (slow), 4 (fast)

Table 5.6: Contract details for the experiments.

### 5.4.1 Contract values with the LSMC and COS method

The contract values that were obtained with the LSMC and COS method are presented in Tables 5.7-5.9. For Gas Test 3 we used  $L = 1$ , instead of  $L = 10$  for the COS method. The relative high values for  $\lambda$  and  $\sigma_J$  make that the integration range  $[a, b]$  based on the cumulants is very wide. By setting  $L = 1$  we make it artificially shorter. We take  $N = 256$  terms in the Fourier cosine expansion to improve the accuracy.

		LSMC 95% c.i.						COS	
$\sigma$	Slow/Fast	$N = 50$	Time	$N = 500$	Time	$N = 5000$	Time	$N = 128$	Time
0.1	Slow	172.97-173.85	9.2s	171.24-171.58	38.4s	171.32-171.45	302s	171.38	14.9s
0.1	Fast	288.52-292.03	10.3s	270.68-271.16	40.8s	268.74-268.88	322s	268.59	14.5s
0.5	Slow	238.69-255.32	9.3s	186.73-190.97	36.2s	179.24-181.25	299s	179.54	14.4s
0.5	Fast	561.64-599.12	9.6s	340.28-346.12	40.1s	302.69-305.33	314s	301.78	14.2s

Table 5.7: Contract values and CPU times with the LSMC and COS method for Gas Test 1.

		LSMC 95% c.i.						COS	
$\sigma$	Slow/Fast	$N = 50$	Time	$N = 500$	Time	$N = 5000$	Time	$N = 128$	Time
0.1	Slow	152.19-153.26	9.2s	151.47-151.74	43.1s	151.47-151.53	285s	151.50	14.7s
0.1	Fast	299.26-301.31	9.6s	292.47-292.72	45.0s	291.99-292.13	306s	292.08	14.7s
0.5	Slow	229.26-243.58	9.3s	199.16-203.10	40.0s	196.73-198.34	300s	197.79	14.5s
0.5	Fast	542.69-582.90	9.8s	388.74-394.18	42.3s	370.15-372.77	330s	370.30	14.9s

Table 5.8: Contract values and CPU times with the LSMC and COS method for Gas Test 2.

		LSMC 95% c.i.						COS	
$\sigma$	Slow/Fast	$N = 50$	Time	$N = 500$	Time	$N = 5000$	Time	$N = 256$	Time
0.5	Slow	362.82-392.07	9.3s	360.73-368.59	36.8s	360.34-362.73	279s	361.29	23.3s
0.5	Fast	1436.1-1608.5	9.6s	1501.3-1558.8	40.0s	1499.0-1510.2	320s	1504.7	24.0s
3	Slow	762.48-805.83	9.3s	768.06-775.72	35.9s	768.97-772.06	295s	770.97	23.0s
3	Fast	3644.0-3795.3	9.6s	3605.6-3648.8	40.8s	3611.3-3629.9	322s	3615.5	24.4s

Table 5.9: Contract values and CPU times with the LSMC and COS method for Gas Test 3. We used  $L = 1$  instead of  $L = 10$  in the valuation with the COS method.

When simulating more trajectories in the LSMC method, the confidence intervals move to the value obtained with the COS method. We need to take at least  $N = 5000$  in the LSMC method to get close to the value obtained with the COS method. However, the COS method is many times faster. In [2], the authors report about simulation times of 40s for the case  $N = 5000$  in the LSMC method. Even if we could get close to these computation times with our simulations, the COS method is faster.

### 5.4.2 Average volume of gas in storage with LSMC

In this section the average volume of gas in storage, obtained with the LSMC method for natural gas storage contracts is shown for the three tests that we defined before. It gives an idea what volumes should be maintained to make maximal profit of the fluctuations in the natural gas spot price. We provided error bars with one standard error of uncertainty. The wider these error bars, the more profit can be made from a volatile natural gas spot price. Each figure is accompanied with a short explanation.

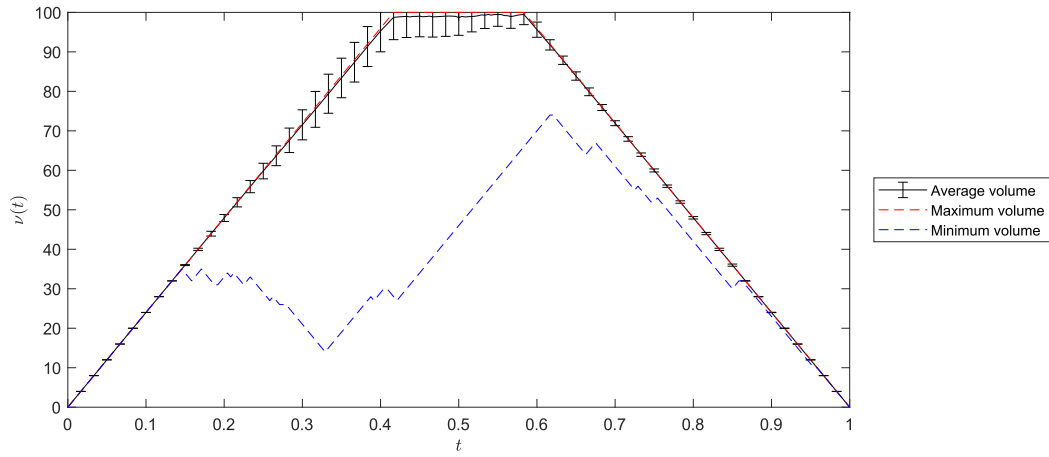


Figure 5.9: Average volume of gas in storage for Gas Test 1 for a slow storage with  $\sigma = 0.1$ . The strategy is to fill up the storage at the beginning and wait until the last moment to empty the storage. For this specific simulation the value of the contract is  $v(0, S(0)) = 171$

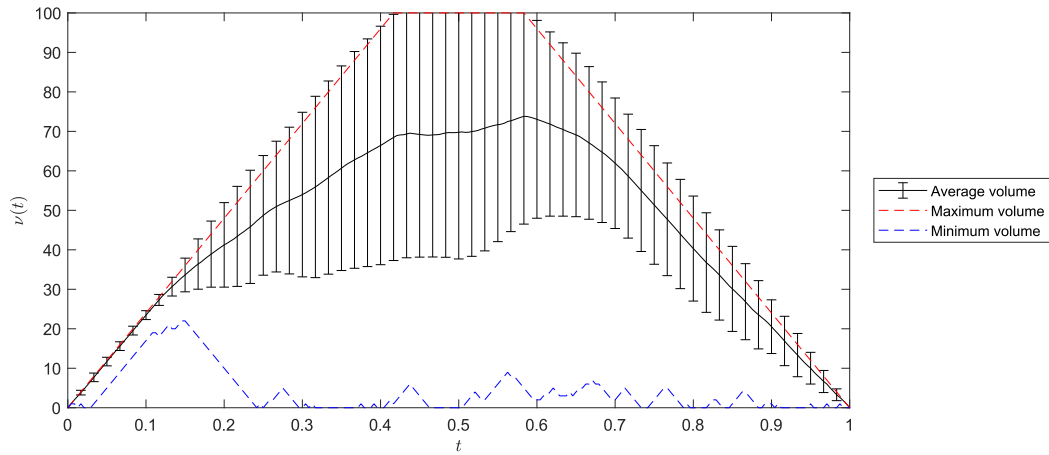


Figure 5.10: Average volume of gas in storage for Gas Test 1 for a slow storage with  $\sigma = 0.5$ . The strategy is to start with filling up the storage at the beginning, but then keep some space to take profit from the high volatility. For this specific simulation the value of the contract is  $v(0, S(0)) = 194$

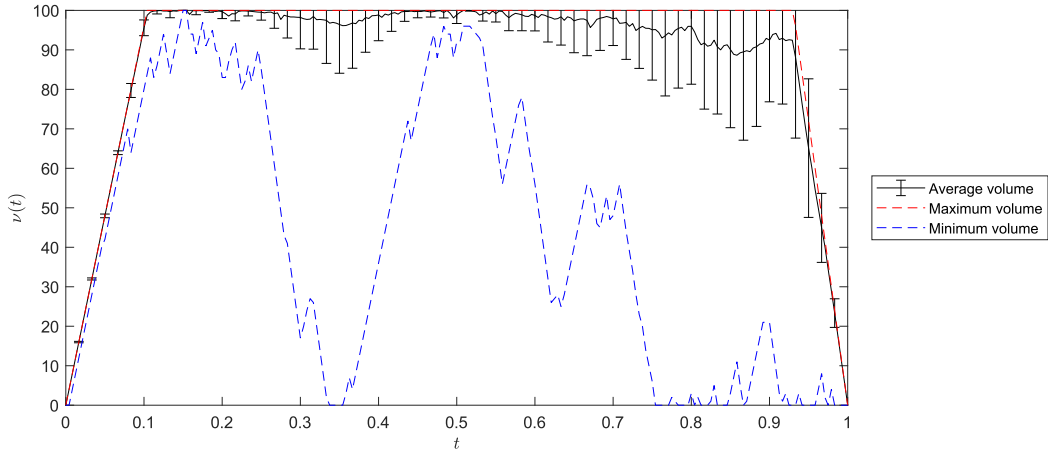


Figure 5.11: Average volume of gas in storage for Gas Test 1 for a fast storage with  $\sigma = 0.1$ . The strategy is to start with filling up the storage at the beginning and wait until the last moment to empty the storage. For this specific simulation the value of the contract is  $v(0, S(0)) = 270$

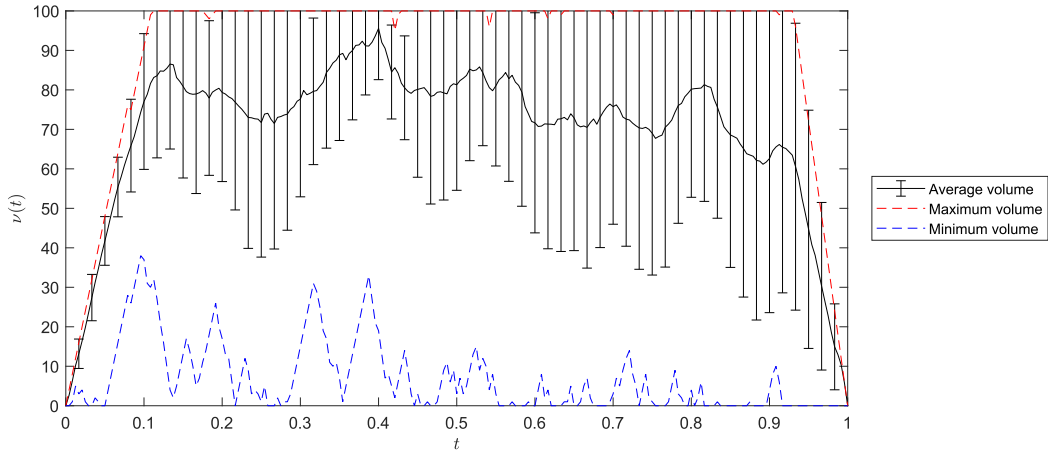


Figure 5.12: Average volume of gas in storage for Gas Test 1 for a fast storage with  $\sigma = 0.5$ . The strategy is to start with filling up the storage at the beginning, but then keep some space to take profit from the high volatility. For this specific simulation the value of the contract is  $v(0, S(0)) = 342$

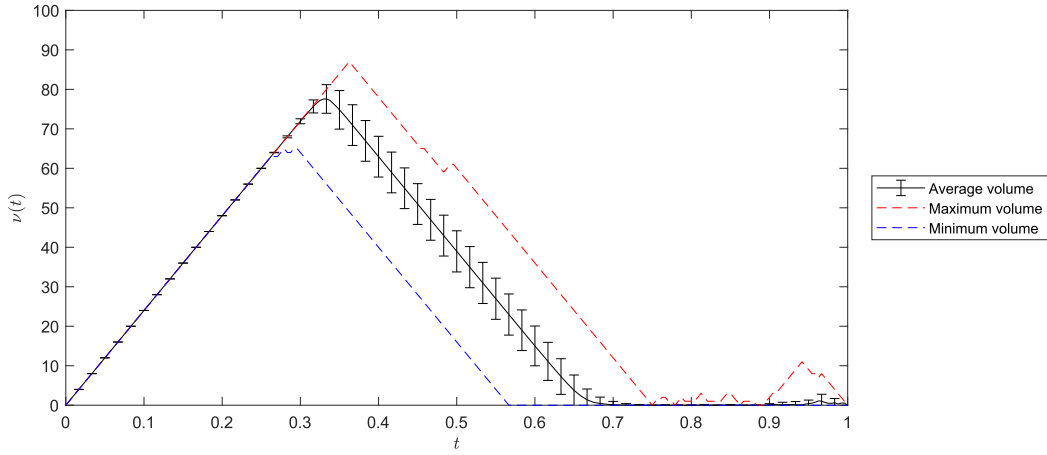


Figure 5.13: Average volume of gas in storage for Gas Test 2 for a slow storage with  $\sigma = 0.1$ . The strategy is to fill up the storage at the beginning and empty the storage when the price drops according to the seasonality function. For this specific simulation the value of the contract is  $v(0, S(0)) = 152$

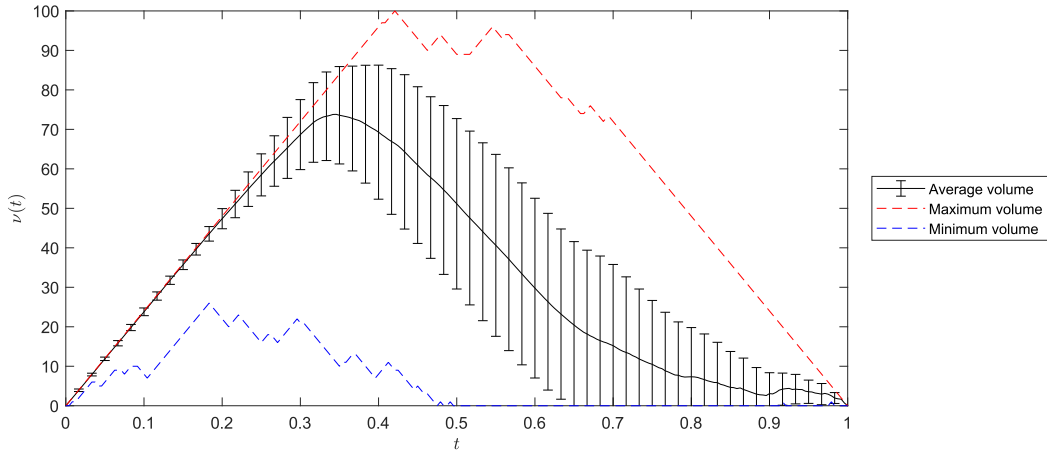


Figure 5.14: Average volume of gas in storage for Gas Test 2 for a slow storage with  $\sigma = 0.5$ . The strategy is to start with filling up the storage at the beginning and empty the storage when the price drops according to the seasonality function. Observe that more space is reserved than in Figure 5.13 to take profit of the higher volatility. For this specific simulation the value of the contract is  $v(0, S(0)) = 200$

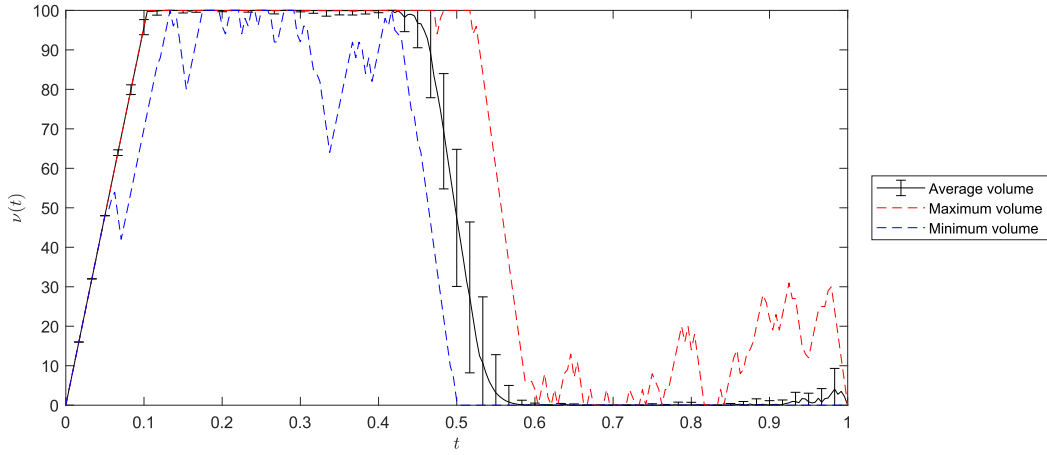


Figure 5.15: Average volume of gas in storage for Gas Test 2 for a fast storage with  $\sigma = 0.1$ . The strategy is to fill up the storage at the beginning and empty the storage when the price drops according to the seasonality function. For this specific simulation the value of the contract is  $v(0, S(0)) = 293$

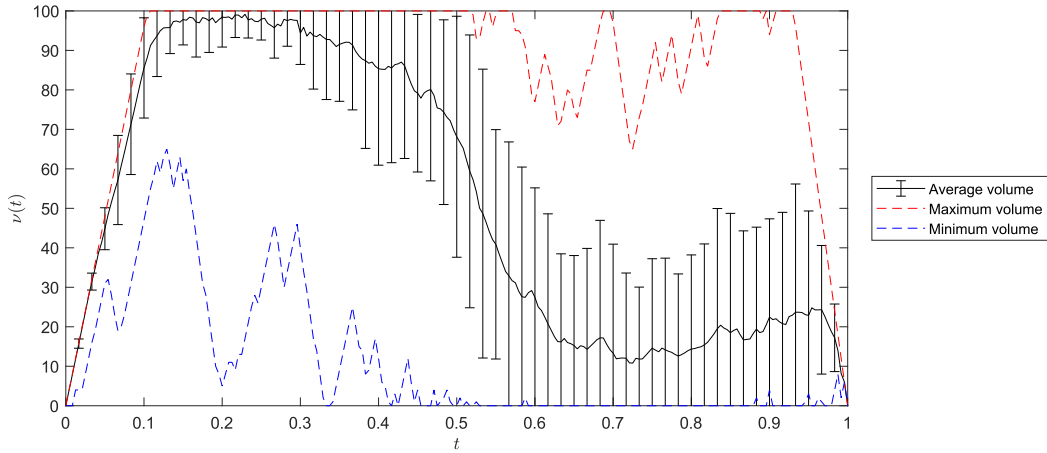


Figure 5.16: Average volume of gas in storage for Gas Test 2 for a fast storage with  $\sigma = 0.5$ . The strategy is to start with filling up the storage at the beginning and empty the storage when the price drops according to the seasonality function. Observe that more space is reserved than in Figure 5.15 to take profit of the higher volatility. For this specific simulation the value of the contract is  $v(0, S(0)) = 385$

### 5.4.3 An experiment with few nomination dates

Start date	$t_0$	0
Last trading date	$T$	1
Nomination	$\Delta t$	1/M
Minimum volume	$\nu^{min}$	0
Maximum volume	$\nu^{max}$	10
Start volume	$\nu(0)$	0
End volume	$\nu(t_{M+1})$	0
Maximum withdrawal	$i^{min}$	-1
Maximum injection	$i^{max}$	1

Table 5.10: Storage contract for test.

For the following test we discretized the volume of the tank onto a smaller grid and compared both methods for small values of  $M$ . The contract details are in Table 5.10.

$M$	LSMC (Mean)	LSMC (Std. error)	COS
1	0	0	0
2	1.1827	0.0018	1.1824
3	1.7030	0.0011	1.7031
4	2.6465	0.0016	2.6456
5	3.2462	0.0018	3.2462
6	4.1155	0.0016	4.1140

Table 5.11: Results for LSMC and COS for the test scenario.

For  $M = 1$ , both methods give a contract value of 0. Intuitively this is correct since there is only one date ( $t_1$ ) on which the storage manager can take an action. If he decides to buy, the storage facility will not be empty at the settlement date which results in a penalty. Therefore the storage manager is implicitly forced to do nothing and the contract has no value. For  $M \geq 2$ , there are two dates on which the storage manager can take an action. So now he can buy at  $t_1$  and sell at  $t_2$ . The profit he is expected to make in this way results in a positive contract value.

It is also noteworthy to see that the increments in contract value from  $M = 2$  to  $M = 3$  and from  $M = 4$  to  $M = 5$  are smaller than the increments from  $M = 1$  to  $M = 2$  and from  $M = 3$  to  $M = 4$ . This can be explained by the flexibility in choices that the storage manager has. If  $M = 3$  the storage manager can buy and sell 1 unit and not 2, because then he is not able to end up with an empty storage facility again. The increase in value from  $M = 2$  to  $M = 3$  can be explained by the fact that he is more flexible in choosing the date he buys and sells 1 unit of gas. The additional increase in value from  $M = 3$  to  $M = 4$  can be explained by the fact that he is now even able to buy and sell 2 units of gas. This effect diminishes when  $M$  becomes larger and larger.



# Chapter 6

## Conclusions and Outlook

### 6.1 Conclusions

In this work we introduced the COS method in determining the value of natural gas storage contracts. As long as the characteristic function of the process which models the natural gas spot price is available, the COS method can be applied. The COS method is at least competitive with existing simulation based valuation methods for natural gas storage contracts in computational time and accuracy.

In anticipation to the derivation of the COS method for the valuation of natural gas storage contracts, we constructed an efficient method for the valuation of options with multiple exercise rights at discrete exercise dates. This efficient computation is driven by the FFT-based algorithm and can only be used if the characteristic function can be written in a special form. For this special case the COS method outperforms the extended LSMC method for options with multiple early exercise rights.

In Section 2.8 we showed how the adjoint expansion method can be used to approximate a characteristic function for processes of the underlying for which the characteristic function is not available. Examples of this are models with a local volatility or state dependent jump measures. We showed that the adjoint expansion method could also be used to approximate the characteristic function of the Ornstein-Uhlenbeck model, especially for short times to maturity. The approximation that is obtained with this method can be used in combination with the FFT-based algorithm because of its special form.

### 6.2 Outlook

In the valuation of natural gas storage contracts with the COS method we approximated the integral that defines the Fourier cosine coefficients of the contract value by using the discrete Fourier cosine transform. This numerical integration is very time consuming in the valuation procedure. It may be beneficial to determine in some way the early decision points such that the FFT-based algorithm can be used to approximate the Fourier cosine coefficients of the continuation value in an efficient way. Because in general there can be made many decisions at a certain time point, it can be a challenge to characterize these decision points, if they exist at all, and to derive the value of the contract in a correct way.

For processes for which the tails of the probability density function are long, we suggest to further investigate the choice of parameter  $L$  that is used in determining the truncation range  $[a, b]$  for the COS method. A smart choice for  $L$  can ensure that less terms are needed in the Fourier cosine expansion, which makes the computation of the contract value faster.



# Appendices



# Appendix A

## Algorithms

In this appendix we present the LSMC algorithm for the valuation of a Bermudan option and the extended LSMC algorithm for the valuation of an option with multiple exercise rights. In Table A.1 we explain the notation that is used in the pseudocode. Do not confuse  $DCF^i$  and  $DCF^{i,j}$  with  $DCF_m^i$ , defined in (3.29), and  $DCF_m^{i,j}$ , defined in (3.32) respectively.  $DCF^i$  and  $DCF^{i,j}$  are the vector and matrix that are updated at every iteration of the algorithm and they contain implicitly all the discounted future cash flows under the optimal strategy.

Two built-in functions in MATLAB are used to do the regression: `polyfit` is a built-in function to do a regression onto the standard polynomials and `polyval` is a built-in function that analyses the function with the coefficients that were obtained with `polyfit`.

$CF_m^i$	The cash flow at time $t_m$ for trajectory $i$
$CF_m^{i,j}$	The cash flow at time $t_m$ for trajectory $i$ for the level of $j$ rights left
$PO_m^i$	The payoff of the option at time $t_m$ for trajectory $i$
$S_m^i$	The spot price at time $t_m$ for trajectory $i$
$CV_m^i$	The continuation value at time $t_m$ for trajectory $i$
$CV_m^{i,j}$	The continuation value at time $t_m$ for trajectory $i$ for the level of $j$ rights left
$V^i$	Approximation of the option price at time $t_0$ for trajectory $i$
$V^{i,j}$	Approximation of the option price at time $t_0$ for trajectory $i$ for the level of $j$ rights left
$DCF^i$	Discounted future cash flows for trajectory $i$ under the optimal strategy
$DCF^{i,j}$	Discounted future cash flows for trajectory $i$ for the level of $j$ rights left under the optimal strategy
$v(t_0, S(t_0))$	The value of the option at time $t_0$
$v^j(t_0, S(t_0))$	The value of the option at time $t_0$ for the level of $j$ rights left

Table A.1: Explained notation for the pseudocode in Algorithms 1-4.

## A.1 LSMC algorithm

---

**Algorithm 1** LSMC algorithm (based on the algorithm presented by Olofsson in [21])

---

```

 $CF_M^i = PO_M^i$  for  $i = 1, \dots, N$ 
for  $t = M - 1, \dots, 1$  do
   $X^i = S_t^i$  for all  $i$  where  $PO_t^i > 0$ 
   $Y^i = \sum_{k>t} e^{-r(k-t)\Delta t} CF_k^i$  for all  $i$  where  $PO_t^i > 0$ 
   $p = \text{polyfit}(X, Y, 3)$ 
   $CV_t^i = \text{polyval}(p, X_t^i)$  for all  $i$  where  $PO_t^i > 0$ 
  for  $i = 1, \dots, N$  do
    if  $CV_t^i < PO_t^i$  then
       $CF_t^i = PO_t^i$ 
       $CF_m^i = 0$  for all  $m > t$ 
    end if
  end for
end for
 $V^i = \sum_{t=1}^M e^{-rt\Delta t} CF_t^i$ 
 $v(t_0, S(t_0)) = \frac{1}{N} \sum_{i=1}^N V^i$ 

```

---



---

**Algorithm 2** LSMC algorithm, vectorized

---

```

 $CF^i = PO_M^i$  for  $i = 1, \dots, N$ 
for  $t = M - 1, \dots, 1$  do
   $DCF^i = e^{-r\Delta t} CF^i$ 
   $X^i = S_t^i$  for all  $i$  where  $PO_t^i > 0$ 
   $Y^i = DCF^i$  for all  $i$  where  $PO_t^i > 0$ 
   $p = \text{polyfit}(X, Y, 3)$ 
   $CV^i = \text{polyval}(p, X_t^i)$  for all  $i$  where  $PO_t^i > 0$ 
  for  $i = 1, \dots, N$  do
    if  $CV^i < PO_t^i$  then
       $CF^i = PO_t^i$ 
    else
       $CF^i = DCF^i$ 
    end if
  end for
end for
 $V^i = e^{-rt\Delta t} DCF^i$ 
 $v(t_0, S(t_0)) = \frac{1}{N} \sum_{i=1}^N V^i$ 

```

---

## A.2 Extended LSMC algorithm

---

**Algorithm 3** LSMC algorithm for an option with multiple exercise rights (based on the algorithm presented by Olofsson in [21])

---

```

for  $j = 1, \dots, R$  do
  for  $t = M, \dots, M - (R - 1)$  do
     $CF_t^{i,j} = PO_t^i$  for  $i = 1, \dots, N$ 
  end for
end for
for  $t = M - 1, \dots, 1$  do
   $X^i = S_t^i$  for all  $i$  where  $PO_t^i > 0$ 
  for  $j = 1, \dots, \min(M - t, R)$  do
     $Y^{i,j} = \sum_{k>t} e^{-r(k-t)\Delta t} CF_k^{i,j}$ 
  end for
  for  $j = 1, \dots, \min(M - t, R)$  do
     $p^j = \text{polyfit}(X, Y^j, 3)$ 
     $CV_t^{i,j} = \text{polyval}(p^j, X_t^i)$  for all  $i$  where  $PO_t^i > 0$ 
  end for
  if  $\min(M - t, R) > 1$  then
    for  $j = \min(M - t, R), \dots, 2$  do
      for  $i = 1, \dots, N$  do
        if  $PO_t^i + CV_t^{i,j-1} > CV_t^{i,j}$  then
           $CF_t^{i,j} = PO_t^i$ 
           $CF_m^{i,j} = CF_m^{i,j-1}$  for all  $m > t$ 
        end if
      end for
    end for
  end if
  if  $PO_t^i > CV_t^{i,1}$  then
     $CF_t^{i,1} = PO_t^i$ 
     $CF_k^{i,1} = 0$  for all  $k > t$ 
  end if
end for
for  $j = 1, \dots, R$  do
   $V^{i,j} = \sum_{t=1}^M e^{-rt\Delta t} CF_t^{i,j}$ 
   $v^j(t_0, S(t_0)) = \frac{1}{N} \sum_{i=1}^N V^{i,j}$ 
end for

```

---

---

**Algorithm 4** Extended LSMC algorithm, vectorized

---

```
for  $j = 1, \dots, R$  do  
   $CF^{i,j} = \sum_{k=1}^j e^{-r(k-1)\Delta t} PO_{M-j+k}^i$    for  $i = 1, \dots, N$   
end for  
for  $t = M - 1, \dots, 1$  do  
   $X^i = S_t^i$    for all  $i$  where  $PO_t^i > 0$   
  for  $j = 1, \dots, \min(M - t, R)$  do  
     $DCF^{i,j} = e^{-r\Delta t} CF^{i,j}$   
     $Y^{i,j} = DCF^{i,j}$    for all  $i$  where  $PO_t^i > 0$   
     $p^j = \text{polyfit}(X, Y^j, 3)$   
     $CV^{i,j} = \text{polyval}(p^j, X_t^i)$    for all  $i$  where  $PO_t^i > 0$   
  end for  
  if  $\min(M - t, R) > 1$  then  
    for  $j = \min(M - t, R), \dots, 2$  do  
      for  $i = 1, \dots, N$  do  
        if  $PO_t^i + CV^{i,j-1} > CV^{i,j}$  then  
           $CF^{i,j} = PO_t^i + DCF^{i,j-1}$   
        else  
           $CF^{i,j} = DCF^{i,j}$   
        end if  
      end for  
    end for  
  end if  
  for  $i = 1, \dots, N$  do  
    if  $PO_t^i > CV^{i,1}$  then  
       $CF^{i,1} = PO_t^i$   
    else  
       $CF^{i,1} = DCF^{i,1}$   
    end if  
  end for  
end for  
for  $j = 1, \dots, R$  do  
   $V^{i,j} = e^{-r\Delta t} DCF^{i,j}$   
   $v^j(t_0, S(t_0)) = \frac{1}{N} \sum_{i=1}^N V^{i,j}$   
end for
```

---

## Appendix B

# Comparison of two numerical integration techniques

In this appendix, we compare the approximation of the Fourier cosine coefficients

$$V_k = \frac{2}{b-a} \int_a^b f(x) \cos\left(k\pi \frac{x-a}{b-a}\right) dx \quad (\text{B.1})$$

for two different methods. For  $f(x)$  we take the smooth function  $f(x) = e^x$ . The first method is with the trapezoidal rule, where the second method is with the discrete Fourier cosine transform. To test the speed of convergence, we choose the interval of integration with  $a = 0$  and  $b = 3$ . We compare the results for both methods for the coefficient  $V_1$  for which the analytic solution is given by

$$V_1 = -\frac{18(1+e^3)}{3(9+\pi^2)}. \quad (\text{B.2})$$

### Speed of convergence of the trapezoidal rule

We use the function `trapz` from MATLAB to approximate the coefficients  $V_1$ .

For  $N = 2^i$ , where  $i = 1 \dots 12$ , we approximated the value of  $V_1$  with the trapezoidal rule. In Table B.1 the error for different values of  $N$  is shown and we observe a second order convergence.

$N$	Error( $N$ )	Error( $N$ )/Error( $2N$ )
2	12.3809331143	10.1970629287
4	1.2141665890	5.6041416319
8	0.2166552291	4.6167423370
16	0.0469281613	4.2760927780
32	0.0109745424	4.1311909581
64	0.0026565081	4.0640091184
128	0.0006536669	4.0316226204
256	0.0001621349	4.0157175829
512	0.0000403751	4.0078355755
1024	0.0000100740	4.0039120115
2048	0.0000025160	4.0019545691
4096	0.0000006287	-

Table B.1: Numerical integration error for the coefficient  $V_1$  with the trapezoidal rule. The numerical integration error decreases when the integration grid becomes more fine. We clearly observe a second order convergence.

## Speed of convergence of the discrete Fourier transform

We use the function `dct` from MATLAB to approximate all  $N$  coefficients  $V_k$  at once. We need to multiply all coefficients by  $\sqrt{2/N}$  and  $V_0$  by  $\sqrt{2}$ , because MATLAB uses a normalization.

For  $N = 2^i$ , where  $i = 1 \dots 12$ , we approximated the value of  $V_1$  by using the discrete Fourier cosine transform. In Table B.2 the error for different values of  $N$  is shown and we observe a second order convergence.

$N$	Error( $N$ )	Error( $N$ )/Error( $2N$ )
2	1.4927065284	4.3709053837
4	0.3415096867	4.1079445168
8	0.0831339580	4.0278830219
16	0.0206396158	4.0070257813
32	0.0051508567	4.0017598677
64	0.0012871479	4.0004401806
128	0.0003217516	4.0001100585
256	0.0000804357	4.0000275155
512	0.0000201088	4.0000068792
1024	0.0000050272	4.0000017236
2048	0.0000012568	4.0000004382
4096	0.0000003142	-

Table B.2: Numerical integration error for the coefficient  $V_1$  with the discrete Fourier cosine transform. The numerical integration error decreases when the integration grid becomes more fine. We clearly observe a second order convergence.

## Comparison

As shown above, the speed of convergence is the same for both techniques. However, a drawback when using the trapezoidal rule is that we have to use it once for every single coefficient  $V_k$ ,  $k = 0 \dots N - 1$ . Also the values of  $\cos\left(k\pi\frac{x-a}{b-a}\right)$  need to be calculated. An advantage when using the trapezoidal rule is that the numerical integration grid can be chosen arbitrarily fine.

When using the discrete Fourier cosine transform, the advantage is that all coefficients  $V_k$ ,  $k = 0 \dots N - 1$  are approximated at once. A condition for this is that the number of grid points for the discrete Fourier cosine transform equals the number of coefficients that need to be approximated.

In Table B.3 we show the CPU times for the approximation of  $V_1$  with both methods. The last column multiplies the computational time for  $V_1$  with  $N$ , to give an indication of the time to compute  $N$  coefficients. The CPU time for the discrete Fourier cosine transform is already the time to compute  $N$  coefficients since all coefficients  $V_k$  can be approximated at once with this technique.

Therefore already for small  $N$ , the discrete cosine transform seems to outperform the trapezoidal rule in the computation of the Fourier cosine coefficients  $V_k$

$N$	All $V_k$ with DCT	$V_1$ with trapezoidal	$\times N$
2	0.16	0.008	0.016
4	0.18	0.010	0.040
8	0.18	0.010	0.080
16	0.18	0.010	0.160
32	0.18	0.011	0.35
64	0.18	0.011	0.70
128	0.18	0.011	1.4
256	0.18	0.012	3.1
512	0.19	0.013	6.7
1024	0.19	0.016	16
2048	0.21	0.022	45
4096	0.23	0.038	$1.5 \cdot 10^2$

Table B.3: CPU times (in msec.)



# Appendix C

## Models for the dynamics of the underlying

In this appendix we recall the characteristics for the models that are mentioned in this report.

### C.1 Geometric Brownian Motion

The simplest model for modelling the spot price is the GBM model. In the GBM model, the spot price is driven by the following stochastic differential equation (SDE):

$$dS(t) = \mu S(t) dt + \sigma S(t) dW(t). \quad (\text{C.1})$$

Substituting  $X(t) = \log(S(t))$  and applying Itô's lemma yields

$$dX(t) = \left( \mu - \frac{1}{2}\sigma^2 \right) dt + \sigma dW(t). \quad (\text{C.2})$$

This can be rewritten in the following integral equation:

$$X(t) = X(0) + \int_0^t \left( \mu - \frac{1}{2}\sigma^2 \right) ds + \int_0^t \sigma dW(s) \quad (\text{C.3})$$

$$= X(0) + \left( \mu - \frac{1}{2}\sigma^2 \right) t + \sigma dW(t). \quad (\text{C.4})$$

Now transforming back to  $S(t)$  by taking the exponential on both sides gives the following solution of the SDE:

$$S(t) = S(0) \cdot \exp \left( \left( \mu - \frac{1}{2}\sigma^2 \right) t + \sigma dW(t) \right). \quad (\text{C.5})$$

In [24] the authors showed that a drawback of GBM is that it cannot capture seasonality and mean-reversion. Therefore GBM is not a realistic process that can be used for the valuation of a gas storage facility. Because it is an easy model to understand and implement, we will use it in our valuation methods for options with (multiple) early exercise rights.

When valuing under the risk neutral measure, the risk-neutral valuation is carried out by taking the drift term  $\mu = r$ , where  $r$  is the risk-free rate.

The characteristic function of the GBM process is given by

$$\phi(\omega; x; \tau) = e^{i\omega x} \varphi_{GBM}(\omega; \tau), \quad (\text{C.6})$$

with

$$\varphi_{GBM}(\omega; \tau) = e^{i\omega \mu \tau - \frac{1}{2}\sigma^2 \omega^2 \tau}. \quad (\text{C.7})$$

## C.2 Merton jump-diffusion

The Merton jump-diffusion process is nothing more than the GBM process with a jump process added to it. The model was first proposed by Merton [20].

The jump magnitude  $J$  in Merton's jump-diffusion model is normally distributed with mean  $\mu_J$  and variance  $\sigma_J^2$ .

When valuing under the risk neutral measure, the risk-neutral valuation is carried out by taking the drift term  $\mu = r - \frac{1}{2}\sigma^2 - \lambda(\exp(\mu_J + \frac{1}{2}\sigma_J^2) - 1)$ , where  $r$  is the risk-free rate.

The characteristic function of Merton's jump-diffusion model is given by

$$\phi(\omega; x; \tau) = e^{i\omega x} \varphi_{Merton}(\omega; \tau), \quad (\text{C.8})$$

with

$$\varphi_{Merton}(\omega; \tau) = \exp\left(i\omega\mu\tau - \frac{1}{2}\sigma^2\omega^2\tau + \lambda\tau\left(e^{i\omega\mu_J - \frac{1}{2}\omega^2\sigma_J^2} - 1\right)\right). \quad (\text{C.9})$$

## C.3 Kou jump-diffusion

Kou proposed the model in his paper [17].

The jump magnitude  $J$  in Kou's jump-diffusion model is asymmetric double exponentially distributed, which means that the probability density function of  $J$  is given by

$$f_J(x) = \begin{cases} p \cdot \eta_1 e^{-\eta_1 x} & \text{if } x \geq 0 \\ q \cdot \eta_2 e^{\eta_2 x} & \text{if } x < 0. \end{cases} \quad (\text{C.10})$$

When valuing under the risk neutral measure, the risk-neutral valuation is carried out by taking the drift term  $\mu = r - \frac{1}{2}\sigma^2 - \lambda\left(p\frac{\eta_1}{\eta_1 - 1} + q\frac{\eta_2}{\eta_2 + 1} - 1\right)$ , where  $r$  is the risk-free rate.

The characteristic function of Kou's jump-diffusion model is given by

$$\phi(\omega; x; \tau) = e^{i\omega x} \varphi_{Kou}(\omega; \tau), \quad (\text{C.11})$$

with

$$\varphi_{Kou}(\omega; \tau) = \exp\left(i\omega\mu\tau - \frac{1}{2}\sigma^2\omega^2\tau + \lambda\tau\left(p\frac{\eta_1}{\eta_1 - i\omega} + q\frac{\eta_2}{\eta_2 + i\omega} - 1\right)\right). \quad (\text{C.12})$$

## C.4 Ornstein-Uhlenbeck mean-reverting process

In this model, the spot price is driven by the following SDE:

$$dS(t) = \kappa(\mu - S(t)) dt + \sigma dW(t). \quad (\text{C.13})$$

The solution of this SDE is given by:

$$S(t) = S(0)e^{-\kappa t} + \mu(1 - e^{-\kappa t}) + \sigma e^{-\kappa t} \int_0^t e^{\kappa s} dW(s) \quad (\text{C.14})$$

In the paper [31] the authors provide the characteristic function for the Ornstein-Uhlenbeck process, which is given by

$$\phi(\omega; x; \tau) = e^{i\omega x e^{-\kappa\tau} + A(\omega, \tau)}, \quad (\text{C.15})$$

with

$$A(\omega, \tau) = \frac{1}{4\kappa} (e^{-2\kappa\tau} - e^{-\kappa\tau}) (\omega^2\sigma^2 + \omega e^{\kappa\tau} (\omega\sigma^2 - 4i\kappa\mu)). \quad (\text{C.16})$$

# Appendix D

## Variations with the COS method

### The log-price process

If we use the  $\log(S(t))$  process where

$$x := \log(S(0)) \quad \text{and} \quad y := \log(S(T)), \quad (\text{D.1})$$

instead of the  $\log(S(t)/K)$  process, where

$$x := \log(S(0)/K) \quad \text{and} \quad y := \log(S(T)/K), \quad (\text{D.2})$$

the payoff function for vanilla options is given by

$$g(y, T) = \begin{cases} \max\{e^y - K, 0\} & \text{for a call,} \\ \max\{K - e^y, 0\} & \text{for a put.} \end{cases} \quad (\text{D.3})$$

Now we calculate the coefficients  $V_k$  for a European option. Because for a call the payoff is zero when  $e^y \leq K$ , or equivalently  $y \geq \ln(K)$ , we have to integrate from  $\ln(K)$  to  $b$  and obtain

$$V_k^{call} = \frac{2}{b-a} \int_{\log(K)}^b (e^y - K) \cos\left(k\pi \frac{y-a}{b-a}\right) dy = \frac{2}{b-a} (\chi_k(\log(K), b) - K\psi_k(\log(K), b)). \quad (\text{D.4})$$

For a put the payoff is zero when  $e^y \geq K$ , or equivalently  $y \leq \ln(K)$ , so we have to integrate from  $a$  to  $\ln(K)$  and obtain

$$V_k^{put} = \frac{2}{b-a} \int_a^{\log(K)} (K - e^y) \cos\left(k\pi \frac{y-a}{b-a}\right) dy = \frac{2}{b-a} (-\chi_k(a, \log(K)) + K\psi_k(a, \log(K))). \quad (\text{D.5})$$

$\chi_k$  and  $\psi_k$  are given by (2.39) and (2.41) respectively. The occurrence of  $K$  in the formulas for  $\chi_k$  and  $\psi_k$  hampers the efficient computation for many strikes simultaneously.

### The put-call parity

As mentioned in the paper [10], the COS method is more sensitive to the choice of the truncation range  $[a, b]$  when it is used for the valuation of call options than for the valuation of put options. The reason for this is that the payoff function for a call option is unbounded. Therefore the suggestion is to use the put-call parity in (D.6) when pricing call options with the COS method.

$$v^{call}(x, t) = v^{put}(x, t) + S_t e^{-q(T-t)} - K e^{-r(T-t)} \quad (\text{D.6})$$

The valuation of Bermudan call options does suffer even more from this effect, because in the recursive algorithm the error is propagated. When valuing Bermudan call options, the problem gets even worse, since in the backward procedure the error is propagated. In [30], the author presents how the put-call parity can be used in the COS method for a Bermudan call option.



# References

- [1] F. E. Benth, R. Kiesel, and A. Nazarova, “A critical empirical study of three electricity spot price models,” *Energy Economics*, vol. 34, no. 5, pp. 1589–1616, 2012.
- [2] A. Boogert and C. De Jong, “Gas storage valuation using a monte carlo method,” *The journal of derivatives*, vol. 15, no. 3, pp. 81–98, 2008.
- [3] A. Borovykh, “Applications of stochastic processes to financial risk computation,” Ph.D. dissertation, University of Bologna, 2018.
- [4] A. Cartea and M. G. Figueroa, “Pricing in electricity markets: a mean reverting jump diffusion model with seasonality,” *Applied Mathematical Finance*, vol. 12, no. 4, pp. 313–335, 2005.
- [5] Z. Chen and P. A. Forsyth, “A semi-lagrangian approach for natural gas storage valuation and optimal operation,” *SIAM Journal on Scientific Computing*, vol. 30, no. 1, pp. 339–368, 2007.
- [6] C. de Jong, “Gas storage valuation and optimization,” *Journal of Natural Gas Science and Engineering*, vol. 24, pp. 365–378, 2015.
- [7] C. de Jong and K. Walet, “To store or not to store,” *Energy Power Risk Management*, pp. 8–11, 2003.
- [8] U. Dörr, “Valuation of swing options and examination of exercise strategies by monte carlo techniques,” Master’s thesis, University of Oxford, 2003.
- [9] F. Fang, “The cos method: An efficient fourier method for pricing financial derivatives,” Ph.D. dissertation, Technische Universiteit Delft, 2010.
- [10] F. Fang and C. W. Oosterlee, “A novel pricing method for european options based on fourier-cosine series expansions,” *SIAM Journal on Scientific Computing*, vol. 31, no. 2, pp. 826–848, 2008.
- [11] —, “Pricing early-exercise and discrete barrier options by fourier-cosine series expansions,” *Numerische Mathematik*, vol. 114, no. 1, pp. 27–62, 2009.
- [12] R. V. Hogg, J. McKean, and A. T. Craig, *Introduction to mathematical statistics*, 7th ed. Pearson, 2013.
- [13] P. Hénaff, I. Laachir, and F. Russo, “Gas storage valuation and hedging: A quantification of model risk,” *International Journal of Financial Studies*, vol. 6, p. 27, 2018.
- [14] A. Ibáñez, “Valuation by simulation of contingent claims with multiple early exercise opportunities,” *Mathematical Finance*, vol. 14, no. 2, pp. 223–248, 2004.
- [15] S. Jain and C. W. Oosterlee, “The stochastic grid bundling method: Efficient pricing of bermudan options and their greeks,” *Applied Mathematics and Computation*, vol. 269, pp. 412–431, 2015.
- [16] V. Kaminski, Ed., *Managing Energy Price Risk*, 4th ed. Risk Books, 2016.
- [17] S. G. Kou, “A jump-diffusion model for option pricing,” *Management science*, vol. 48, no. 8, pp. 1086–1101, 2002.

- [18] F. A. Longstaff and E. S. Schwartz, “Valuing american options by simulation: a simple least-squares approach,” *The review of financial studies*, vol. 14, no. 1, pp. 113–147, 2001.
- [19] J. J. Lucia and E. S. Schwartz, “Electricity prices and power derivatives: Evidence from the nordic power exchange,” *Review of derivatives research*, vol. 5, no. 1, pp. 5–50, 2002.
- [20] R. C. Merton, “Option pricing when underlying stock returns are discontinuous,” *Journal of financial economics*, vol. 3, no. 1-2, pp. 125–144, 1976.
- [21] C. Olofsson, “Pricing swing options in the electricity market,” Master’s thesis, Lund University, 2015.
- [22] S. Pagliarani, A. Pascucci, and C. Riga, “Adjoint expansions in local lévy models,” *SIAM Journal on Financial Mathematics*, vol. 4, no. 1, pp. 265–296, 2013.
- [23] K. R. Rao and P. Yip, *Discrete cosine transform: algorithms, advantages, applications*. Academic press, 1990.
- [24] N. Roelofs, “Incorporating seasonality and volatility updating in gas storage valuation for the purpose of validation,” Master’s thesis, University of Twente, 2015.
- [25] M. J. Ruijter, “Fourier methods for multidimensional problems and backward sdes in finance and economics,” Ph.D. dissertation, Technische Universiteit Delft, 2015.
- [26] E. S. Schwartz, “The stochastic behavior of commodity prices: Implications for valuation and hedging,” *The Journal of Finance*, vol. 52, no. 3, pp. 923–973, 1997.
- [27] R. Seydel, *Tools for computational finance*, 5th ed. Springer, 2012.
- [28] M. Thompson, M. Davison, and H. Rasmussen, “Natural gas storage valuation and optimization: A real options application,” *Naval Research Logistics (NRL)*, vol. 56, no. 3, pp. 226–238, 2009.
- [29] B. Zhang and C. W. Oosterlee, “An efficient pricing algorithm for swing options based on fourier cosine expansions,” *Journal of Computational Finance*, vol. 16, no. 4, pp. 3–34, 2013.
- [30] B. Zhang, “Efficient pricing of early-exercise and exotic options based on fourier cosine expansions,” Ph.D. dissertation, Technische Universiteit Delft, 2012.
- [31] B. Zhang, L. A. Grzelak, and C. W. Oosterlee, “Efficient pricing of commodity options with early-exercise under the ornstein–uhlenbeck process,” *Applied Numerical Mathematics*, vol. 62, no. 2, pp. 91–111, 2012.